UZBEKISTAN ACADEMY OF SCIENCES
ASTRONOMICAL INSTITUTE
INSTITUTE OF NUCLEAR PHYSICS

УДК 530.12:531.51

SHAYMATOV SANJAR RUZIMUROTOVICH

GENERAL RELATIVISTIC ASTROPHYSICAL PROCESSES IN THE VICINITY OF COMPACT GRAVITATIONAL OBJECTS IN THE PRESENCE OF EXTERNAL ELECTROMAGNETIC FIELD

01.03.01- ASTRONOMY

DISSERTATION OF THE DOCTOR OF PHILOSOFY (PhD)
ON PHYSICAL AND MATHEMATICAL SCIENCES

Supervisor: **Ahmedov Bobomurat Juraevich**
doctor of sciences in physics and mathematics, professor

Tashkent- 2018

Contents

INTRODUCTION

Topicality and demand of the theme of dissertation.

Nowadays, much progress has been made in observational studies of stellar mass black holes in X-ray binaries and supermassive black holes through modern astronomical observations. Also, the detection of gravitational waves (GWs) from GW150914, GW151226 and GW170104 and the detection of a high energy neutrino 170922A by IceCube Neutrino Observatory verify the observational progress in the detection of black holes. Thus, the presence of black holes in astrophysics is now taking center stage by the LIGO and VIRGO detection of stellar black hole mergers and recent astronomical investigations of the high-energy neutrino and the output ($L_{quasar} \approx 10^{42} - 10^{47} erg/s$) from active galactic nuclei (AGN) in various forms such as winds and jets, which have been detected by x-ray, VLBI, and γ-ray telescopes.

Throughout the world, developing accurate theoretical investigations in the context of testing cosmic censorship conjecture for presence of black holes, modeling the energy extraction from black holes being candidates for such energy sources via infalling test particles or magnetic fields surrounding compact objects is the most important issues of modern astrophysics in getting more information about the properties of black holes and providing the proof to the relevant observations by ground and space-based telescopes. The investigation of the astrophysical processes in the vicinity of black holes and the effect of the electromagnetic field on the rich phenomenology of astrophysical processes in the strong gravitational field regime, which allows us to verify the general theory of relativity, is one of the most important tasks of modern relativistic astrophysics.

In our country, great attention has been paid to the development of experimental and theoretical researches in the field of relativistic astrophysics, as well as fundamental research in this direction at the international level. The fundamental research topics, which are of great importance for the progress of science and its further application in practice in our country, are reflected in the

Strategy[1] for Further Development of the Republic of Uzbekistan for 2017-2021. Thus, theoretical and observational studies of the role of the external magnetic field on the motion of test particles around compact gravitational objects in testing cosmic censorship conjecture, analyzing bound and isofrequency pairing non-geodesic orbits around black holes, and developing energy extraction processes from black holes in the field of relativistic astrophysics play a significant role.

This research carried out in the dissertation fully corresponds to the tasks stipulated in the Decrees of the President of the Republic of Uzbekistan No. PR-2789 “On measures of further improvement of the activities of the Academy of Sciences, organization, management and financing of scientific research works” from February, 2017, Decree No. PD-4947 “On the strategy of Actions on Further Development of the Republic of Uzbekistan” from February 7, 2017, and Decree No. PD-3275 “On the creation of the state specialized secondary school named after Mirzo Ulugbek and Astronomy and Aeronautics park” from September 14, 2017, and in legal and regulatory documents accepted in this field as well.

Relevance of the research to the priority areas of science and technology development of the Republic of Uzbekistan. The dissertation research has been carried out in accordance with the priority areas of science and technology in the Republic of Uzbekistan: II. “Power, energy and resource saving”.

Degree of study of the problem. Many scientists in the world, for instance, Japan scientists (I. Takahisa, H. Tomohiro, K. Masashi), Indian scientists (N. Dadhich, S. Ghosh, P. Joshi, M. Patil), Italian scientists (C. Bambi, L. Rezzolla, L. Modesto, D. Malafarina, O. Zanotti), Russian scientists (M. Yu. Piotrovich, Yu. N. Gnedin; A. Zakharov, D. Galtsov), Czech scientists (Z. Stuchlik, M. Kolos, J. Schee, J. Kovar, V. Karas), German scientists (C. Laemmerzahl, J. Kuntz, E. Hackmann, D. Kunst, V. Perlick), and others have done huge number of theoretical and observational investigations to study the energetic processes, particle motion and isofrequency pairing bound orbits around rotating black hole and cosmic censorship

[1] Decree of the President of the Republic of Uzbekistan “On the Strategy for the Further Development of the Republic of Uzbekistan” No. 4947 of 07 February 2017

and overspinning process for rotating black hole as well. Also, uzbek scientists (B. Ahmedov, A. Abdujabbarov, V. Morozova, F. Atamuratov, A. Tursunov, B. Toshmatov and others) have done theoretical investigations in analysing the influence of a magnetic field on the innermost stable circular orbit (ISCO) so as to provide the upper limit for the different parameters of the black hole and in studying the orbits of magnetized particles around black holes immersed in an asymptotically uniform magnetic field in the alternative theory of gravity and optical properties of black holes.

Previous research works on energetic processes around black hole and cosmic censorship have been done for axial symmetric compact gravitating objects. However, one can consider the magnetic field effect on those astrophysical processes. Since an external magnetic field plays an important role in the vicinity of compact objects, its effect could be used as a useful tool in constructing new tests of general relativity, in testing cosmic censorship conjecture, in producing the observed enormous energy from rotating black holes, and in studying isofrequency pairing nongeodesic circular orbits around black hole.

The idea of the cosmic censorship was proposed by Penrose, according to which the singularities are hidden inside the horizon of black holes and not observable outside; black holes with event horizon in astrophysics also take center stage by the LIGO and VIRGO detection of stellar black hole mergers registered by GW150914 recently. The cosmic censorship conjecture has been studied in detail for the various parameters of the black hole in scientific papers.

However, testing cosmic censorship conjecture with infalling test particles has recently become an active scientific object irrespective of fact that it remained unproven yet. The influence of an external magnetic field on cosmic censorship conjecture, the amount of energy extracted from black hole, and isofrequency pairing nongeodesic circular orbits around black hole has not been investigated yet in detail.

Connection of dissertational research with the plans of scientific research works of the scientific research institution, where the dissertation was

conducted. The dissertation was done in the framework of the scientific projects of the Institute of Nuclear Physics and Astronomical Institute, Uzbek Academy of Sciences: EF-2A-FA-1-10 "Particles and fields in the vicinity of relativistic gravitational objects from dark energy and wormholes" (2010-2011); F2-FA-F113 "Gravitational and electromagnetic processes in relativistic astrophysics and cosmology, a system of bosons at low temperatures" (2012-2016); EF2-FA-O-25046 "The motion of particles with spin and propagation of electromagnetic waves in the vicinity of compact objects gravity" (2014-2015); VA-FA-F-2-008 "Astrophysical Processes in Stationary and Dynamic Relativistic Gravitation Objects" (2017-2020).

The aim of the research of dissertation is to develop a theoretical formalism describing high-energetic processes, the dynamics of overspinning processes in testing cosmic censorship conjecture, and the process of isofrequency pairing nongeodesic orbits of charged particles in the vicinity of black holes in the presence of an external electromagnetic field.

The tasks of the research:

- to study isofrequency pairing of the circular non-geodesic orbits in the vicinity of the Schwarzschild black hole immersed in external asymptotically uniform magnetic field;

- to study the particle motion around a rotating black hole with a non-zero brane parameter, and consider the dependence of the ergosphere of the rotating black hole on cosmological constant;

- to consider and investigate the electromagnetic field and the charged particles motion in the vicinity of the rotating and nonrotating black hole with quintessential energy immersed in an external uniform magnetic field;

- to obtain the dependence of the extracted energy from compact object on NUT (Newmann-Unti-Tamburino) parameter;

- to investigate the high energetic processes around a rotating and non-rotating black hole with quintessential energy immersed in an external magnetic field; to investigate the influence of an external magnetic field on the amount of energy extracted from black hole;

- to consider a process of over-spinning a near-extremal rotating black hole; to analyze the effect of magnetic field on such process in testing cosmic censorship conjecture.

The objects of the research are relativistic compact gravitating objects: astrophysical and supermassive black holes.

The subjects of the research are isofrequency pairing non-geodesic orbits of charged particles around black holes, the effect of the external magnetic fields on the efficiency of extracted energy from black holes and the process of destroying a near-extremal rotating black hole in testing cosmic censorship conjecture.

The methods of the research. The research methods are mathematical apparatus of general relativity and metric affine differential geometry, analytical and numerical methods for solving differential equations of particle motion and field.

The scientific novelty of the research is the follows:

- Isofrequency pairing of non-geodesic orbits under the grav¬itational field of the Schwarzschild black hole immersed in external asymp¬totically uniform magnetic field and the dependence of the surface of region where isofrequency pairing of non-geodesic orbits occur around Schwarzschild black hole from the external magnetic field have been developed;

- it has been shown that a test magnetic field can affect the process of destroying black holes and restore the cosmic censorship in the astrophysical context;

- it has been shown that energy extraction through Penrose process is more realistic process for the energy extraction from the rotating black hole in the Kerr-Taub-NUT spacetime. The dependence of the extracted energy from compact object on NUT parameter $\tilde{l}$ (gravitomagnetic charge) has been found;

- it has been shown that the influence of the cosmological constant and the brane parameter may also cause a limitation for the efficiency of the ultrahigh-energy of the colliding particles; it has been established that the mechanism of this limitation is related to splitting the ISCO radius from the event horizon.

Practical results of the research are as follows:

- A decrease in the surface of the isofrequency pairing of nongeodesic orbits as nearly (7-10) % for the maximal values of the external uniform magnetic field $B \approx 10^6 - 10^7$ Gauss around astrophysical black holes has been found;

- it has been obtained that a test magnetic field would act as a cosmic censor beyond a certain threshold value of the magnetic field B_{cr} = 0.6872;

- it has been demonstrated that the magnetic field, although small, can strongly affect the value of energy efficiency and play a decisive role in the amount of energy extracted from quintessential black hole, giving rise to an increase in the amount of the upper bound of the efficiency up to 50% for the extremal rotating black hole as compared to the upper bound 42% for the extremal Kerr black hole;

- the analytical expressions for the vacuum electromagnetic field of quintessential rotating black hole in the external asymptotically uniform magnetic field have been obtained; it has been demonstrated that due to the existence of quintessential field intensity parameter $\tilde{c}$ charged particles are prevented from acceleration to infinitely high energies;

- it has been obtained that the center of mass energy starts becoming finite once the value of cosmological parameter Λ and quintessential parameter $\tilde{c}$, being responsible for the form of dark energy, increases even for the extremal quintessential rotating black hole.

Reliability of the research results is provided by the followings: in the dissertation new methods of general relativity and modern numerical methods and algorithms are used; obtained theoretical results are compared with modern astronomical observations, as well as the results of other authors; conclusions of results are well consistent with the general principles of compact gravitational objects.

Scientific and practical significance of the research results.

The scientific significance of the research results is devoted much attention to explaining the arbitrarily high energy processes around a rotating black hole by the mechanisms developed in the dissertation so as to analyze the jets being spewed out of a black hole. The results, in the dissertation, concerning isofrequency pairing nongeodesic orbits can make easier to identify signals coming from infinity in studying the data-analysis problem for gravitational-wave detectors. In addition, the scientific significance of results consists in an original strict mathematical proof to the validity of cosmic censorship in an astrophysical scenario by using the effect of a test magnetic field.

The practical significance of the research results consists in constructing and verifying processes of astrophysical models of general relativity in the vicinity of compact gravitating objects on the basis of general relativity. The results in the dissertation obtained in theoretical point of view can be used to build new astrophysical models in the framework of the classical standard four-dimensional and multi-dimensional gravity. They can also be useful for the analysis of the nature and dynamics of the gravitational field in the field of developing observational experiments for the detection and identification of signals coming far away from gravitational objects. Also, analysis of the results concerning the process of destroying a near-extreamal rotating black hole could be used to analyze objects so-called naked singularities by using a new generation of radiotelescope networks in the near future and to test the general relativity and other alternative theories of gravity in strong field regime.

Implementation of the research results. Based on investigations of general relativistic astrophysical processes in the vicinity of compact gravitational objects in the presence of external electromagnetic field:

isofrequency pairing of non-geodesic orbits under the gravitational field of the Schwarzschild black hole immersed in external asymptotically uniform magnetic field has been used to obtain the isofrequency pairing circular orbits of spinning particles in various gravity models presented in scientific papers of international scientific journals (Physical Review D, **92**, 024029, 2015; Physical Review D, **93**, 084012, 2016; Astronomische Nachrichten, **339**, 341, 2018). Application of these results allowed to develop fundamental theories of isofrequency pairing orbits by the effect of cosmological constant and spinning particles in other gravity models;

the obtained research results of the magnetic field that can affect the process of destroying black hole and restore the cosmic censorship in the astrophysical context have been used to develop the process of destroying black holes in various gravity models presented in scientific papers of international scientific journals (Classical and Quantum Gravity, **33**, 175002, 2016; Physical Review D, **96**, 024016, 2017; International Journal of Modern Physics A, **32,** 1750125-85**,** 2017; Classical and Quantum Gravity, **35**, 045008, 2018). Application of these results allowed to develop fundamental theories of process of destroying a black hole horizon by charged particles and test fields in other gravity models;

the obtained research results on the energy extraction through Penrose process and energetic properties of rotating black holes with gravitomagnetic charge and cosmological constant have been used to examine the results of high energies related to the observations and the results of energetic properties obtained through the numerical calculations in different gravity models presented in scientific papers of international scientific journals (Physical Review D, **89**, 024023, 2014; Physical Review D, **89**, 104048, 2014; Classical and Quantum Gravity, **31**, 195013, 2014; Physical Review D, **93**, 104031, 2016; Physical Review D, **94**, 086006, 2016; The European Physical Journal C, **76**, 104, 2016; The European Physical Journal C, **76**, 643, 2016; Physical Review D, **96**, 104050, 2017; The European Physical Journal C, **78**, 335, 2018; Physical Review D, **98**, 024022, 2018). Application of these results allowed to develop a model of the influence of various parameters of black holes on the high energy collisions for different gravity models;

theoretical research results and methods of the influence of the cosmological constant and the brane parameter on the efficiency of the ultra-high energy of the colliding particles near a rotating black hole in a Randall-Sundrum brane have been used in the frame of the program "Supporting Integration with the International Theoretical and Observational Research Network in Relativistic Astrophysics of Compact Objects" supported by the Operational Programme Education for Competitiveness funded by Structural Funds of the European Union and State Budget of the Czech Republic and registered by number CZ.1.07/2.3.00/20.0071 (2010-2014). Research results provided a possibility to explain energetic properties of the regular black hole.

Approbation of the research results. The research results were reported and discussed at 12 international and local scientific conferences.

Publication of the research results. In the field of dissertation theme, 19 scientific works were published, of which 7 scientific papers in scientific journals recommended by the Supreme Attestation Commission of the Republic of Uzbekistan for publishing basic scientific results of PhD theses, including 6 international ones.

Volume and structure of the dissertation. The dissertation consists of an introduction, four chapters, conclusion, one appendix, and bibliography. The size of the dissertation is 122 pages.

List of published papers [1, 2, 3, 4, 5, 6, 7].

1. Abdujabbarov A.A., Ahmedov B.J., Shaymatov S.R., Rakhmatov A.S. Penrose process in Kerr-Taub-NUT spacetime // Astrophysics and Space Science. - Berlin Heidelberg: Springer (Germany), 2011. - vol. 334, N 2. - pp.237-241.

2. Shaymatov S.R, Ahmedov B.J., Abdujabbarov A.A. Particle acceleration near a rotating black hole in a Randall-Sundrum brane with a cosmological constant // Physical Review D. - New York (USA), 2013. - vol. 88, N 2. - id.024016. - 12p.

3. Atamurotov F., Ahmedov B., Shaymatov S. Formation of black holes through BSW effect and black holeyblack hole collisions // Astrophysics and Space Science. - Berlin Heidelberg: Springer (Germany), 2013. - vol. 347, N 2. - pp. 277-281.

4. Shaymatov S., Atamurotov F., Ahmedov B. Isofrequency pairing of circular orbits in Schwarzschild spacetime in the presence of magnetic field // Astrophysics and Space Science. - Berlin Heidelberg: Springer (Germany), 2014. -vol. 350, N 1. - pp. 413-419.

5. Shaymatov S., Patil M., Ahmedov B., Joshi P.S. Destroying a near-extremal Kerr black hole with a charged particle: Can a test magnetic field serve as a cosmic censor? // Phys. Rev. D. - New York (USA), 2015. - vol. 91, N 6. id.064025. - 11p.

6. Shaymatov S.R., Atamuratov F.S., Hakimov A.A. Solar system effects by potentials of galaxy // Uzbek Journal of Physics. - Tashkent (Uzbekistan), 2015. - V. 17, N 2. - pp. 178-186.

7. Shaymatov S., Ahmedov B., Stuchlik Z., Abdujabbarov A., Effect of an external magnetic field on particle acceleration by a rotating black hole surrounded by quintessential energy // International Journal of Modern Physics D. - Singapore, 2018. - vol. 27, N 08. –id1850088. – 33p.

CHAPTER I. ASTROPHYSICAL AND OBSERVATIONAL PROPERTIES OF BLACK HOLES

§1.1 Introduction

In general, astrophysical black holes (stellar mass) are cosmological garbage of stars in the universe, that is, stars are born and died, but at the end of their life stage black holes are formed as a result of gravitational collapse, depending on the initial masses of collapsing stars. However, black holes are mainly classified into many groups: supermassive, intermediate-mass, stellar-mass and primordial black hole candidates. So far astronomical observations by ground and space-based telescopes have made supermassive and stellar-mass black hole candidates to be more interesting objects to the broad scientific community. Second type of objects called intermediate-mass black holes with intermediate mass being between astrophysical and supermassive black holes is likely to be occurred in the universe as well [8]; however, measuring these class of objects is not suitable for enough difficulty. It is believed that early universe after the Big Bang was so dense, thus giving rise to the formation of so-called primordial black holes. They were not a result of stellar gravitational collapse due to the fact that their mass could be much comparable as that of one solar mass. The problem was that primordial black holes could have disappeared through Hawking radiation until the present Universe. Therefore, their existence among the stars was predicted to be just one of the consequences of general relativity. A black hole itself is a simple object and exerts so strong gravitational field that nothing can come out from its pull to infinity, and it is covered by the event horizon from which any escape is impossible. In general relativity, the first exact solution was obtained by Karl Schwarzschild [9] whose solution totally characterizes a black hole. The discovery of neutron stars, quasars and other active galactic nuclei (AGN) in the late 1960s gave rise to interest in pointing all out to the physics of collapsed gravitational objects because black holes had been regarded as just prediction of general relativity. It then began expecting that stellar mass black holes with a mass about $3-100\ M_{\odot}$

of sun would be formed once massive stars collapse at the end process of their life. Meanwhile it is expected that supermassive black holes with millions of solar masses $M_\odot$ would form differently, absorbing other nearby stars and joining with other black holes. Moreover, it is worth noting that white dwarfs can be also formed after gravitational collapse of stars provided that a remaining mass is less than 1.4 $M_\odot$ solar mass (Chandrasekhar limit). With the help of modern observations, type Ia supernovae are expected to be white dwarfs as standard candles in the night sky and very useful to help us estimate distances. They would appear in binary stars, pulling mass from its pair. Also, their location gives out some indirect signs.

Recently, a group of German astronomers from the Institute for Extraterrestrial Physics Society of Max Planck, England astronomers from the Institute of Astronomy, Cambridge University, astronomers from the United States from California Institute of Technology, and European astronomers, etc. shown the data of 10 years of observations of the stars concentrated in the center of our Galaxy. As a result, it was possible to show that in the Galactic Center there is a single super-dense and supermassive object as a black hole with a mass of four million solar masses. In the past decade, astronomers have already been assured that the presence of supermassive black holes (SMBH) in the centers of galaxies is an integral part of the structure of stellar systems. The presence of a cluster of massive objects (or one supermassive object) in the center of the Galaxy has long been unchallenged. Now it is generally believed that galaxies with AGN and subsequently also those with non-active nuclei are suspected of hosting a supermassive black hole with mass of order $M \approx 10^6 - 10^9 M_\odot$ in their centers, such as M87 AGN of $\approx 10^9 M_\odot$ or Sagittarius A^*, non-active nucleus of our Galaxy with $M \approx 4.4 \times 10^6 M_\odot$ [10].

Sources emitting radio waves with highly redshifted have been discovered by Astronomers [11], which is very distant from us $(\approx 0.3 - 3)\, Gpc$ as stated by Hubble's law. Based on the observed visual magnitude of these objects, called quasars, their huge power output is nearly 100 times greater than the total luminosity of average galaxy ($L_{quasar} \approx 10^{42} - 10^{47}\ erg/s$). Quasars also appeared to emit significantly in $X-ray$ and even in gamma part of the spectrum. Apart from quasars, there are also new objects, called blazars or radio galaxies (RGs) and Seyfert galaxies, in the universe. They are all classified by their spectrum and luminosity coming from a small volume ($\approx 10^{-6}\, pc^3$). Since no consistent way appears to explain the mechanism of those energy sources, compact objects and the black holes exerting strong gravitational fields were considered as candidates for such energy sources. In this sense, the rotating black holes like Kerr black hole appear to be an appropriate model so as to get more information about the properties of AGN. The matter accreted from its vicinity would form an accretion disk becoming heated by accretion process and then emits radiation of various types, depending on temperature and many other properties of accretion disk. In the accretion process, approximately 40 % of rest mass of the accreted matter can be transformed into radiation which is significantly large as compared to the case of thermonuclear synthesis of helium (≈ 7% of the rest mass) [12]. So-called BSW (Banados, Silk and West) effect and the well known Penrose processes were theoretically proposed to explain recent astronomical observations regarding energetic processes around black holes. These effects attracted strong attention in recent years. In the dissertation, energetic processes of black holes are investigated in detail.

Nowadays, much progress has been made in observational studies of stellar mass black holes in $X-ray$ binaries and supermassive black holes through modern x-ray, VLBI, and $\gamma-ray$ telescopes. Also, the detection of gravitational waves (GWs) from GW150914, GW151226 and GW170104 [13, 14] verifies the observational progress. This pre-eminent direct detection of GWs was significant result for general relativity and a great victory of observational astronomy as a new method. The discovery of GWs from merging two black holes has opened a qualitatively new stage of observational astronomy. However, developing new mechanisms explaining gravitational radiation energy has been the most important issues of modern astrophysics in getting more information about the properties of black holes and providing the proof to the relevant observations. In addition, Very Long Baseline

Interferometry (VLBI) on short wavelengths ($\lambda \lesssim 1{:}3mm$) of the Event Horizon Telescope (EHT) with an angular resolution of better than 10^{-5} seconds is being realized [15, 16, 17, 18]. To test the presence of black holes, EHT were first proposed to obtain real images of event horizon by observing the center of our galaxy Sagittarius A^* and the center of M87 galaxy. Also, the idea of cosmic censorship hypothesis proposed by Penrose strongly supports the presence of black holes, concealing singularity from observers outside [19]. Testing the presence of black holes with infalling test particles or fields have recently become the object of active scientific research despite the fact that it has remained unproven yet. Moreover, EHT will also claim the presence of black holes in the near future. Thus, taking into account all facts mentioned above, the existence of black holes is now becoming realistic.

A high energy neutrino with$\sim 290\ TeV$ has been very recently detected by Ice-Cube Neutrino Observatory on 22 September 2017 [20, 21, 22]. This event was first announced by NSF (The National Science Foundation) on 12 July 2018. It was a great discovery in observation of the location from where the high energy neutrino was produced. Its location was identified that a gamma-ray flare is coming from the blazar TXS 0506+056 with power $\sim 10^{45-46} erg/s$. The high energy neutrino event, IceCube-170922A (YY/MM/DD), claims that blazars are recognizable and candidate sources for the high-energy neutrino flux. However, observations emphasize that blazars can be characterized in various energetic range in high energy gamma-rays and variable sources. Neutrino observation shows that blazars can be regarded sources for high energy neutrino. In conclusion, it is expected that blazars emitting gamma-rays are likely to be source of the observed astrophysical neutrinos as stated by neutrino emission. On the other hand, blazars are also supermassive black hole candidates because of its active galactic nucleus with relativistic jets accelerating cosmic rays to the energies in the order of several PeV and traveling toward the Earth. These observations show that SMBHs could only produce such high energy astrophysical neutrinos as well.

In Sec. 1.2 we briefly give information about supermassive black holes and demonstrate their candidates in detail. In Sec. 1.3, we describe stellar-mass black holes and give information regarding their candidates in detail. We conclude our results in the Sec. 1.4.

§1.2 Supermassive black hole candidates

Current modern astronomical observations have confirmed a number of black hole candidates [23]. It is expected that each active galactic nucleus consists of supermassive black hole. SMBHs with a mass of a million solar masses can be found only in the center of galaxies. Thus, galaxies with AGN and with non-active nuclei are believed in hosting a supermassive black hole with mass of order $M \approx 10^6 - 10^6\, M_\odot$ in their centers. For instance: M87 is referred to as AGN, which also has the accretion disc surrounding around it. The accretion disk produces large amount of energies in the spectra. This is the main property of AGN as compared to the inactive galaxies which are supposed to not have an accretion disc around it. Sagittarius A* is type of non-active nucleus of our Galaxy [10]. Supermassive Black hole physics has been investigated for over the last quarter century despite the fact that their origin has remained an open field of research. However, several hypotheses are available for the formation mechanisms of supermassive black holes. The existence of other galaxies like our galaxy Sagittarius A* in the universe was discovered only in the mid-20th century. By that time almost all scientists had assumed that the universe consisted of stars only that continuously distributed through the universe. With this motivation, black hole physics has been also developed since the discovery of such different type of galaxies. Black hole candidates are expected to be rotating black holes in astrophysics in general relativity. There is only way, according to which one can test black hole candidates by studying analysis of electromagnetic radiation emitted by various type of materials forming accretion disk and orbiting around such objects.

The following observational objects being candidates for black holes IRAS

13224-3809, Mrk 110, 1H 0707-495, RBS 1124, Swift J0501.9-3239, Ark 564, Ton S180, 1H 0419-577, Mrk 509, 3C 382, Mrk 359, Mrk 1018, Mrk 1018, and Fairall 9 were reported and given the detailed information for all required parameters in Refs. [24, 25, 26]. Observations of AGN like a nearby Seyfert 1: Fairall 9, MCG-6-30-15, NGC 3516, 3783 and 4051 were analyzed in detail and presented [27]. Relativistic Fe K line emission observed in the spectrum of NGC 3516 and relativistic Fe Ka emission along with energy 6.4 keV for Fairall 9, MCG-6-30-15 and NGC 3783 with spin calculation $a = 0.67^{+0.10}_{-0.11}$ and $a = 0.49^{+0.20}_{-0.12}$ were accurately demonstrated in the following Ref.s [24, 27, 28]. The Seyfert 1.2 galaxy MCG -06-30-15 was presented in [39] on the basis of broad iron line observations. The detailed analysis of the $X-ray$ with energy 2-10 keV for Seyfert galaxy NGC 1365 through the XMM-Newton observation and analysis of $X-ray$ observations of NGC 1365 through 10-30 keV were presented in Ref.s [30, 31]. Seyfert 1 galaxy 1H0707-495 through a long XMM-Newton observation of the narrow-line with energy 7 keV [32] and the Seyfert 2 Galaxy IRAS 00521-7054 [33] were presented and investigated in detail. Also the following black hole candidates registered by 3C 120 and Mrk 79 were presented in detail in [34, 35, 36].

Table 1.1

The latest Supermassive black bole candidates registered as a result of iron line measurements. These black hole candidates are regarded as rotating black holes under the assumption that almost all black holes are rotating astrophysical black holes in general relativity [24, 25] (for detailed information).

SMBH Candidates (AGN)	a_* (iron)	L_{Bol} / L_{Edd}
IRAS 13224-3809	> 0.995	0.71
NGC 4051	> 0.99	0.03
MrK110	> 0.99	0.16 ± 0.04
MCG-6-30-15	> 0.98	0.40 ± 0.13
1H 0707-495	> 0.98	~ 1

NGC 3783	> 0.98	0.06 ± 0.01
RBS 1124	> 0.98	0.98 ± 0.15
NGC 1365	$0.97^{+0.01}_{-0.04}$	$0.06^{+0.06}_{-0.04}$
Swift J0501.9-3239	> 0.96	–
Ark 564	$0.96^{+0.01}_{-0.06}$	> 0.11
3C 120	> 0.95	0.31 ± 0.20
Ark 120	0.94 ± 0.01	0.04 ± 0.01
Ton S180	$0.91^{+0.02}_{-0.09}$	$2.1^{+3.2}_{-1.6}$
1H 0419-577	> 0.88	1.3 ± 0.4
Mrk 509	$0.86^{+0.02}_{-0.01}$	–
IRAS 00521-7054	> 0.84	–
3C 382	$0.75^{+0.07}_{-0.04}$	–
Mrk 335	$0.70^{+0.12}_{-0.01}$	0.25 ± 0.07
Mrk 79	0.7 ± 0.1	0.05 ± 0.01
Mrk 359	$0.7^{+0.3}_{-0.5}$	0.25
NGC 7469	0.69 ± 0.09	–
Swift J2127.4+5654	0.6 ± 0.2	0.18 ± 0.03
Mrk 1018	$0.6^{+0.4}_{-0.7}$	0.01
Mrk 841	> 0.56	0.44
Fairall 9	$0.52^{+0.19}_{-0.15}$	0.05 ± 0.01

§1.3 Stellar mass black hole candidates

As a result of Einstein's general theory of relativity stellar mass black holes are formed due to the gravitational collapse of stars when they run out of their fuel, thus being not possible to sustain its own gravity. In black hole astrophysics, as was mentioned above one can call stellar-mass black hole candidates in the case in which their masses should be in the range [3-100] $\boldsymbol{M}_{\odot}$. In this respect an accurate mass of such candidates is very essential for measuring them. Typically, the masses of stellar mass black hole candidates can be determined by the properties of companion star's orbital and radiative properties. In many cases almost all known stellar-mass black hole candidates are one of the object of binary system and in a class of $\boldsymbol{x-ray}$ binaries. Thus, stellar mass black holes candidates can be detected in binary stellar systems by $\boldsymbol{X-ray}$ radiation, caused by the absorption of the matter of the companion star. Spectral states of stellar mass and supermassive black hole candidates differs from each other due to the fact that their masses, environments and radiation mechanisms in the accretion disk as well are totally different. Spectral state of stellar-mass black hole candidates can be changed in a couple of weeks or months, whereas spectral states for supermassive BH candidates are long lived [37]. This is because SMBH candidates are observed in its usual spectral state. Note that it is very important task in modern astrophysics to have relevant correct models in order to explain some spectral behaviors and their physical interpretations. However, there are many models which are being used recently: among them continuum-fitting (CF) and iron line methods have been applied in measuring black hole candidates.

Stellar-mass black hole candidates are tabulated in Table 1.2 for various methods being referred to as continuum-fitting and iron line measurements, see [24, 38] for more details. This enables us to distinguish which one is more accurate in determining black hole spin. However, both of them are currently realistic methods for observers analyzing spectral states and revealing physical interpretation of observing objects. From Table 1.2, one may deduce the accuracy of the results obtained by iron line method is a bit comparable as that of CF method.

Table 1.2

The latest Stellar-mass black hole candidates registered as a result of the iron line and continuum-fitting measurements. These black hole candidates are also regarded as rotating ones.

Stellar-mass BH Candidates	a_* (CF)	a_* (iron)
GRS 1915-105	> 0.98	0.98 ± 0.01
Cyg X-1	> 0.98	$0.97^{+0.014}_{-0.02}$
LMC X-1	0.92 ± 0.06	$0.97^{+0.02}_{-0.25}$
GX 339-4	< 0.9	$0.95^{+0.03}_{-0.05}$
MAXI J1836-194	–	0.88 ± 0.03
M33 X-7	0.84 ± 0.05	–
4U 1543-47	0.80 ± 0.10	–
Swift J1753.5	–	$0.76^{+0.11}_{-0.15}$
XTE J1650-500	–	$0.84 \sim 0.98$
IC 10 X-1	$\gtrsim 0.7$	–
GRO J1655-40	0.70 ± 0.10	> 0.9
GS 1124-683	$0.63^{+0.16}_{-0.19}$	–
XTE J1752-223	–	1.52 ± 0.11
XTE J1652-453	–	< 0.5
XTE J1550-564	0.34 ± 0.28	$0.55^{+0.15}_{-0.22}$
LMC X-3	0.25 ± 0.15	–
H1743-322	0.2 ± 0.3	–
A0620-00	0.12 ± 0.19	–
XMMU J004243.6	< -0.2	–

The binary X-ray source GRS 1915-105 was analyzed in detail as stated by a spectral analysis of the X-ray, and it was shown that this source is a rapidly rotating black hole [39]. The following sources are stellar mass black hole candidates: the X-ray binary Cygnus X-1 was the first black hole, which was established through dynamical observations [40]; Cygnus X-1 and LMC X-1 were also reported in Refs. [41, 42] for along with its spin parameter $\boldsymbol{a} > \mathbf{0.95}$; the source A0620-00 was reported in detail [43], according to which it was shown that A0620-00 has the low spin due to its disk. Using the models for disc emission GX 339-4 was analyzed and reported in [44]. Decisions for confirmation of two sources 4U 1543-47 and GRO J1655-40 were made on the basis of the X-ray spectral data in the thermal-dominant, and their spin parameters were also estimated with high accuracy [45]. The following sources IC 10 X-1, XTE J1550-564, LMC X-3, and H1743-322 were presented in detail Refs. [42, 46 - 48]. Recently Xray binary MAXI J1836-194 were discovered and reported that its spectral state corresponds to the intermediate spectral state with broadened iron emission line [49]. Newly discovered sources registered by Swift J1753.5 and XTE J1752-223 were presented in Refs. [50, 51]. By comparing the stellar mass black hole binary XTE J1650-500 with AGN MCG-6-30-15 [29], the same emission properties at the spectral energy 4-7 keV were obtained and such properties were regularly observed in both sources [52]. A broad and strong Fe Ka emission line were observed in the XMM-Newton spectrum of the black hole candidate XTE J1652-453 and it was presented in [53] for more detailed information.

§1.4 Conclusion

The presence of black holes has been just considered a generic prediction of general relativity till the detection of gravitational waves (GWs) [13, 14]. However, the detection of GWs not only verifies the prediction of Einestein but also verifies the presence of black holes in the universe. Thus, the presence of black holes in astrophysics is now becoming more realistic due to the first observation of GWs from signal by GW150914 as a consequence of two solar mass black hole mergers about a couple of billion light-years away and recent modern astronomical observations. On the other hand, a huge scientific attention is nowadays focused on investigation of properties of black holes through gravitational radiation, dynamics of binary systems, and energetic processes around black holes. In recent years, the best observation methods have been developed year by year. In this respect various class of black hole candidates have been detected and analyzed, and at the end their catalogues have been listed for supermassive and stellar-mass black hole candidates. However, two black hole candidates, M87 and Sagitarius A*, has been considered as more interesting objects to reveal the mysteries of black holes. This is because that Sagitarius A* is located at the near distance and M87 has big size as that of other nearby galaxies. This is the reason almost all scientific projects in the world regarding the black hole problems have been given to scientific groups working on the physical properties of M87 and Sagitarius A* in order to answer to open questions of black hole properties. Nowadays these two objects become the object of active scientific research as a main source of black hole candidate. In addition, direct observational evidence of black hole candidates and their analysis have shown that all black holes are rapidly rotating black hole candidates and even rotating ones in the nature. In conclusion, there is, however, still an unanswered question in the black hole astrophysics. In the near future, these hidden properties of black holes could be probed by analyzing gravitational waves and observation data of observed objects being candidates for black holes.

CHAPTER II. THE MOTION OF PARTICLES IN THE BOUND GEODESIC AND NON-GEODESIC ORBITS AROUND COMPACT GRAVITATING OBJECTS IMMERSED IN AN EXTERNAL MAGNETIC FIELD

§ 2.1 Introduction

The motion of test particles in the gravitational field of rotating and non-rotating black holes has been investigated for a long time. Much of these investigations concentrated to understand the properties of binary systems or radiative inspirals as sources of gravitational waves for future possible signals through astrophysical observations. With this motivation, Warburton, Barack and Sago [54, 55] also studied the isofrequency pairing of geodesic orbits in Schwarzschild and Kerr geometry, and they described the region in the parameter space where such orbits occur and also provide an intuitive explanation as to why isofrequency pairing must occur. In this section, we also extended recent research [54] concerning isofrequency pairing of circular orbits to the case when the Schwarzschild black hole is embedded in magnetic field. We then investigated the motion of the particles and the effect of the magnetic field on the isofrequency pairing of circular orbits in the background of Schwarzschild black hole embedded in external, uniform, axisymmetric magnetic field. Based on theoretical approaches and observational data one may expect the presence of magnetic field around black holes [56].

The motion of charged particle around a Schwarzschild black hole immersed in an external asymptotically uniform magnetic field was explored both analytically and numerically for the first time in [57]. An extensive analysis of the motion of charged particles in the magnetic field surrounding gravitational objects can be found in [3, 4,56, 58- 71]. Off-equatorial motion of charged particles in background gravitational and electromagnetic fields has been studied in [72, 73]. Observational evidences of the existence of magnetic field around black holes can be found in [74, 75]. Recently, we have noticed that there is the new paper analyzing the observation of the twin-jet system of NGC 1052 at 86 GHz with the Global mm-VLBI Array, deriving the magnetic field that would be between 200G and 8.3 x 10^4G at 1 Schwarzschild radius [76]. This is in agreement with the strength of the magnetic field B for supermassive black holes. It has been shown by Ref. [77] that the strength of the magnetic field can be calculated to be Bi ~ 10^4G and B_2 ~ 10^8G for the supermassive and stellar mass black holes, respectively. The estimation of the strength of the magnetic field was also constructed recently in [78, 79]. The self-magnetic field generated by the string loop around a black hole was studied in Ref. [80, 81].

In general relativity gravitational collapse should decay with t^{-1} [82, 83]. Consequently, black hole does not have own magnetic field. However, a magnetic field near a black hole can arise due to external factors, such as the presence of a nearby magnetars or neutron stars [58, 59, 84]. The gravitational energy is comparable with electromagnet energy when the strength of magnetic field surrounding black hole with mass M is of order B_M ~ 10^{19} $\frac{M}{M_{\odot}}$G. In reality the magnetic field surrounding black holes is much smaller than the value of B_M [56]. It is clear that with this value B_M of the magnetic field the space-time geometry near a black hole will be significantly distorted [85, 86], however, when B << B_M there is definitely a region near the black hole where the space-time is not distorted by the external magnetic field and the latter can be considered as a perturbation. In what follows we assume that magnetic field is weak B << B_M and its energy-momentum does not modify the background black hole geometry, being considered as a test field in the given gravitational background.

As it is mentioned in [54] eccentric geodesics of the Schwarzschild geometry are characterized by two frequencies: an azimuthal frequency Ω^{φ} and a radial frequency $\Omega^{\hat{r}}$, associated with the periodic motions in the Schwarzschild coordinates p and r, respectively. Unlike in the analogous Keplerian problem where $\Omega^{\varphi} = \Omega^{\hat{r}}$, here one always finds $\Omega^{\varphi} > \Omega^{\hat{r}}$, giving rise to what we interpret as periastron advance.

Based on the Boyer-Lindquist time frequencies introduced in [87, 88], Warbur- ton et. al. [54] described orbits in several special cases in the following way: The equatorial orbits (θ = n/2) become biperiodic with frequencies $\Omega^{\hat{r}}$ and Ω^{φ}, where T^{r} = 2n/$\Omega^{\hat{r}}$ is a radial period. $\Omega^{\hat{r}}$ becomes meaningless when the orbits of the particles are circular ($r_p = r_a$) and become periodic with frequency Ω^{φ} . Consequently, particles orbiting around the gravitational object at the equatorial plane can have the two frequencies $\Omega^{\hat{r}}$ and Ω^{φ} simultaneously in the Boyer-Lindquist coordinate system.

There may exist infinite number of pairs of circular orbits of particles in a particular area of a gravitational object where pairs of orbits having different quantities of energy and angular momentum can possess similar values of frequencies Ω^{φ} and $\Omega^{\hat{r}}$, in this sense such orbits are referred as "isofrequency" circular orbits [54]. Consequently they could be synchronized in phase where pairs of the isofrequency circular orbits passing their periastra at one time and with similar azimuthal phase $\Delta\boldsymbol{\varphi}$ are referred as "synchronous" [54]. The main aim of this chapter is to study the effect of the asymptotically uniform magnetic field surrounding a Schwarzschild black hole on the isofrequency pairing of non-geodesic orbits.

Cosmological observations of supernova explosions confirm an accelerating rate of expansion of our universe at present, commonly explained by a dark energy endowed with repulsive gravitational effect. Usually, the dark energy is related to the vacuum energy associated with the cosmological-constant term $\Lambda g_{\alpha\beta}$ in the standard Einstein equations. The cosmological observations suggest the value of the cosmological constant to be $\Lambda \sim 10^{-52}m^{-2}$ [89, 90]. There are many works revealing the significant role of the cosmological constant in wide range of astrophysical phenomena [91- 109]. The quintessential scalar fields were suggested instead of the cosmological constant A as an alternative form of the dark energy, serving as an explanation of the accelerating rate of the present expansion of the universe [89, 110, 111]. The spherically symmetric black hole solution surrounded by a dynamical quintessential field, characterized by the equation of state p = $u_q p$ with the quintessence parameter $u_q \in$ (-1; -1/3) and the field intensity parameter c, was introduced in [112]. A quintessential rotating black hole solution was constructed in [113].

Contrary to the standard general relativistic vacuum black-hole solutions that are Ricci flat ($R_{\alpha\beta} = 0$), both the cosmological-constant (de-Sitter) and quintessential black hole spacetimes are not Ricci flat ($R_{\alpha\beta} \neq 0$), due to the presence of a non-zero vacuum-energy or quintessential-energy density. In both de-Sitter and quintessential black holes the geometry is not asymptotically flat. Contrary to black hole spacetimes with the cosmological constant (vacuum energy) term where the energy density radial profile remains constant, in the quintessential black hole spacetimes the quintessential energy density is modified by the black hole space-time, being thus radius dependent [112, 113]. The non-zero Ricci tensor then influences substantially behaviour of the external magnetic fields surrounding the black holes. Therefore, it is essential to investigate in detail the repulsive role of the quintessential field in the astrophysical processes in the vicinity of black holes associated with an external magnetic field.

In Sec. 2.2 we consider (biperiodic) synchronous orbits in Schwarzschild geometry in the presence of the magnetic field and describe the region in the parameter space where such orbits occur. We study the contribution of the magnetic field on the isofrequency pairing of non-geodesic orbits. In Sec. 2.3, we consider the charged particle motion in an uniform magnetic field around the quintessential rotating black hole and calculate trajectory of charged particles due to effect of magnetic field that is assumed to have its intensity parallel to the black hole axis. We obtain the effective potential for charged test particle with a specific angular momentum and energy as a function of the external magnetic quintessential field parameters. Finally, Sec. 2.4 summarizes our main results.

§2.2 Influence of magnetic field on isofrequency orbits around Schwarzs-child black hole

§2.2.1 The non-geodesic equations of motion

We consider a charged particle with the rest mass m and charge q in the vicinity of the Schwarzschild black hole of mass M immersed in external asymptotically uniform magnetic field. Presence of the magnetic field in the Schwarzschild spacetime metric in spherical coordinates reads

$$ds^2 = -f(r)dt^2 + f^{-1}(r)dr^2 + r^2(d\theta^2 + \sin^2 d\varphi^2) , \qquad (2.1)$$

where the metric function

$$f(r) = 1 - \frac{2M}{r} \qquad (2.2)$$

is expressed through the total mass M of the black hole.

The covariant components of the 4-vector potential of the electromag-netic field around the Schwarzschild space-time will take the form

$$A_t = A_r = A_\theta = 0, \quad A_\varphi = \frac{B}{2} r^2 \sin^2\theta. \qquad (2.3)$$

Next, the non-geodesic equations of charged test particles in the quatorial plane $\theta = \pi/2$ of a Schwarzschild black hole immersed in external asymptotically uniform magnetic field are described as follows

$$\begin{aligned} \dot{t} &= \frac{\mathcal{E}}{f(r)} , \quad \dot{\varphi} = \frac{\mathcal{L}}{r^2} + \beta , \\ \dot{r}^2 &= \mathcal{E}^2 - V_{eff} , \end{aligned} \qquad (2.4)$$

where a dot denotes differentiation with respect to the proper-time τ and the effective potential for the radial motion of charged test particles has the following form

$$V_{eff}(r; \mathcal{L}) = \left(1 - \frac{2M}{r}\right)\left[1 + r^2\left(\frac{\mathcal{L}}{r^2} + \beta\right)^2\right] . \qquad (2.5)$$

Here let us represent

$$\mathcal{E} = \frac{E}{m} , \quad \mathcal{L} = \frac{L}{m} , \quad \beta = \frac{qB}{2m} , \qquad (2.6)$$

where $\mathcal{E}$ and $\mathcal{L}$ are constants of the motion corresponding to the particle's specific energy and angular momentum, respectively. Bound orbits exist for

$$\sqrt{6}/3\left[1+4M^2\left(\beta+\left(\beta^2+1/12M^2\right)^{1/2}\right)^2\right]^{1/2}<\mathcal{E}<1\ ,$$

with

$$\mathcal{L}>12M^2\left(\beta+\left(\beta^2+1/12M^2\right)^{1/2}\right)\ . \tag{2.7}$$

The motion of particles around the gravitational object takes place between the turning points such as the periastron r_p and the apastron r_a in the limit of each specific energy and angular momentum represented in Eq. (2.7). The pair of values $\{r_a, r_p\}$ can be expressed as

$$r_a=\frac{p_\beta M}{1-e},\qquad r_p=\frac{p_\beta M}{1+e}. \tag{2.8}$$

As implied by Eq. (2.8), *semi-latus rectum* p_β represented in Table 2.1 measures the size of the orbit, while *eccentricity* e measures its degree of noncircularity [114]. The relationship between $\{p, e\}$ and $\{\mathcal{E},\mathcal{L}\}$ can be obtained from the two conditions $V_{eff}(r_p) = V_{eff}(r_a) = \mathcal{E}^2$. Explicitly,

$$\begin{aligned}\mathcal{E} &= \frac{1}{p^{1/2}\left(p-3-e^2\right)}\Bigg[(p-2)\left(p-3-e^2\right)^2\\ &+ p^2M^2\left(\beta+\left(\beta^2+\frac{p-3-e^2}{p^2M^2}\right)^{1/2}\right)^2\left(p-2+e^2(p-6)\right)\Bigg]^{1/2},\\ \mathcal{L} &= \frac{p^2M^2}{p-3-e^2}\left[\beta+\left(\beta^2+\frac{p-3-e^2}{p^2M^2}\right)^{1/2}\right].\end{aligned} \tag{2.9}$$

§ 2.2.2 Influence of magnetic field on orbital frequencies and separatrix

We consider orbital frequencies in the presence of the magnetic field via the non-geodesic equations of motion. Non-geodesic elliptical bound orbits can be formed when the eccentricity takes the range $0 \leq e < 1$ with the boundary $P_\beta \geq p_s(e) = 6 + 2e$, being referred to as the *separatrix* confining bound orbits, in the vicinity of gravitational massive object [115]. On the other hand the separatrix curve describes the innermost stable circular orbit (ISCO). The presence of a separatrix in black hole spacetimes represents a main difference from the Newtonian dynamics. It was shown by Warburton et al. [54], the presence of a separatrix gives rise to an increase in number of the isofrequency orbits.

Following to [115], the integration of the non-geodesic equations for the *t(r)* and *φ(r)* is introduced as follows

$$t(r) = \mathcal{E} \int \frac{dr}{f(\mathcal{E}^2 - V_{eff})^{1/2}}, \tag{2.10}$$

and

$$\varphi(r) = \mathcal{L} \int \frac{dr}{r^2(\mathcal{E}^2 - V_{eff})^{1/2}} + \beta \int \frac{dr}{(\mathcal{E}^2 - V_{eff})^{1/2}} \,. \tag{2.11}$$

Substituting the form $r(x) = Mp/(1 + e \cos x)$ into Eq. (2.7), and using (2.9), (2.10) and (2.11) one can obtain the following equations with the parameter x, which is related to t and φ as

$$\begin{aligned} \frac{dt}{d\chi} &= \frac{p\big(p-6-2e\cos\chi\big)^{-1/2}}{b\big(p-2-2e\cos\chi\big)\big(1+e\cos\chi\big)^2}\Big[(p-2)(p-3-e^2)^2 \\ &\quad +p^2M^2b^2\big(p-2+e^2(p-6)\big)\Big]^{1/2}, \end{aligned} \tag{2.12}$$

$$\frac{d\varphi}{d\chi} = \left(1 + \frac{\beta\big(p-3-e^2\big)}{b\big(1+e\cos\chi\big)^2}\right)\frac{p^{1/2}}{\big(p-6-2e\cos\chi\big)^{1/2}}, \tag{2.13}$$

where parameter b is defined as follows

$$b = \beta + \left(\beta^2 + \frac{p-3-e^2}{p^2M^2}\right)^{1/2}.$$

From above expressions the radial period and radial frequency can then be described

[54, 115] as

$$T^{\hat{r}} = \int_0^{2\pi} \frac{dt}{d\chi} d\chi \,, \qquad \Omega^{\hat{r}} = \frac{2\pi}{T^{\hat{r}}} \,. \tag{2.14}$$

The frequency of the orbit will take the form

$$\Omega^{\hat{\varphi}} = \frac{1}{T^{\hat{r}}} \int_0^{T^{\hat{r}}} \frac{d\varphi}{dt} dt = \frac{\Delta\varphi}{T^{\hat{r}}} \,, \tag{2.15}$$

where azimuthal phase $\Delta\varphi$ is computed as

$$\begin{aligned} \Delta\varphi &= \int_0^{2\pi} \frac{d\varphi}{d\chi} d\chi == \int_0^{2\pi} \left(1 + \frac{\beta(p-3-e^2)}{b(1+e\cos\chi)^2}\right) \frac{p^{1/2}}{(p-6-2e\cos\chi)^{1/2}} d\chi \\ &= \left(\frac{2p}{e}\right)^{1/2} \left(1 - \frac{\beta(p-3-e^2)(p-6-2e)^{1/2}}{b(p-4)(e+1)e^{1/2}}\right) \left[K\left(-\frac{4e}{\epsilon}\right) + \dots\right] , \end{aligned} \tag{2.16}$$

where $e = p_\beta - p_s(e) = p_\beta - 6 - 2e$ is the small parameter and $K(x) = \int_0^{\pi/2} d\theta (1 - x \sin^2\theta)^{-1/2}$.

§ 2.2.3 Isofrequency orbits in the presence of magnetic field

The purpose of this subsection is devoted to the study of the isofrequency and bound orbits of the Schwarzschild spacetime in the presence of the magnetic field. In order to estimate the divergent quantities of the azimuthal phase and the radial period and their ratio in Eq. (2.15) we consider orbits lying extremely close to the separatrix *e*. Considering the near-separatrix analytic expansions we derive corresponding expressions for T^r, $\Delta\varphi$ [54, 115]

$$\begin{aligned} \Delta\varphi &\approx \left(\frac{2p}{e}\right)^{1/2} \left(1 - \frac{\beta(p-3-e^2)(p-6-2e)^{1/2}}{b(p-4)(e+1)e^{1/2}}\right) \\ &\quad \times \left[1 + \mathcal{O}\left(\frac{\epsilon}{4e}\right)\right] \ln\left(\frac{64e}{\epsilon}\right) , \end{aligned} \tag{2.17}$$

$$
\begin{aligned}
T^{\hat{r}} \;\approx\; & \frac{4(3+e)^2}{pb}\Bigg[\frac{(p-2)(p-3-e^2)^2}{e(1+e)^3(p-2-2e)(p-2+2e)} \\
& + \frac{p^2M^2b^2(p-2-e^2(p-6))}{e(1+e)^3(p-2-2e)(p-2+2e)}\Bigg]^{1/2} \\
& \times \left[\ln\left(\frac{64e}{\epsilon}\right) + eI(e) + \frac{\pi e(9+6e-7e^2)}{4(1-e^2)^{3/2}} + \mathcal{O}\left(\frac{\epsilon}{4e}\ln\frac{4e}{\epsilon}\right)\right]
\end{aligned} \tag{2.18}
$$

Here, we denote the parameter

$b = \beta + \ \beta^2 + (p - 3 - e^2)/p^2M^2)^{1/2}$ again, and the integral

$I(e) = \int_0^{\pi} d\chi(1 + e\cos\chi)^{-2} D(\cos\chi)$ being finite for any e, with

$$
\begin{aligned}
D(\cos\chi) \;=\; & \frac{3+2e-e^2\cos^2\chi}{2+e(1-\cos\chi)}\Big[2(1-\cos\chi)\Big]^{1/2} \\
& - \; 3+e-\frac{1}{4}\Big(7e-3\Big)\Big(1+\cos\chi\Big)\,,
\end{aligned} \tag{2.19}
$$

can be easily calculated numerically.

Using Eq. (2.15) with Eqs. (2.17) and (2.18) we make the relevant numerical calculations and plot the *separatrix* $e = e_s(\Omega^\varphi, \beta)$ as shown in Fig. 2.1 in the (Ω^φ, e) plane. Following from observations we describe the region in the parameter space where isofrequency pairing of non-geodesic orbits occurs. In Fig. 2.1 we have shown the effect of the magnetic field on the parameter space (e, Ω^φ) for bound non-geodesic orbits around Schwarzschild black hole embedded in external asymptotically uniform magnetic field.

We delineate the *separatrix* $e = e_s(\Omega^\varphi, \beta)$ represented as solid lines in Fig. 2.1 when the parameter $\Omega^r = 0$. We study the influence of the magnetic field on the *separatrix* being referred to as boundary. The existence of the *separatrix* gives rise to occurrence isofrequency pairing of circular orbits. From Fig. 2.1, one can easily see that the presence of the magnetic field causes the *seperatrix* line to modify surrounding of the object, in which an increase in magnetic field forces *seperatrix* to shift outward the central object.

Using the relevant numerical calculations shown in Table 2.2 we describe the dot-dashed line. Since the Jacobian matrix of the transformation [Eq. (2.20)] is singular, the isofrequency orbits are available inside and outside of the singular curve. Namely, it is essential to consider the singular curve in the particular area of the massive gravitational object because a pair of isofrequency orbits occur between the separatrix and singular curve as well as between the singular curve and *circular-orbit duals* (COD) in the range (r_{isco},r_b) [54]. From Fig. 2.1 one can see that the shape of the singular curve shifts upward due to the influence of the magnetic field, in turn, the value of the frequency Q becomes smaller with the certain radius r_b of a circular orbit in the limit $e \to 0$. More detailed analysis of radius r_b is shown in Table 2.1.

We will concentrate on the dashed lines and give a more detailed analysis to it which represent circular orbit duals (COD) introduced in [54]. The COD also plays important role as a boundary region keeping pairs of isofrequency orbits to be existed in a particular area of gravitational object. The trajectory of all nongeodesic circular orbits of radius r is defined in the range $r_{isco} = 6M + \delta r_{isco}(\beta) < r < r_b + \delta r_b(\beta)$ with nonvanishing magnetic field in the Schwarzschild spacetime, where $\delta r_{isco}(\beta)$ and $\delta r_b(\beta)$ are delineating the contribution of the magnetic field. However, the COD is in the $r_{isco} = 6M < r < r_b$ range with vanishing magnetic field, where r_b is radius of the circular orbit at the limit $e \to 0$. This phenomenon explains the behavior of the COD in the presence of magnetic field in Table 2.1.

Based on the above discussions the occurrence of isofrequency pairing is more related to the presence of boundary regions such as *separatrix* and COD. Each and every circular orbit in the range $\xi = r_b - r_{isco}$ is becoming smaller with increasing the magnetic field. Consequently we conclude that the region between the *separatrix* and the *circular-orbit duals* (COD), where all isofrequency pairs are confined and every orbit has an isofrequency dual, becomes smaller due to the effect of the magnetic field.

According to [54], isofrequency orbits Ω^{φ} are estimated using Taylor expansion at point b and then the Jacobian determinant $J = |\partial(\Omega^r, \Omega^\varphi)/\partial(p, e)|$ in the limit $e \to 0$ with $p = r_b/M$ will take the form

$$J(e \to 0) = \frac{9\left(p^3 - 18p^2 + 102p - 176\right)\left(p - \beta\sqrt{p-3}\right)}{2M^2 p^{11/2}(p-2)(p-6)^{3/2}} - \frac{3\left(2p^3 - 32p^2 + 165p - 266\right)}{4M^2 p^{11/2}(p-2)(p-6)^{3/2}} \times \left(3p - \beta(\sqrt{p-6} - \sqrt{p-3})\right). \tag{2.20}$$

Indeed, the frequency of any pairs of isofrequency orbits $\Omega^\varphi = (M/r_b^3)^{1/2}$ are givin Tables 2.1 and 2.2 together with radius of non-geodesic circular orbit r_b. In this respect the range of such orbits is represented in Table 2.2 for the different values of the magnetic field

$$\tilde{\Omega}^{\hat{\varphi}}(e=0) \lesssim \tilde{\Omega}^{\hat{\varphi}} < \tilde{\Omega}^{\hat{\varphi}}(e=1). \tag{2.21}$$

In Table 2.2, the values of the frequency Ω^φ of the particles moving around the Schwarzschild black hole in the presence of the magnetic field have been shown. From the results obtained one may see that the value of the frequency is becoming smaller with increasing magnetic field, but the radius of the ISCO is becoming larger. However, with the increasing the module of the magnetic field both the radius of ISCO and radius of the circular orbit r_b are slightly increased and going to be close to each other; therefore, the distance ξ between r_{isco} and r_b is becoming smaller. This causes in turn to restrict the motion of the particles and to decrease the amount of isofrequency pair in the region between the *separatrix* and *circular- orbit duals* (COD). This phenomena explains the behavior of the plots in Fig. 2.1 and the numerical results shown in Table 2.1.

Table 2.1

The radius of innermost stable circular orbits, the radius r_b, and the value of the small quantity $\xi = r_{isco} - r_b$ of the isofrequency pairing of non-geodesics orbits around the Schwarzschild black hole in the presence of the magnetic field for the different values of the magnetic parameter β.

β	0	0.001	0.005	0.01	0.05	0.1
r_b	6.38019	6.38022	6.38025	6.38029	6.38068	6.38118
r_{isco}	6	6.0036	6.0085	6-.Q145	6.0621	6.1203
$\xi = r_b - r_{isco}$	0.3802	0.3766	0.3717	0.3658	0.3185	0.2608

Here, we describe the dependence of the surface of region where isofrequency pairing of non-geodesic orbits occur around Schwarzschild black hole by external asymptotically uniform magnetic field. From numerical analysis, the expression for the ratio of the surface of the region can be delineated as $S(\beta \neq 0)/S(\beta = 0) \approx 0.90 - 0.93$ for the maximal values of the magnetic field in the fixed area B ~ $10^6 - 10^7$ Gauss. For the ratio, one can easily get the reduction of the surface of region between the *separatrix* and *circular-orbit duals* (COD), which corresponds to decreasing of the surface to nearly (7 − 10)% with compare to the one in Schwarzschild black hole without magnetic field.

Table 2.2

Numerical values for the frequency Ω^{φ} of isofrequency pairing of non-geodesic orbits around the Schwarzschild black hole for the different values of the magnetic parameter β and eccentricity e.

B	0	0.001	0.01	0.05	0.1
E	Ω^{φ} *(β)*	Ω^{φ} *(β)*	Ω^{φ} *(β)*	Ω^{φ} *(β)*	Ω^{φ} *(β)*
0	0.062051	0.0620508	0.0620496	0.062044	0.0620367
0.3	0.068	0.06798	0.0678	0.067	0.066
0.4	0.07395	0.07393	0.07374	0.0729	0.07187
0.5	0.0799	0.07988	0.07967	0.078798	0.07769
0.624	0.0918	0.091776	0.09155	0.090556	0.0893

0.768	0.1037	0.10367	0.1034	0.10233	0.10097
0.832	0.10965	0.1096	0.10936	0.108224	0.106798
0.896	0.1156	0.11557	0.1153	0.11412	0.1126
0.96	0.12155	0.12152	0.12124	0.120015	0.11848
1	0.125	0.1249	0.12468	0.12343	0.121875

§2.3 The electromagnetic field and charged particle motion in the gravitational field of a quintessential rotating black hole combined with an uniform magnetic field

The line element of the quintessential rotating black hole spacetime introduced in Ref. [113], generalizing thus the solution for a static quintessential black hole [112], takes in the Boyer-Lindquist coordinate system (t,r,θ,φ) the form

$$\begin{aligned} ds^2 &= -\left(1-\frac{2Mr+\tilde{c}r^{1-3\omega_q}}{\Sigma}\right)dt^2+\frac{\Sigma}{\Delta}dr^2-2a\sin^2\theta\left(\frac{2Mr+\tilde{c}r^{1-3\omega_q}}{\Sigma}\right)d\varphi dt \\ &+ \Sigma d\theta^2+\sin^2\theta\left[r^2+a^2+a^2\sin^2\theta\left(\frac{2Mr+\tilde{c}r^{1-3\omega_q}}{\Sigma}\right)\right]d\varphi^2\,, \end{aligned} \qquad (2.22)$$

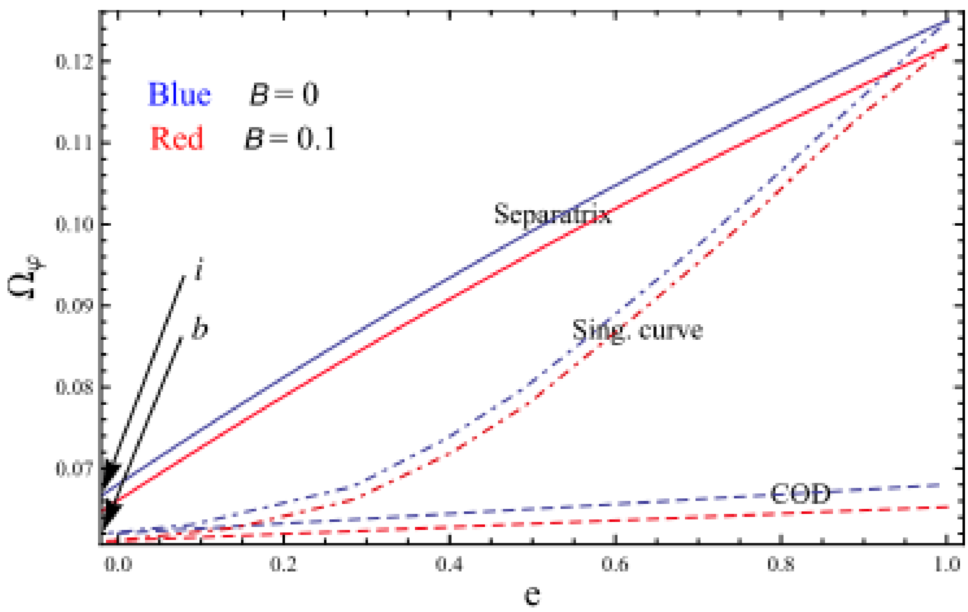

Figure 2.1: The dependence of the parameter space (e, Ω^φ) for bound non-

geodesic orbits from the magnetic parameter β in Schwarzschild black hole embedded in external asymptotically uniform magnetic field B. The point b corresponds to a circular orbit of radius r_b at the limit $e \to 0$ while the point i corresponds to the innermost stable circular orbit of radius r_{ISCO}.

Where

$$\Delta = r^2 - 2Mr + a^2 - \tilde{c} r^{1-3\omega_q} \text{ and } \Sigma = r^2 + a^2 \cos^2\theta \,. \tag{2.23}$$

The spacetime metric (2.22) reduces to the Kerr one when $c = 0$. More details on the rotating quintessential black hole background can be found in [113].

We study motion of a charged (test) particle, with the rest mass m and charge q, in the gravitational field of a quintessential rotating black hole that is also immersed in an external magnetic field which is assumed to be uniform at large distances from the black hole; namely, we can assume the uniformity of the external magnetic field at vicinity of the static radius of the quintessential black hole spacetime where the black hole spacetimes related to the vacuum energy, or alternatively to the quintessential energy, are closest to the flat spacetime [116].

We assume that the electromagnetic field is not disturbing the background geometry and is not directly interacting with the quitessential field, being also stationary and axisymmetric. In fact, the electromagnetic fields observed in the systems containing the astrophysical black hole candidates would be quite small as compared to the gravitational field of the black hole. Nevertheless, the influence of such small electromagnetic field on the charged particle motion could be significant, as demonstrated in [60, 70, 71].

It can be shown from the asymptotic properties that B turns out to be the magnetic field at large distances (near the static radius) where the spacetime is nearly flat, resembling thus the asymptotic flatness of the Kerr spacetime at infinity, where the magnetic field is assumed to be uniform and oriented along the axis of symmetry of the black hole. We thus study the charged particle motion in a stationary and axisymmetric electromagnetic field oriented along the symmetry axis of a quintessential rotating black hole. The Hamiltonian of the system can be then defined as [12]

$$H \equiv \frac{1}{2} g^{\alpha\beta}(\pi_\alpha - qA_\alpha)(\pi_\beta - qA_\beta) \tag{2.24}$$

where π_a is the canonical (generalized) momentum of a charged particle and the value of the Hamiltonian is constant as $H=-m^2/2$. The explicit expression with the derivation of four-vector potential of the electromagnetic field $A_\alpha = A_\alpha(r, \theta)$ appeared in Eq. (2.24) is given in A.1.7.

The four-momentum of a charged particle is

$$p^\alpha \equiv \frac{dx^\alpha}{d\lambda} = g^{\alpha\beta}(\pi_\beta - qA_\beta) \ , \tag{2.25}$$

where $\lambda = \tau/m$ is an affine parameter and t is the proper time. The Lorentz-force equation is equivalent to Hamilton's equations written in terms of x^a and π_α:

$$\frac{dx^\alpha}{d\lambda} = \frac{\partial H}{\partial \pi_\alpha} \ , \tag{2.26}$$

$$\frac{d\pi_\alpha}{d\lambda} = -\frac{\partial H}{\partial x^\alpha} \ . \tag{2.27}$$

With the help of equations (2.26) and (2.27) given above we are able to write down the equations of motion for the charged particle around the black hole placed in the magnetic field. Here, we restrict our attention to charged particle motion in the equatorial plane ($\theta = \pi/2$), so that $n^\theta = 0$. Then, the equations of motion for the charged particle take the form [4]

$$p^t = \frac{1}{r^2}\left[a(\pi_\varphi + a\pi_t) + \frac{r^2+a^2}{\Delta}P\right] , \tag{2.28}$$

$$p^\varphi = \frac{1}{r^2}\left[(\pi_\varphi + a\pi_t) + \frac{a}{\Delta}P\right] , \tag{2.29}$$

$$p^r = \left(\frac{P^2 - \Delta\left[r^2 + (\pi_\varphi + a\pi_t)^2\right]}{r^4}\right)^{1/2} , \tag{2.30}$$

where $P = (r^2 + a^2)(-\pi_t) - a\pi_\varphi$.

Note that in the case of general 3D motion the action S of the Hamilton-Jacobi equation can be separated in the following form

$$S = \frac{1}{2}m^2\lambda - Et + L\varphi + S_r(r) + S_\theta(\theta)\ , \tag{2.31}$$

where the parameters $E = -\pi_t$ and $L = \pi_\varphi$ are, along with the rest energy m, the motion constants, namely, energy and axial angular momentum of the charged particle, while S_r and S_θ are functions of r and θ, respectively. By virtue of Eqs (2.24) and (2.31), one can easily obtain the Hamilton-Jacobi equation in the form

$$\begin{aligned} &- \left[\frac{(r^2+a^2)^2}{\Delta} - a^2\sin^2\theta\right](E+qA_t)^2 + \Delta\left(\frac{\partial S_r}{\partial r}\right)^2 \\ &+ \frac{2a(2M+\tilde{c}r^{-3\omega_q})r}{\Delta}(E+qA_t)(L-qA_\varphi) + \left(\frac{\partial S_\theta}{\partial\theta}\right)^2 \\ &+ \left[\frac{1}{\sin^2\theta} - \frac{a^2}{\Delta}\right](L-qA_\varphi)^2 + m^2\Sigma = 0\,. \end{aligned} \tag{2.32}$$

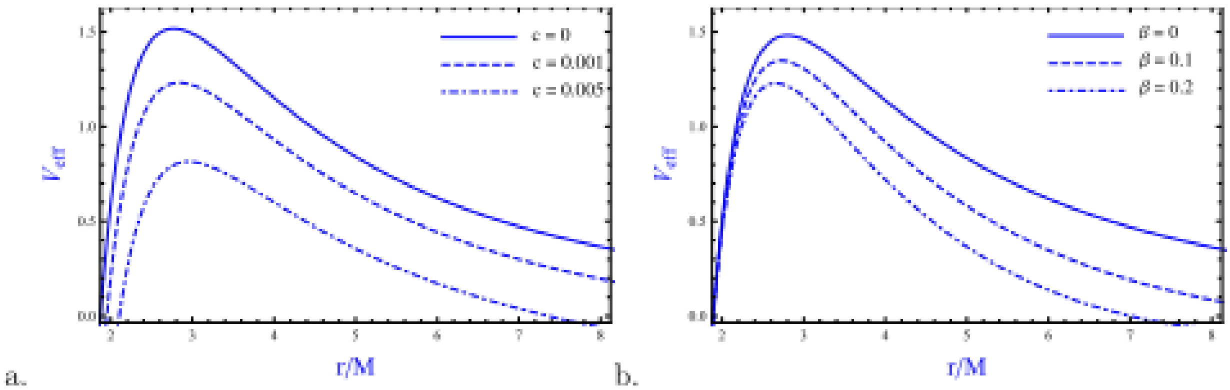

Figure 2.2: The dependence of the effective potential near the quintessential rotating black hole placed in a magnetic field of strength B on the radial motion of charged particles a) for the different values of quintessence matter parameter $\tilde{c}$ for the vanishing magnetic parameter $\beta = 0$ b) for the different values of the magnetic parameter β for the fixed c in the case in which the spin parameter $a = 0.5$ and the quintessence matter state parameter $\omega_q = -2/3$.

Then the fourth constant of motion can be obtained due to separability of the action. As the forth constant of motion is related to the latitudinal motion of test particles, we do not consider this motion constant here, being concentrated on the equatorial motion.

§ 2.3.1 Radial motion in the equatorial plane

By virtue of Eq. (2.32), the radial equation of the equatorial motion ($\theta = \pi/2$) of charged test particles can be written in the form

$$\frac{1}{2}\dot{r}^2 + R(\mathcal{E}, \mathcal{L}, r, a, c, \beta) = 0, \tag{2.33}$$

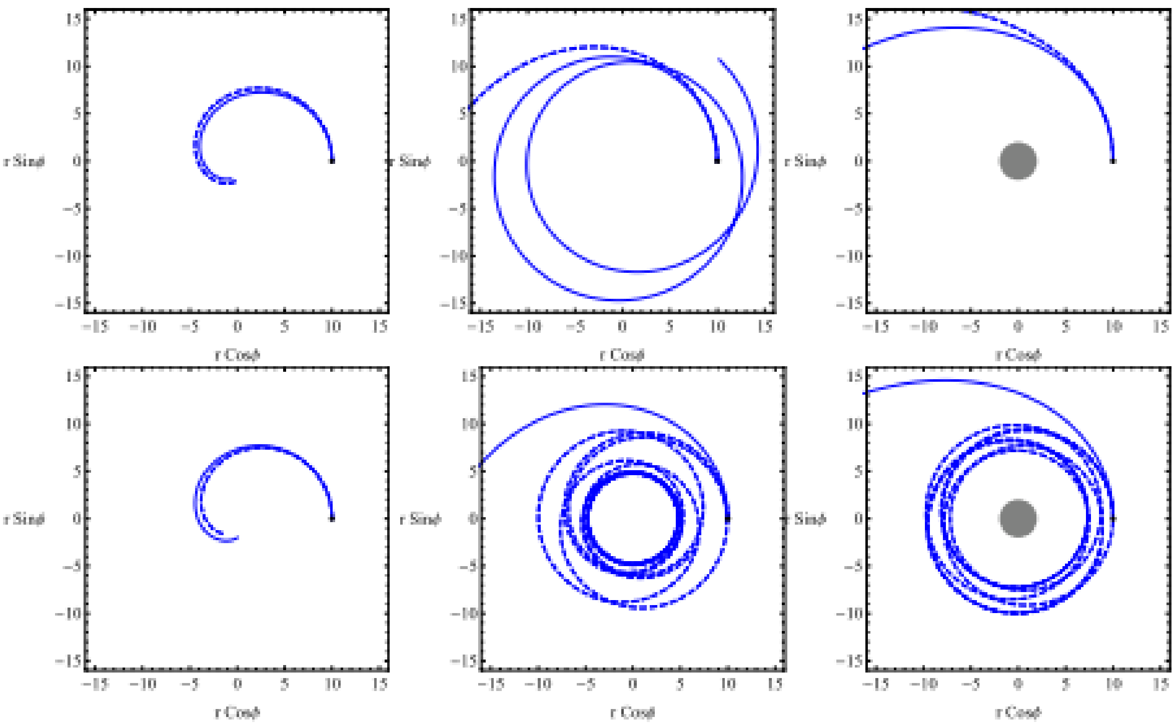

Figure 2.3: Trajectories of the charged particle at the equatorial plane around the quintessential rotating black immersed in an external magnetic field of strength *B*. For the top of this figure, the quintessence matter parameter $\tilde{c} = 0$ (solid curve) and $\tilde{c} = 0.001$ (dashed curve) for the $\beta = 0$, while for the bottom plots there is magnetic parameter $\beta = 0$ (solid curve) and $\beta = 0.01$ (dashed curve) for fixed quintessential parameter c = 0.001, in the cases in which the angular momentum (from left to right) $L = 3$, $L = 4$, and $L = 5$ for all possible orbits. In each case particle

starts moving from $r_o = 10$ towards the black hole.

where the Radial function $R(\mathcal{E}, \mathcal{L}, r, c, \beta)$ governing the radial motion is defined by the relation

$$
\begin{aligned}
R(\mathcal{E}, \mathcal{L}, r, a, \tilde{c}, \beta) \;=\; & -\frac{1}{2r^2}\left[\left(r^2 + a^2 + \frac{2A(r)a^2}{r}\right)\left(\mathcal{E}^2 - \frac{\beta^2}{4}\left(1 + \frac{\tilde{c}r^3}{3M^2}\right)^2 \Delta\right)\right. \\
& - \left(1 - \frac{2A(r)}{r}\right)\mathcal{L}^2 - \frac{4A(r)\; a\; \mathcal{E}\; \mathcal{L}}{r} \\
& \left. - \;\Delta\left(1 - \beta\;\left(1 + \frac{cr^3}{3M^2}\right)\;\mathcal{L}\right)\right], \qquad (2.34)
\end{aligned}
$$

where we use specific constants of motion, $\mathcal{E} = E/m$, $\mathcal{L} = L/m$, the magnetic parameter $\beta = qB/m$ measuring influence of the magnetic field on charged particle motion, and the parameter $A(r)$ defined by the relation

$$
A(r) = M + \tilde{c}r^{-3\omega_q}/2\,. \qquad (2.35)
$$

The effective potential $V_{eff}\,(\mathcal{L}, r, a, c, \beta)$ of the radial motion is determined by the relation

$$
\dot{r}^2 = (\mathcal{E} - \mathcal{E}_+(\mathcal{L}, r, \tilde{c}, \beta))(\mathcal{E} - \mathcal{E}_-(\mathcal{L}, r, \tilde{c}, \beta)), \qquad (2.36)
$$

and $V_{eff}\,(\mathcal{L}, r, a, c, \beta) = \mathcal{E}_+(\mathcal{L}, r, c, \beta)$, if we restrict attention to the physically relevant particles in the so called positive-root states [117].

The Radial function appearing in Eq. (2.34) gives the turning points of the radial motion and its properties thus map the role of the quintessential field related to the black hole and the external magnetic field in the charged particle motion. Fig. 1.2(a) reflects the role of the quintessential field, showing the radial profiles of the Radial function for fixed rotational parameter and vanishing of the magnetization parameter. Fig. 2.2(b) reflects the role of the external magnetic field, showing the radial profiles of the Radial function for fixed rotational parameter and the quintessential field intensity parameter.

As can be seen from Fig. 2.2, the height and range of the Radial function decreases with increasing quintessential parameter c while the other parameters are fixed; in a similar way we observe that the range of the Radial function decreases with increasing magnetic parameter β while the other parameters are fixed. As the turning points of the radial motion are given by the condition $R = 0$, we conclude that both the quintessential field intensity and the magnetic parameter have tendency to restrict the range of the charge particle motion.

Note that the condition for the turning points of the equatorial radial motion, $R(\mathcal{E}, L, r, a, c, \beta) = 0$, can be considered as a quadratic function of ε and can be thus expressed in the form $(\mathcal{E} - V_{eff+}(L, r, a, c,\beta))(\mathcal{E} - V_{eff-}(L, r, a, c,\beta)) = 0$ where the effective potentials related to the conservative energy of the particle motion are determined by the solution of the quadratic equation. Above the black hole horizon, physically relevant for the test particle motion is the effective potential V_{eff+} [113]. The turning points are then given by the equation $\mathcal{E} = V_{eff+}(L, r, a, c,\beta)$. Minima (maxima) of the effective potential $V_{eff+}(L, r, a, c,\beta) = V_{eff}$ govern the stable (unstable) circular orbits of charged test particles. The innermost stable circular orbit is determined by the inflex point of the effective potential.

Finally, we illustrate the charged particle equatorial motion by their trajectories in the black hole vicinity. The top part of Fig. 2.3 presents trajectories of uncharged particles with vanishing magnetic parameter β and illustrated the role of the quintessential parameter cc, while the bottom part is constructed for fixed parameter c and illustrates the role of the magnetic parameter β. From Fig. 2.3 it is obvious that various orbits can occur: bound orbits, orbits captured by the black hole, and escaping orbits, if the parameters are properly tuned.

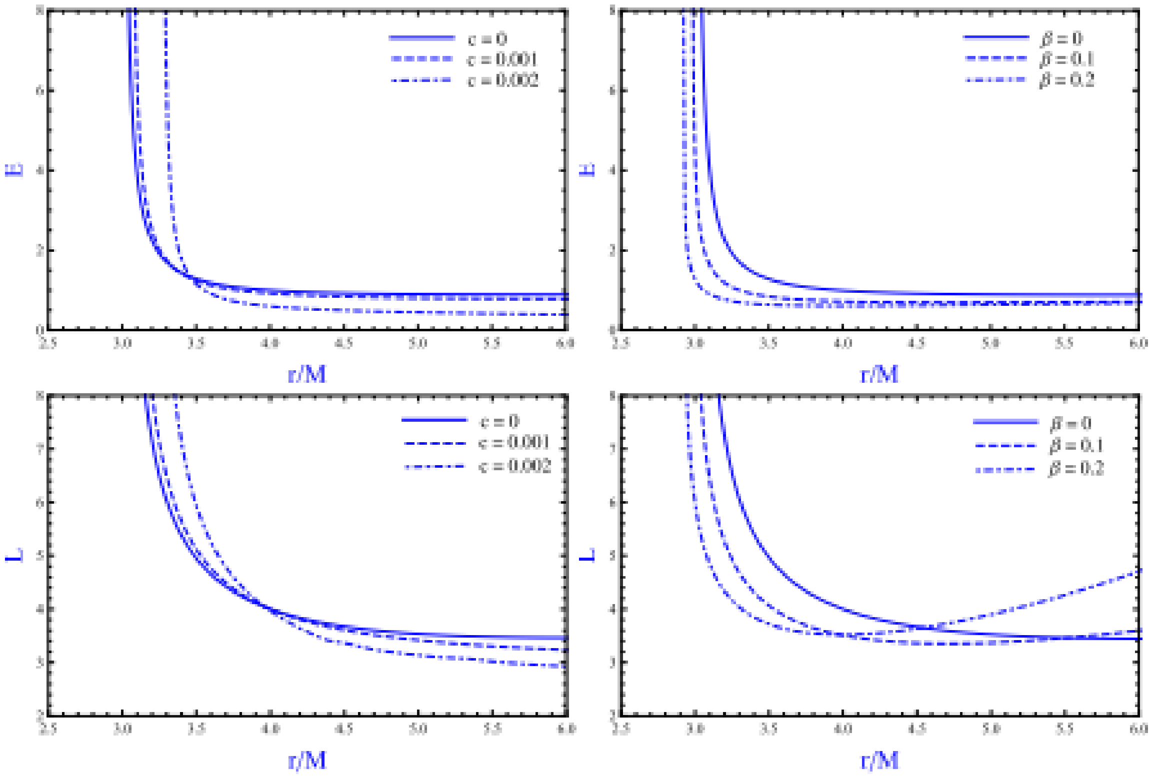

Figure 2.4: The dependence of the specific angular momentum and energy on the radial motion of the charged particles moving in the vicinity of the rotating black hole with quintessential energy is plotted for the magnetic parameter β = 0 (left panel) for the different values of quintessential matter parameter $\tilde{c}$, and $\beta \neq 0$ (right panel) for the given $\tilde{c}$ = 0.001 in the case in which matter state parameter $\omega_q = -2/3$.

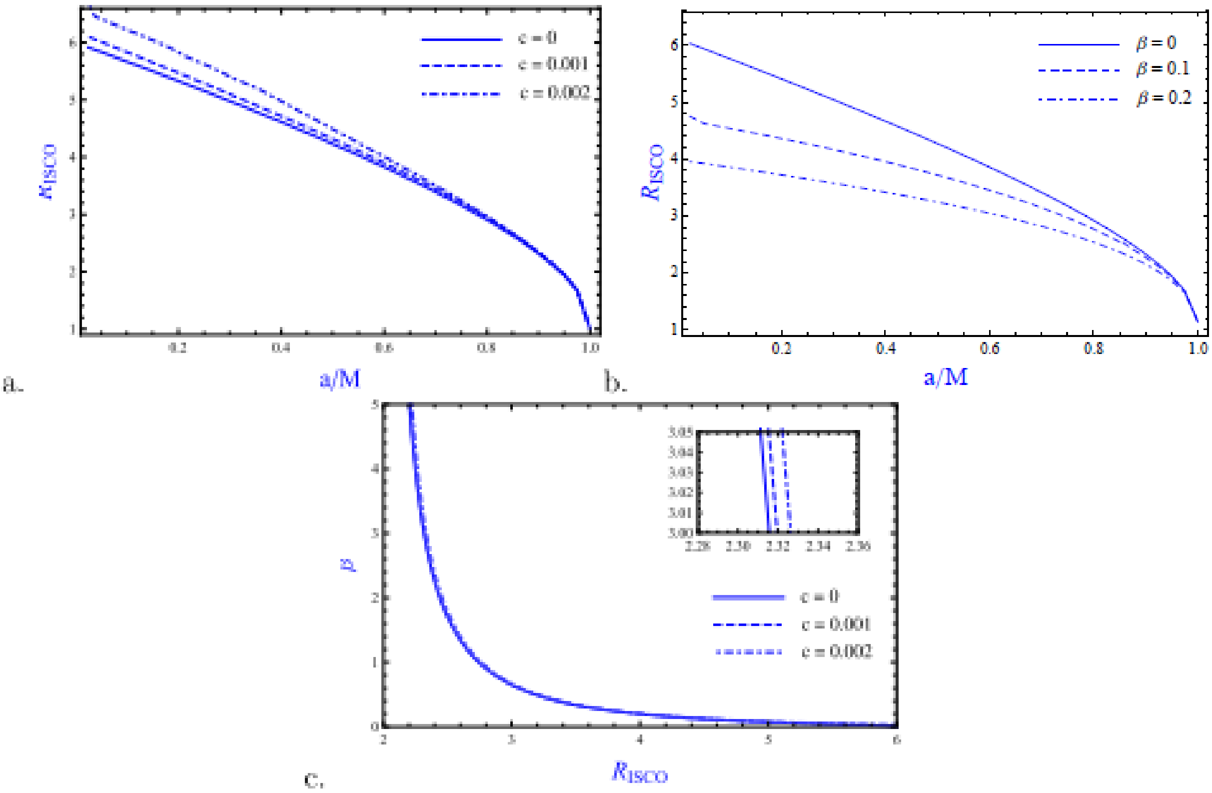

Figure 2.5: The dependence of the radius of the innermost stable circular orbits (ISCO) of the charged particles moving in the vicinity of the rotating black hole with quintessential energy on the spin parameter a is plotted for the a) $\beta = 0$ and b) $\beta \neq 0$ cases. The ISCO radius increases due to the effect of quintessential matter parameter $\tilde{c}$, and then it decreases once the magnetic parameter β starts becoming larger for the given $\tilde{c}$ = 0.001. The dependence of an external magnetic field on ISCO of the charged particles is plotted for c) the different values of parameter c with vanishing spin parameter $a = 0$. Here, in all cases in which matter state parameter is considered as $\omega_q = -2/3$.

§ 2.3.2 The innermost stable circular orbits (ISCO)

The equatorial circular orbits of charged test particles can be obtained by simultaneous solution of the equations

$$R(r) = 0, \frac{\partial R(r)}{\partial r} = 0. \tag{2.37}$$

Solution of these equations gives the radial profiles of the specific energy $\mathcal{E}$ $(r, a, c,$

β) and axial angular momentum $\mathcal{L}$ (r, a, c, β) related to the circular orbits.

In Fig. 2.4, we illustrate behavior of the radial profiles of the specific energy and the specific axial angular momentum of the charged particle circular orbits demonstrating dependence on the quintessential field parameter cc, and the magnetic parameter β. We can see in Fig. 2.4 that the energy E and angular momentum $\mathcal{L}$ radial profiles are shifted outwards due to increasing parameter $\tilde{c}$, while they are shifted towards the black hole with increasing magnetic parameter β.

For the innermost stable circular orbits (ISCO) we have to satisfy also equation

$$\frac{\partial^2 R(r)}{\partial r^2} = 0 \, . \tag{2.38}$$

Using the radial profiles of $\mathcal{E}$ and $\mathcal{L}$ in the expression governing the innermost stable circular orbits, we can obtain the condition that has to be satisfied by the ISCO radii r_{ISCO}. Detailed discussion of the ISCO radii in the field of magnetized black holes (without the quintessential field) can be found in [69, 71]. Here we illustrate results of numerical calculations in Fig. 2.5 in order to demonstrated the role of the black hole spin a, the quintessential parameter cc and the magnetic parameter β. The first pair of Fig. 2.5 illustrates the dependence of the radius of the innermost stable circular orbits of the charged particles on the spin parameter *a*. The ISCO radius increases with increasing quintessential field parameter c in contrast to the Schwarzschild geometry. On the other hand, the ISCO radius decreases with increasing the magnetic parameter β.

We give the estimated of the ISCO radius in dependence on the quantesential parameter c and magnetic parameter β for the case of static black holes when the situation is simplified. In the limit of a → 0, the effective potential (2.34) of the test particle motion takes the following relatively simple form

$$V_{eff}(r) = \left(1 - \frac{2M}{r} - \frac{\tilde{c} r^{1-3\omega_q}}{r^2}\right)\left(1 + \frac{\left[\mathcal{L} - \beta\left(1 + \frac{\tilde{c} r^3}{3M^2}\right) r^2\right]^2}{r^2}\right), \tag{2.39}$$

which allows us to find the equation governing the ISCO radius using the first and second derivatives of (2.39) with respect to r. The resulting condition then reads

$$
\begin{aligned}
& r(6-r)+4\left(\tilde{c}r^2+\sqrt{(6-r)(3r-6\tilde{c}r^2-2)}\right) \\
- & \left(\tilde{c}r^2+\sqrt{(6-r)(3r-6\tilde{c}r^2-2)}\right)^2 \frac{[12+r(\tilde{c}r-3)]}{(6-r)} \\
- & 3\tilde{c}r^2(6-r)-\frac{2(6-r)}{\beta^2 r^2}=0\,.
\end{aligned}
\tag{2.40}
$$

Then we can obtain the angular momentum in the form

$$
\begin{aligned}
\mathcal{L} \;=\; & \left(\frac{2(6-r)}{r}\right)^{1/2} \\
\times\; & \left[r(6-r)+4\left(\tilde{c}r^2+\sqrt{(6-r)(3r-6\tilde{c}r^2-2)}\right)-3\tilde{c}r^2(6-r)\right. \\
-\; & \left.\left(\tilde{c}r^2+\sqrt{(6-r)(3r-6\tilde{c}r^2-2)}\right)^2 \frac{[12+r(\tilde{c}r-3)]}{(6-r)}\right]^{-1/2} \\
\times\; & \frac{\left[(6-r)(3r-6\tilde{c}r^2-2)\right]^{1/2}+\tilde{c}r^2}{2(6-r)}r^2\,.
\end{aligned}
\tag{2.41}
$$

From the equation (2.40), we can easily obtain the parameter β as a function of r. The bottom plot of Fig. 2.5 demonstrates the magnetic parameter β expressed at the ISCO radius for various values of the quintessential field parameter c. The plot shows that the ISCO radius is slightly shifted outwards due to the effect of the quintessential parameter c. However, as can be seen from Fig. 2.5(c), once magnetic parameter $\beta\to\infty$, the ISCO radius reaches its minimum irrespective of presence of the parameter $\tilde{c}$.

In the limit of small quintessential matter parameter, $\tilde{c} \ll 1$, and strong magnetic field, $\beta \gg 1$, one can solve equation (2.40) to obtain the following form for the ISCO radius

$$r_{ISCO} \;=\; 2+\frac{1}{\beta}\left(\frac{2}{\sqrt{3}}+\frac{91+29\sqrt{2}}{192\sqrt{3}}\tilde{c}+\mathcal{O}(\tilde{c}^2)\right)+\left(\frac{5+\sqrt{2}}{6}\right)\tilde{c}+\mathcal{O}(\beta^{-2})\,. \tag{2.42}$$

It is obvious from equation (2.42) that for $\tilde{c}=0$ one can express the r_{ISCO} radius in the form

$$r_{ISCO}=2+\frac{2}{\sqrt{3}\beta}+\mathcal{O}(\beta^{-2})\,, \tag{2.43}$$

which coincides with the results given in [56, 60], and is also in agreement with the results of [118, 119].

In the Table 2.3 the values of the ISCO radius of the charged particles circling around the rotating black hole with quintessential energy are given in dependence on the magnetic parameter β. The results listed in Table 2.3 demonstrate the behavior of innermost stable circular orbits for various values of the quintessential parameter *c*. One can notice that with increasing magnetic field the innermost stable circular orbits are getting closer to the black hole horizon.

§2.4 Conclusion

Here, we have studied isofrequency pairing of non-geodesic orbits under the gravitational field of the Schwarzschild black hole immersed in external asymptotically uniform magnetic field. It was pointed out by Warburton et al. [54] that the isofrequency pairing of geodesic orbits can be occurred in the Schwarzschild and the Kerr geometry, and they gave an intuitive explanation concerning occurrence of the isofrequency pairing of geodesic orbits in the area between the *separatrix* and *circular-orbit duals* (COD).

Our results show that the presence of the magnetic field gives rise to r_{ISCO} and r_b to be slightly shifted from the central black hole and the distinction between

Table 2.3:

The value of the radius of the innermost stable circular orbits of the charged particles moving around the quintessential black hole and the values of center of mass energy of collision between charged particle orbiting at the ISCO and neutral particle freely falling far away from infinity for the different values of quintessential parameter.

$\tilde{c}$	r_{ISCO}	$E_{c.m.}$ /m
0.00000	2.00000 + 1.15470P^{-1}	1.74337$P^{1/4}$
0.00001	2.00001 + 1.15471P^{-1}	1.73824$P^{1/4}$
0.00005	2.00005 + 1.15472P^{-1}	1.73818$P^{1/4}$
0.00010	2.00011 + 1.15475P^{-1}	1.7 3722$P^{1/4}$
0.00050	2.00053 + 1.15494P^{-1}	1.73656$P^{1/4}$
0.00100	2.00107+ 1.15519P^{-1}	1.73556$P^{1/4}$
0.00500	2.00535 + 1.15713P^{-1}	1.72903$P^{1/4}$

them $\xi = (r_b - r_{ISCO})$ to become smaller, which also causes the region allowing isofrequency pairing of non-geodesic orbits to be decreased; consequently, the amount of the isofrequency pairing of circular orbits decreases when the value of the magnetic field increases. We have studied the dependence of the surface of region where isofrequency pairing of non-geodesic orbits occur around Schwarzschild black hole from the external magnetic field. To make our conclusion more concrete, we have found a decrease in the surface of the isofrequency pairing of nongeodesic orbits as nearly (7 –10) % for the maximal values of the external uniform magnetic field B ~ 10^6 –10^7Gauss. The results obtained from our analysis can make easier to identify signals coming from infinity for colleagues studying the data-analysis problem for gravitational-wave detectors.

We have investigated the ISCO radius of quintessential black hole in the presence of quintessential field, according to which it starts getting away from black hole with increasing the value of quintessential parameter $\tilde{c}$, but this approach is contrary for the effect of magnetic field. Rather, the center of mass energy infinitely grows when the ISCO of the charged particle becomes arbitrarily close to the horizon by the influence of the external magnetic field. Also, in this paper, we have also shown that the center of mass energy can be decreased due to the effect of parameter cc; however, it can be approached to its maximum energy, although it is slightly comparable with the result in Ref. [60], in the collision between a neutral particle radially falling and a charged particle moving at the ISCO for the huge magnetic parameter β.

CHAPTER III. THE DYNAMICS OF OVERSPINNING PROCESS OF BLACK HOLE AND THE ROLE OF ELECTROMAGNETIC

§3.1 Introduction

In this chapter, we study a Gedanken experiment to destroy a black hole with the infalling test particle. The infalling particle would add to the mass, angular momentum, and charge of the black hole and can make it go past the extremality, thus turning the black hole into the naked singularity. Such a process was examined by Wald for the first time, who found that it is impossible to overspin an extremal Kerr black hole by throwing in a neutral test particle [120]. If the angular momentum of the infalling particle is large enough for the purpose of overspining the black hole, it turns back before it could enter a black hole. Whereas if the particle enters the black hole, it would not add a sufficient amount of angular momentum to overspin the black hole.

Recently, it was shown by Jacobsan and Sotiriou [121] that it would be possible to destroy a black hole with an infalling test particle if we start with a near-extremal configuration, rather than an extremal black hole as in the case of Wald's analysis. There is a narrow range of the energy and angular momentum of the infalling particles for which it would be possible for it to enter a black hole and also overspin it past the extremality. It was also shown that it would be possible to destroy near-extremal Reissner-Nordstrom black holes with the charged test particle [122]. The process of destroying a rotating black hole with the charged test particle was investigated in Ref. [123]. In all these calculations, it was assumed that the test particle follows a geodesic motion and effects of the conservative and dissipative backreaction were ignored. There are investigations that suggest that the radiation reaction and selfforce would act as a cosmic censor [124-126]. It was also shown that it would be possible to destroy a regular black hole with the test particles even when the backreaction effects are taken into account [127]. There are also works extending the process of destroying to a massive complex scalar test field around a four-parameter extreme black hole and massless integer spin test fields [128, 129].

We approach this issue from a different perspective. Typically, in the astro-physical scenarios, black holes are surrounded with the magnetic field, which affects the motion of the charged particle and thus influences the process of destroying the black hole. With this motivation in mind, in this paper, we investigate whether or not a magnetic field could possibly serve as a cosmic censor. For this purpose, we introduce a test magnetic field on the Kerr space-time following a procedure that is described in Ref. [84].

The Wald solution was recently extended to a black hole that is also moving at constant velocity in Refs. [130-133]. The magnetic field respects the axial symmetry of the Kerr space-time, and it takes a constant value asymptotically at infinity. We show that for a large enough value of the magnetic field it serves as a cosmic censor.We try to gauge the magnitude of the magnetic field required by comparing its backreaction on the background geometry as compared to that of a test particle. The density of the energy-momentum tensor of the magnetic field is a good measure of its backreaction on the background Kerr space-time. We compute the square root of the difference in the Kretschmann scalar at the horizon between extremal and near-extremal geometry, which is a fair indicator of the backreaction of the test particle on the background spacetime. We show that the backreaction of the magnetic field is as much as or slightly larger than that of the tiny backreaction of the test particle when it starts acting as the cosmic censor. Thus, an extremely weak magnetic field is sufficient to restore the cosmic censorship in the process of destroying the near-extremal Kerr black hole.

The magnetic field respects the axial symmetry of the Kerr space-time, and it takes a constant value asymptotically at infinity. We show that for a large enough value of the magnetic field it serves as a cosmic censor. We try to gauge the magnitude of the magnetic field required by comparing its backreaction on the background geometry as compared to that of a test particle. The density of the energy-momentum tensor of the magnetic field is a good measure of its backreaction on the background Kerr space-time. We compute the square root of the difference in the Kretschmann scalar at the horizon between extremal and near-extremal geometry, which is a fair indicator of the backreaction of the test particle on the background spacetime. We show that the backreaction of the magnetic field is as much as or slightly larger than that of the tiny backreaction of the test particle when it starts acting as the cosmic censor. Thus, an extremely weak magnetic field is sufficient to restore the cosmic censorship in the process of destroying the near-extremal Kerr black hole.

This analysis also suggests that we must in principle take into account the backreaction of the magnetic field on the background geometry since the change in the metric due to the magnetic field will be comparable to that of the test particle. It is difficult to implement it in the absence of any exact solution representing magnetized near-extremal geometry. However, we argue that our conclusions will not change even after taking into account the backreaction of the magnetic field.

If black holes could indeed turn into the naked singularities, i.e., if cosmic censorship hypothesis [19] could be violated, it would have serious implications from a theoretical as well as observational perspective. Kerr and Kerr-Newmann naked singular geometries are associated with the absence of global hyperbolicity and also with the existence of the closed time like curves. However, it was suggested that string theory could potentially resolve the naked singularities, and all these issues would disappear [134], rendering their existence legal. From an observational point of view, it was shown that the near-extremal naked singularities can host ultrahigh-energy particle collisions and thus can serve as an astrophysical probe of high-energy physics [135-139]. We also note that there are many investigations in which it is demonstrated that the naked singularities can form as an end state of the continual gravitational collapse [140-143].

In Sec. 3.2, we describe the process of destroying the near-extremal Kerr black hole with a charged test particle. In Sec. 3.3, we introduce a test magnetic field on the background of the Kerr black hole and analyze its effect on the process of destroying a near-extremal Kerr black hole with a charged test particle. In Sec. 3.4, we compare the backreaction of the test magnetic field with that of the test particle and analyze whether magnetic field could possibly serve as a cosmic censor. We summarize our concluding remarks of the obtained results in the Sec. 3.5.

§3.2 Particle motion around a near-extremal Kerr black hole and dynamics of overspinning process with a charged particle

In what follows we describe the process of destroying the near-extremal Kerr black hole with the charged test particle. We calculate the range of the energy and angular momentum of the particle for it to turn the Kerr black hole into the Kerr-Newmann naked singularity. We then analyze allowed range of the parameters for which a particle can enter the black hole.

We restrict our attention to the particles that follow geodesic motion on the equatorial plane of the Kerr black hole with mass M and angular momentum J. There are two constants of motion associated with the particle, namely, conserved energy δE and conserved angular momentum δJ. We assume that these quantities are much smaller compared to that of the black hole $\delta E \ll M$, $\delta J \ll J$, so the test particle approximation holds well. Let q be the charge associated with the test particle, which is also assumed to be small. We neglect the radiation reaction and self-force. When a particle enters the black hole, it adds to the mass, angular momentum, and charge of the black hole. The final mass, angular momentum, and charge of the black hole are given by $M + \delta E$, $J + \delta J$, and q, respectively.

If the particle were to turn a Kerr black hole into the Kerr-Newman naked singularity, the following condition must hold:

$$(M + \delta E)^2 < \left(\frac{J + \delta J}{M + \delta E}\right)^2 + q^2. \tag{3.1}$$

This yields the lower bound on the angular momentum of the particle:

$$\delta J > \delta J_{min} = (M^2 - J) + 2M\delta E + \delta E^2 - \frac{q^2}{2}. \tag{3.2}$$

As it was pointed out in Ref. [121], the null energy condition on the matter of which the test particle consists puts an upper bound on the angular momentum

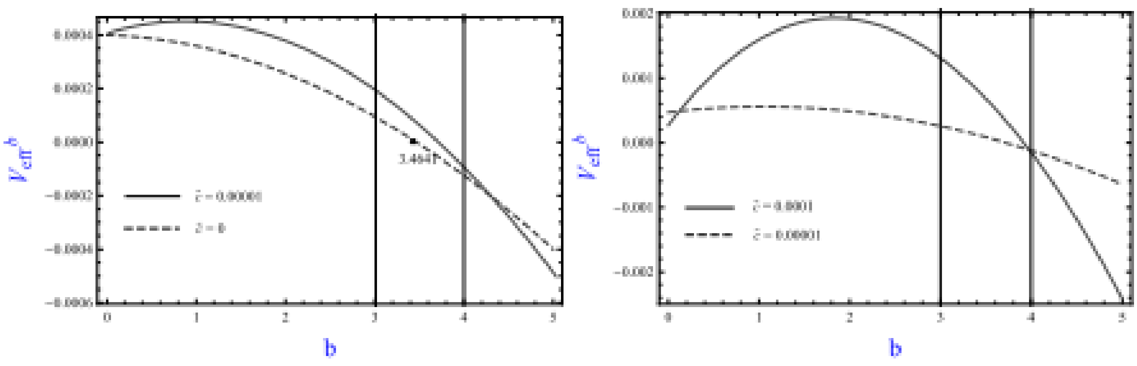

Figure 3.1: The dependence of the value of the effective potential at given maximum radius r_{max} on the parameter b is plotted here for the different values of charge parameter e. The allowed range of b increases as we increase the charge q.

of the particle,

$$\delta J < \delta J_{max} = \frac{2Mr_+}{a}\delta E, \tag{3.3}$$

where the three parameters, a, M and r_+, denote a specific angular momentum, mass, and event horizon of a Kerr black hole, respectively. In case of the extremal black hole, it turns out that $J_{max} < J_{mm}$, and thus it is not possible to overspin it.

Here, we deal with the near-extremal black hole with the dimensionless spin parameter close to unity. We take $J/M^2 = a/M = 1 - 2\epsilon^2$, with $\epsilon << 1$ being a small dimensionless parameter. Hereafter, we set $M = 1$. The maximum and minimum values of δJ are given by

$$\delta J_{min} = 2\epsilon^2 + 2\delta E + \delta E^2 - \frac{q^2}{2}, \tag{3.4}$$

$$\delta J_{max} = (2 + 4\epsilon)\delta E, \tag{3.5}$$

and the allowed range of δE is

$$\left(2 - \sqrt{2}\sqrt{1 + \left(\frac{q}{2\epsilon}\right)^2}\right)\epsilon < \delta E < \left(2 + \sqrt{2}\sqrt{1 + \left(\frac{q}{2\epsilon}\right)^2}\right)\epsilon. \tag{3.6}$$

The value of charge q is taken to be small as compared to ϵ. Thus, we have δE of the order of ϵ. For the given δE, we get $\delta J \sim \delta E$, and the particle under consideration can be thought of as a test particle.

We must ensure that the particle in the allowed range of the energy and angular momentum starting from a distant location indeed enters the black hole if it were to turn it into a naked singularity. Thus, we need to understand the geodesic motion of the particle. As stated earlier, we focus on the particle that is restricted to move on the equatorial plane. The motion of the particle in the radial direction can be described in terms of the effective potential as stated in the equation below. Thus, we must analyze the behavior of the effective potential to understand whether or not particle enters the black hole,

$$\frac{\dot{r}^2}{2} + V_{\text{eff}}(r, \delta\tilde{E}, \delta\tilde{J}) = 0, \tag{3.7}$$

where $\delta E = \delta E/m$ and $\delta J = \delta J/m,$ and m is the rest mass of the particle.

For the chosen value of the energy δE, one can write the allowed range of the angular momentum of the body falling into the black hole as

$$(2 + 3\epsilon)\delta\tilde{E} - \frac{q^2}{2m} < \delta\tilde{J} < (2 + 4\epsilon)\delta\tilde{E}. \tag{3.8}$$

As we have already mentioned, the initial black hole is nearly extremal, but now we can be somewhat more quantitative. For example, we take $\epsilon = 10^{-2}$. All the plots in this paper are made with this value of ϵ. The spin parameter of the Kerr black hole in this case is given by $a = 0.9998$. We can imagine even smaller values of ϵ in principle.

We parametrize the range of allowed specific angular momentum with

$$\delta\tilde{J} = (2 + b\ \epsilon)\ \delta\tilde{E} - (4 - b)\ \tilde{e}, \tag{3.9}$$

where $b \in [3,4]$ and $\tilde{e} = q^2/2m$ is charge parameter.

We now investigate the effective potential for the radial motion of the particle. The charged particle is assumed to start from a distant location falling in toward the black hole. We must make sure that $V_{eff} < 0$ everywhere outside the horizon so that the particle enters the black hole. The effective potential that appears in (3.7) is given by

$$V_{eff} = -\frac{\delta\tilde{E}^2}{2}\left[1 - \frac{3 + b\tilde{e}(b-4) + 4b\epsilon + (4+b^2)\epsilon^2}{r^2} + \frac{2 - 2b\tilde{e}(b-4) + 4b\epsilon - 4\tilde{e}(4-b)\epsilon + 2(4+b^2)\epsilon^2}{r^3} - \gamma\left(\frac{8b + (4-b)^2\gamma - 32}{4r^2} - \frac{4b + (4-b)^2\gamma - 16}{2r^3}\right)\right], \quad (3.10)$$

where $\gamma = \tilde{e}/\varepsilon$. Here, we assume that the specific energy of the infalling particle is large, $\delta E >> 1$, as in Ref. [121].

We compute the maximum value of the effective potential attained at a location outside the horizon and write it as $V_{eff} = \delta E^2\ E^b_{eff}/2$. For a particle to enter the event horizon, E^b_{eff} defined by the expression given in the brackets of Eq. (3.10) must be positive at the radial location stated above where the effective potential attains the maximum. For given value of $\tilde{e}$, the parameter b must take a value in the range (3, b_{cr}) as can be seen in Fig 3.1. The upper critical values of the parameter b_{cr} for the different values of charge parameter e are tabulated in Table 3.1. We also compute the upper critical values of the parameter b_{cr} for the different values of parameter ϵ so as to understand the behavior of the process in a better way and tabulate these values in Table 2.2. From Table 2.2, one may observe that the value of parameter b_{cr} starts getting closer toward b = 4 with increasing the value of charge parameter e. However, it keeps particles entering into the black hole.

The parameter b can take values in the range [3,4]. As shown in Ref. [121], the allowed range for the uncharged particle to enter the black hole is given by

Table 2.1:

The values of b_{cr} for the different values of charge parameter c for the given value of nonextremality *e*.

ϵ	0.01	0.01	0.01	0.01	0.01	0.01
$\tilde{e}$	10^{-3}	10^{-4}	$5x10^{-5}$	10^{-5}	5×10^{-6}	0
b_{cr}	3.9863	3.8846	3.8034	3.6093	3.5558	3.4641

Table 2.2:

The values of b_{cr} for the different values of charge parameter $\tilde{e}$ for various values of ϵ.

ϵ	$\tilde{e}$	b_{cr}
0.0001	1×10^{-3}	3.9999988860
	1×10^{-4}	3.9999888610
	5×10^{-5}	3.9999777225
	1×10^{-5}	3.9999228631
	5×10^{-6}	3.9998886303
0.000001	1×10^{-3}	3.9999999998
	1×10^{-4}	3.9999999988
	5×10^{-5}	3.9999999977
	1×10^{-5}	3.9999999888
	5×10^{-6}	3.9999999777

$[3, \sqrt{12}]$. As can be seen in Fig. 3.1, the effective potential V_{eff}^{b} at r_{max} is positive in this range. Here, we analyze the process of destroying the Kerr black hole with the charged particle. The allowed range of parameter b for which the test particle enters the near-extremal black hole and turns it into the Kerr-Newman naked singularity increases as we increase the charge parameter. As can be seen from Fig. 3.1, the intersection point of the effective potential curve moves toward b = 4. Consequently, it becomes easier to destroy the black hole if the incoming particle is charged.

In this section, we described the process of destroying a near-extremal Kerr black hole with a charged test particle. In the next section, we introduce a test magnetic field around the Kerr black hole and analyze its effect on the process of destroying a black hole.

§3.3 The effect of magnetic field on the particle motion around near-extremal Kerr black hole

We analyze the effect of a magnetic field in the process of destroying a Kerr black hole with a charged particle. We describe a process to set up a test magnetic field on the space-time containing the Kerr black hole. The magnetic field takes a constant value at infinity and is oriented along the axis of symmetry of the Kerr geometry. The motion of the charged particle could be influenced by the test magnetic field, and it can also affect the process of destroying the black hole. We try to understand whether or not the magnetic field can stop particles with the appropriate values of geodesic parameters from entering the black hole and thus serve as a cosmic censor.

The metric of the Kerr geometry in the Boyer-Lindquist coordinates is given by

$$ds^2 = -\left(\frac{\Delta - a^2\sin^2\theta}{\Sigma}\right)dt^2 - \frac{2a\sin^2\theta(r^2+a^2-\Delta)}{\Sigma}dtd\phi + \frac{\Sigma}{\Delta}dr^2 + \Sigma d\theta^2 + \frac{(r^2+a^2)^2 - \Delta a^2\sin^2\theta}{\Sigma}\sin^2\theta d\phi^2, \tag{3.11}$$

where $\Sigma = r^2 + a^2\cos^2\theta$ and $\Delta = r^2 + a^2 - 2Mr$.

We write down the conserved quantities for the particle motion in the equatorial plane,

$$\pi_t = -g_{\mu\nu}(\xi_t)^\mu\pi^\nu = g_{tt}\pi^t + g_{t\varphi}\pi^\varphi + qA_t, \tag{3.12}$$

$$\pi_\varphi = -g_{\mu\nu}(\xi_\varphi)^\mu\pi^\nu = g_{\varphi t}\pi^t + g_{\varphi\varphi}\pi^\varphi + qA_\varphi, \tag{3.13}$$

where π^ν is the 4-velocity defined by $\pi^\nu = \frac{dx^2}{d\tau}$ and τ is the proper time for timelike geodesics.

The covariant components of the 4-vector potential of the electromagnetic field for the Kerr spacetime is given by

$$
\begin{aligned}
A_t &= -\frac{1}{2\Sigma}\left\{aB\left[\Delta\left(1+cos^2\theta\right)+\left(r^2-a^2\right)\sin^2\theta\right]-2aB\left(\Sigma-2Mr\right)\right\},\\
A_r &= A_\theta = 0\ ,\\
A_\varphi &= \frac{1}{\Sigma}\left\{\frac{B}{2}\left[\Delta a^2\left(1+cos^2\theta\right)+r^4-a^4\right]-2QMBa^3\right\}\sin^2\theta\,. \qquad (3.14)
\end{aligned}
$$

Solving Eqs. (3.12) and (3.13) associated with electromagnetic potentials (3.14), we write down the equation of motion for the charged particle motion in the Maxwell field around black holes,

$$
\pi^t = \frac{1}{r^2}\left[a(\pi_\varphi + a\pi_t) + \frac{r^2+a^2}{\Delta}P\right], \qquad (3.15)
$$

$$
\pi^\varphi = \frac{1}{r^2}\left[(\pi_\varphi + a\pi_t) + \frac{a}{\Delta}P\right], \qquad (3.16)
$$

$$
(\pi^r)^2 = \frac{P^2 - \Delta\left[r^2 + \left(\pi_\varphi + a\pi_t\right)^2\right]}{r^4}, \qquad (3.17)
$$

where $P = (r^2 + a^2)(-\pi_t) - a\pi_\varphi$.

The effective potential for the radial motion of a charged particle at the equatorial plane $\theta = \pi/2$ of the Kerr black hole placed in an external magnetic field is given by

$$
V_{eff}(r) = \frac{\Delta\left[r^2 + \left(\pi_\varphi + a\pi_t\right)^2\right] - P^2}{2r^4}\,. \qquad (3.18)
$$

Now, we discuss and analyze the charged particle motion around a Kerr black hole immersed in a uniform magnetic field. Again, we analyze the effective potential

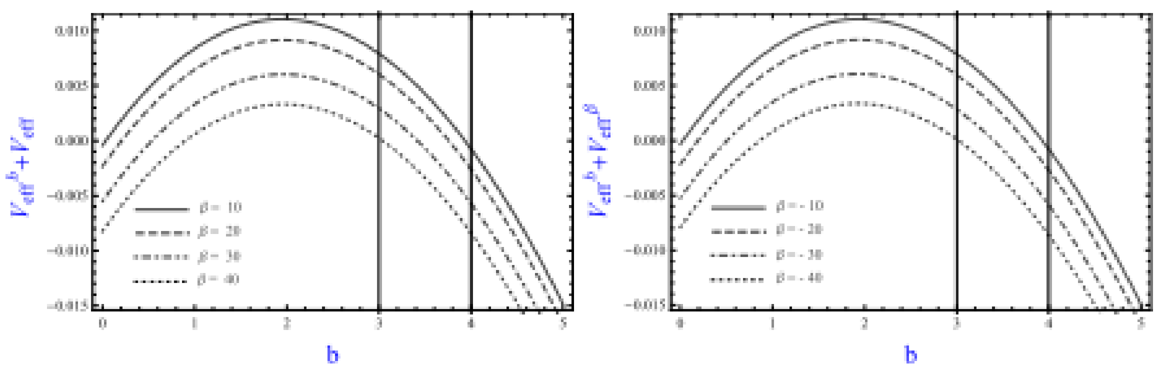

Figure 3.2: The dependence of the effective potential at the maximum point r_{max} near the extremal rotating black hole placed in a magnetic field of strength B on the parametrization parameter b for both the negative $\beta < 0$ and positive $\beta > 0$ cases for the different values of magnetic parameter β in the case in which the charge parameter $\tilde{e} = 10^{-3}$.

Using Eq. (3.18), the effective potential for radial motion can be given as

$$V_{\text{eff}} = -\frac{1}{2r^2}\left[\left(r^2 + a^2 + \frac{2Ma^2}{r}\right)\left(\delta\tilde{E}^2 - \frac{\beta^2}{4M^2}\Delta\right) - \left(1 - \frac{2M}{r}\right)\delta\tilde{J}^2 - \frac{4Ma\,\delta\tilde{E}\,\delta\tilde{J}}{r} - \Delta\left(1 - \frac{\beta\,\delta\tilde{J}}{M}\right)\right], \tag{3.19}$$

where the magnetic parameter $\beta = qBM/m$ measures the influence of the magnetic field on charged particle motion.

We study the effective potential in order to understand the effect of magnetic field on the process of destroying a black hole. We would like to be sure that the particle with the energy and angular momentum in the appropriate range as described in the earlier section will start from a infinity and fall toward the black hole without encountering any turning point.

The effective potential can be written in the form

$$V_{eff} = -\frac{\delta\tilde{E}^2}{2}\left(V^b_{eff} + V^\beta_{eff}\right), \tag{3.20}$$

Where V^β_{eff} is defined as

$$V^\beta_{eff} = \beta\left[\frac{2 + b\epsilon}{\delta\tilde{E}} - \frac{8\tilde{e} - 2b\tilde{e} + \beta(1 - 4\epsilon^2)}{2\delta\tilde{E}^2} - \frac{(4 + 2b\epsilon)/\delta\tilde{E} - (8\tilde{e} - 2b\tilde{e})/\delta\tilde{E}^2}{r} + \frac{(16b\tilde{e} - 64\tilde{e} + 3\beta)/\delta\tilde{E}^2}{4r^2} + \frac{(2 + b\epsilon - 8\epsilon^2)/\delta\tilde{E} - (4b\tilde{e} - 16\tilde{e} + 2\beta)(\epsilon/\delta\tilde{E})^2}{r^2} - \frac{\beta(1 - 8\epsilon^2)/\delta\tilde{E}^2}{2r^3}\right], \tag{3.21}$$

and V_{eff}^{b} was given in Eq. (3.10). We have expanded the potential (3.19) out to second order in ϵ.

We now try to understand the effect of the test magnetic field on the motion of the test particle and see whether or not it can serve as a cosmic censor in the process of destroying a black hole.

For a particle with a given mass and charge, the magnetic parameter β increases with the increasing magnetic field. For low values of the magnetic fields and parameter β it will not be possible for magnetic field to prevent particles from entering the black hole and turning it into the naked singularity. However, with increase of the magnetic field and parameter β the motion of the charged particles is significantly affected. We plot effective potential at the maximum $V_{eff}^{b}+V_{eff}^{\beta}$ as a function of parameter b. The allowed range of the angular momenta for which it is possible to destroy black hole is given by (3, b_{cr}) where $V_{eff}^{b}+V_{eff}^{\beta}$ is positive. As we can see from the Fig. 3.2, b_{cr} tends to decrease as we increase the magnitude of parameter β. At a certain critical value of β, we have $b_{cr} = 3$. Beyond this value, it is not possible for the charged particle to enter the black hole, and the test magnetic field serves as a cosmic censor.

The effective potential for the radial potential is plotted in Fig. 3.3. When the magnetic field is zero, the maximum of the effective potential is negative, thus allowing an infalling particle to enter the black hole. As we increase the magnetic field, the height of maximum tends to increase. Beyond a certain value of the magnetic field, the maximum value crosses zero and is positive. Thus, the infalling particle will turn back and will not be able to enter the black hole.

We have shown that if the magnetic field is sufficiently large it can prevent an infalling particle from entering the black hole and thus could in principle serve as a cosmic censor. In the next section, we try to gauge how large the critical magnetic field is by comparing its backreaction to that of the test particle.

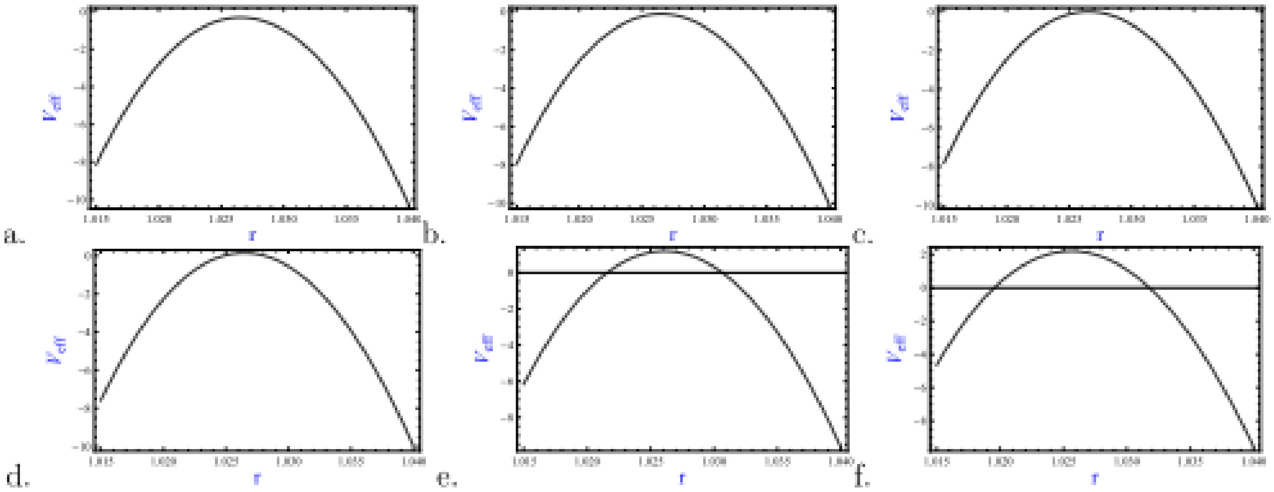

Figure 3.3: Radial dependence of the effective potential on the radial motion of the charged particle moving around the nearextremal rotating black hole immersed in a magnetic field of strength B for the different values of magnetic parameter β. For this figure, β = 0 (a), β = 0.01 (b), β = 0.1 (c), β = 1 (d), β = 5 (e), and β =10 (f) in the case when parametrization parameter b = 3.9863 and charge parameter $\tilde{e} = 10^{-3}$.

§3.4 Analyzing the backreaction of the magnetic field on background spacetime

We have shown that the test magnetic field can potentially serve as the cosmic censor, preventing a particle that can turn a near-extremal black hole into a naked singularity in the absence of magnetic field from entering the black hole. In this section, we try to understand how large the threshold magnetic field is. As we describe below, we do that by comparing the strength of the perturbation of the magnetic field on the background space-time with that of the test particle.

The effect of the test particle on the background spacetime can be understood in terms of the change in the Kretschmann scalar between extremal and near-extremal geometry at the horizon. The backreaction of the magnetic field can be expressed in terms of the density of the energy momentum tensor of the test magnetic field calculated at the horizon of the black hole. The trace of the energy momentum tensor has units of density, whereas the Kretschmann scalar has units of the square of the density. Thus, to compare the backreaction of the test particle on the background geometry to that of test magnetic field, we compare square root of the change in the Kretschmann scalar to the density of the energy-momentum tensor.

The Kretschmann scalar for the Kerr metric is given by the expression

$$K = R^{\alpha\beta\mu\nu}R_{\alpha\beta\mu\nu} = \frac{48M^2\left(r^2-a^2x^2\right)}{\left(r^2+a^2x^2\right)^6}\left((r^2+a^2x^2)^2-16a^2r^2x^2\right), \quad (3.22)$$

where $x = \cos\theta$.

We calculate the square root of the difference of the Kretschmann scalar at the horizon for extremal and nearextremal geometries, subtract, and take a square root,

$$K = (K_1-K_2)^{1/2} = 6\sqrt[4]{2}\left[2\sqrt{2}\left(\frac{1-7x^6+35x^4-21x^2}{(1+x^2)^7}\right)^{1/2}(\epsilon)^{1/2} - \frac{7-2x^{10}+47x^8-224x^6+434x^4-182x^2}{(1+x^2)^8\left(\frac{1-7x^6+35x^4-21x^2}{(1+x^2)^7}\right)^{1/2}}(\epsilon)^{3/2}\right], \quad (3.23)$$

which measures the change in the curvature in the background space-time due to the test particle.

We now calculate the density of the magnetic field:

$$T^{\mu\nu} = \frac{1}{4\pi}(F^{\mu}_{\sigma}F^{\nu\sigma} - \frac{1}{4}g^{\mu\nu}F_{\sigma\lambda}F^{\sigma\lambda}). \quad (3.24)$$

The density of the magnetic field is given by

$$
\begin{aligned}
T = &-\frac{B^2}{2\Sigma^8}\left(\Sigma^2 - 4M^2r^2\right) \\
&\times \left[\frac{\Sigma^2 x^2\left((\Xi - 4a^2Mr)(r^2+a^2) - a^2\Sigma\Delta(1-x^2)\right)^2}{\Xi}\right. \\
&-\frac{4a^6M^2r^2\Sigma^2x^2(x^2-1)(1+x^2)^2}{\Sigma+2Mr} \\
&+\frac{(\Xi+4M^2r^2)\Sigma^2(1-x^2)}{\Xi(\Sigma+2Mr)}\left[-\Xi r + 4a^2Mr^2 + 2\Sigma r^3 + a^2(r-M)\Sigma(1+x^2)\right]^2 \\
&+\frac{a^2x^2(1-x^2)}{\Xi(\Sigma+2Mr)}\left[\Xi\left(\Sigma r^2 + a^2(\Sigma+4Mr) - 1\right)\right. \\
&\left.-a^2(\Sigma+2Mr)\left(4a^2Mr + 4Mr^3 + \Delta\Sigma(1-x^2)\right)\right]^2 \\
&-\frac{a^2M^2}{\Xi}\left[\frac{\Xi\Sigma(1+x^2)(r^2-a^2x^2)}{\Sigma+2Mr} - r(1-x^2)\left(-\Xi r + 4a^2Mr^2\right.\right. \\
&\left.\left.\left.+2\Sigma r^3 + a^2(r-M)\Sigma(1+x^2)\right)\right]^2\right].
\end{aligned} \tag{3.25}
$$

Here, we have S = $(r^2 + a^2)^2 - a^2\Delta(1 - x^2)$. At the horizon, the density is given by

$$
T = \frac{B^2\left(25 + 77x^2 + x^4 - 99x^6 - 109x^8 + 11x^{10} + 63x^{12} + 27x^{14} + 4x^{16}\right)}{2\left(1+x^2\right)^8\left(3+x^2\right)}, \tag{3.26}
$$

We now find the critical value of the magnetic field for which the square root of change in the Kretschmann scalar between the extremal and near-extremal configurations at the horizon is equal to the density of the magnetic field at the horizon:

$$
K = (K_1 - K_2)^{1/2} \sim T, \tag{3.27}
$$

We set $x = \cos\theta = 0$ as we restrict ourselves to the equatorial plane.

For the value chosen in this analysis, $\epsilon = 0.01$, the critical value of the magnetic field is given by

$$
B_{cr} \sim 0.6872. \tag{3.28}
$$

We have shown that the magnetic field can possibly act as a cosmic censor, preventing a charged test particle from entering the black hole that can turn it into a naked singularity. We now compare the strength of the requisite magnetic field by comparing its backreaction to that of the test particle. That can be done by comparing the strength of the magnetic field to that of the critical magnetic field defined above, B_{cr}.

Table 3.3:

The values of parameter b_{cr} for the different values of e for the charge parameter $\tilde{e}$ $= 10^{-3}$.

β		b_{cr}	
	$\epsilon = 0.01$	$\epsilon = 0.0001$	$\epsilon = 0.000001$
3.84×10^{1}	2.982423607	2.954112182	2.954934151
3.84	3.979232348	3.992297928	3.992304539
19.2×10^{-1}	3.984852247	3.998076544	3.998079014
11.52×10^{-1}	3.985953499	3.999307076	3.999308666
7.68×10^{-1}	3.986259107	3.999691452	3.999692771
3.84×10^{-1}	3.986401494	3.999922037	3.999923197
3.84×10^{-2}	3.986390120	3.999998118	3.999999231
3.84×10^{-4}	3.986380799	3.999998881	3.9999999998
3.84×10^{-6}	3.986380698	3.999998886	3.9999999999

We stated the values of parameters β and $\tilde{e}$ while calculating the effective potential in the previous sections to understand whether the magnetic field can prevent the charged particle from entering the black hole. To compare the back-reaction of the magnetic field to that of test particle, we have to calculate the value of the magnetic field and compare it to the critical value. Eliminating the charge e in the expression for the parameter β, one can get

$$\beta = \sqrt{\frac{2\tilde{e}}{m}} MB. \tag{3.29}$$

This equation allows us to relate the magnetic field B with β and $\tilde{e}$ for the given mass of the test particle m. We may take M = 1. Since we assume that $\widetilde{\delta E}$ δE $\sim 2\delta E/m$ is large and $\delta E \sim \epsilon$, we take $m \sim \epsilon^{2}$.

We now analyze the effective potential for the same values of parameters we have chosen and see whether magnetic field can act as a cosmic censor by calculating the critical value $b_{\rm cr}$. We compute and compare the magnetic field to the critical value.

We get the results for the different near-extremal cases tabulated in Table 3.3. For the values of β, we find that $b_{\rm cr}$ initially increases and then it tends to decrease as we increase parameter β. In Table 3.4, we have tabulated the values of β beyond which the magnetic field starts acting as a cosmic censor and the ratio B/B_{cr}. Thus, the backreaction of the magnetic field on the background space-time is comparable to the tiny backreaction of the test particle. Thus, the magnetic field necessary to restore the cosmic censorship is extremely small. The behavior of the results presented in Table 3.4 is also explained in Fig. 3.4.

However, since the backreaction of the magnetic field on the background spacetime is comparable to that of the test particle, one must take into account the effect of magnetic field on the background space-time while analyzing whether or not it can act as a cosmic censor. Various exact magnetized black hole solutions have been obtained [144, 145]. However, there is no exact solution that represents a near-extremal black hole. Thus, it is a daunting task to take into account the effect of the magnetic field on the background metric.

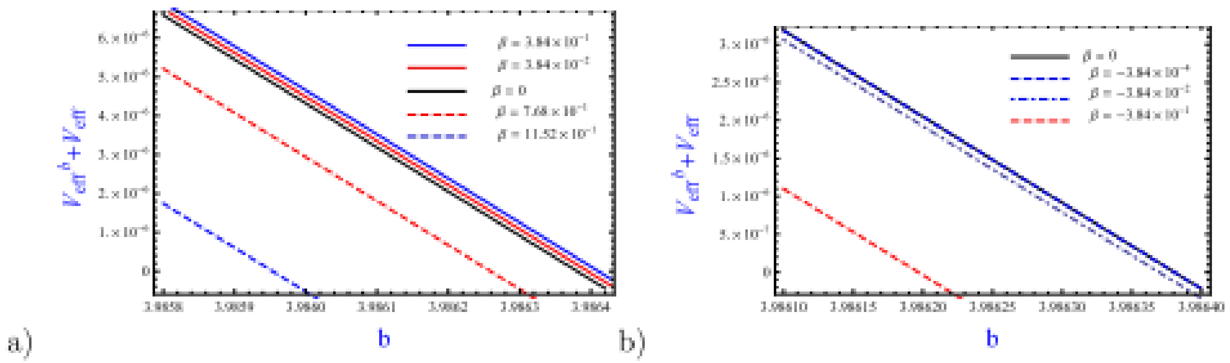

Figure 3.4: The value of the effective potential at the maximum as a function of b is plotted for positive as well as negative values of β and for charge parameter $\tilde{e} = 10^{-3}$. The magnetic field is sufficiently smaller than the critical value b_{cr} initially increases, and then it decreases. We have $b_{cr} > 3$. Thus, when backreaction of the magnetic field can be ignored, it does not serve as a cosmic censor.

To understand the effect of the backreaction of the magnetic field, we carried out a slightly different investigation involving the process of destroying a near-extremal Reissner-Nordstrom black hole with a radially moving charged particle. We then involve the magnetic field. Since the exact solution depicting a magnetized Reissner-Nordstrom black hole is available in the literature [145], we can take into account the effect of the magnetic field both on the background geometry as well as the charged particle motion. We find that the magnetic field acts as a cosmic censor beyond a threshold value.

§3.5 Conclusion

Here, we studied the process of turning a black hole into a naked singularity by throwing in the test particle with appropriate values of the geodesic parameters. It is possible to turn a near-extremal Kerr black hole into a Kerr-Newmann naked singularity using a charged test particle. Typically, in the astrophysical context, black holes are surrounded with a magnetic field that would exert a Lorentz force on the charged particle affecting its motion. Thus, we study the effect of the test magnetic field on the process of destroying a black hole. We invoke a weak magnetic field that takes a constant value at infinity and is aligned with the axis of symmetry of Kerr geometry.

We have shown that for sufficiently large values of the magnetic field it is not possible for a particle with the appropriate values of geodesic parameters to enter the black hole and turn it into the naked singularity. Thus, it appears that test magnetic field could serve as a cosmic censor. To gauge the strength of the requisite magnetic field, we compute the density of the magnetic field and compare it with the square root of the change in the Kretschmann scalar at the horizon between extremal and near-extremal configurations, which is a measure of the effect of the test particle on the background space-time.

We have found that when the magnetic field acts as a cosmic censor its back-reaction is slightly larger than that of the test particle. Therefore, we need an extremely small magnetic field to restore the cosmic censorship in the process of destroying a near-extremal Kerr black hole with a charged test particle. However, since the backreaction of the magnetic field is stronger than that of the test particle, one must take account its effect on the metric, which is difficult to implement in the absence of any near-extremal rotating magnetized black hole solution. We expect that the results obtained without considering the backreaction of the magnetic field are expected to hold well even in the presence of the backreaction and that the magnetic field would act as a cosmic censor.

Table 3.4:

The value of parameter β_{cr} at which we have b_{cr} = 3 and the magnetic field starts acting as a cosmic censor is tabulated here. The ratio of the magnetic field to the critical value is also specified. We find that the magnetic field is around ten times larger than the critical magnetic field B_{cr} when it starts acting as a cosmic censor. The result is similar for different nonextremal cases.

$b_{cr} = 3$					
m	0.0001	0.0001	0.0001	0.0001	0.0001
$\tilde{e}$	10^{-3}	10^{-4}	5×10^{-5}	10^{-5}	5×10^{-6}
$\epsilon = 0.01$					
β_{cr}	37.0809	12.3265	9.1618	5.4369	4.7714
	-36.8021	-12.3011	-9.1490	-5.4342	-4.7699
B/B_{cr}	9.6514	10.1457	10.6644	14.1512	17.5631
	9.5788	10.1248	10.6495	14.1442	17.5576
$\epsilon = 0.0001$					
β_{cr}	37.8413	11.9930	8.4816	3.7937	2.6827
	-37.8242	-11.9937	-8.4819	-3.7938	-2.6828
B/B_{cr}	9.8493	9.8711	9.8727	9.8742	9.8748
	9.8448	9.8717	9.8730	9.8745	9.8752
$\epsilon = 0.000001$					

β_{cr}	37.8510	11.9963	8.4838	3.7945	2.6832
	-37.8365	-11.9972	-8.4844	-3.7947	-2.6833
B/B_{cr}	9.8510	9.8739	9.8752	9.8763	9.8766
	9.8481	9.8746	9.8759	9.8768	9.8770

CHAPTER IV. ENERGY EXTRACTION FROM GRAVITATIONAL COMPACT OBJECTS

§4.1 Introduction

At present there is no any observational evidence for the existence of gravito-magnetic monopole so-called NUT (Newman, Unti & Tamburino [146]) parameter or *magnetic mass.* Therefore study of the motion of the test particles and energy extraction mechanisms in NUT spacetime may provide new tool for studying new important general relativistic effects which are associated with nondiagonal components of the metric tensor and have no Newtonian analogues [147-149], where solutions for electromagnetic waves and interferometry in spacetime with NUT parameter have been studied. Kerr-Taub-NUT spacetime with Maxwell and dilation fields is recently investigated by [150]. The plasma magnetosphere around a rotating, magnetized neutron star and charged particle motion around compact objects immersed in external magnetic field in the presence of the NUT parameter have been studied in Refs. [64, 151].

Penrose process [19] for the extraction of energy from rotating black hole is based on the existence of negative energy orbits in the ergosphere, the region bounded by the event horizon and the static limit. The possibility that astro- physical jet collimation may arise from the geometry of rotating black holes and the presence of high-energy particles resulting from a Penrose process rather than from effect of the magnetic fields has been examined [152]. Detailed study of the energetics of the Kerr-Newman black hole by the Penrose process is given by [153]. Energetics of a rotating charged black hole in 5-dimensional supergravity has been recently considered by [154].

The geodesics of the Kerr-Taub-NUT spacetime share many of the properties of the ergosphere in the field of a magnetic monopole. A thorough discussion and comparison of these orbits can be found in papers [155, 156].

The ultra-high center-of-mass energy can be produced by particles colliding near the horizon of fastly rotating black holes. Really, it has been shown by Banados, Silk and West [157] (the BSW effect) that an extremal Kerr black hole acts as a particle accelerator to arbitrary high energies in the center of mass frame, if two particles with fine tuned motion constants collide near its horizon. Therefore, the extremal rotating black hole could be considered as Planck-energy- scale colliders.

The BSW effect attracted strong attention in recent years [2, 3, 60, 66, 121, 135, 159-165]. It has been studied in the framework of standard general relativity for spinning black holes [121], charged black holes [160], weakly magnetized black holes [60], Kerr naked singularity [135, 167, 168], weakly magnetized non-rotating black holes with magnetic charge [66], Kerr-Taub- NUT black holes [166]. It was demonstrated that the ultra-high energy collisions obtained in the field of rotating black holes can be also strongly enhanced by the black hole charges, or by the external magnetic field. In this sense, ultra- high energy collisions were also studied near the horizon of a rotating black hole immersed in an external magnetic field [118], under assumption that the back- reaction effect of the magnetic field does not modify the background geometry, being infinitesimal in real astrophysical scenarios. Relations of the BSW effect and the well known Penrose processes were studied in [1]. The mechanism of formation of black holes from collisions of particles in vicinity of a supermassive black hole acting as a BSW particle accelerator was investigated in [3], along with possibility of the black hole collisions.

Later, studies of the BSW effect were extended to the black hole solutions related to alternate gravity theories, or to the complementary versions to the black hole solutions, as the naked singularity solutions, or the regular no-horizon solutions complementary to the regular black hole solutions [169]. Large efficiency of the BSW effect, even in relation to their observability by distant observers, has been demonstrated in the case of near-extreme Kerr superspinars [170]. Ultra- high-energy collisions of charged particles have been shown to exist in the field of near-extreme Kehagias-Sfetsos (Horava-Lifshitz quantum gravity) black holes and naked singularities [170, 172], the rotating black holes in the Randall-Sundrum braneworld [2], the rotating regular black holes [173], or in multidimensional space- times of black string [81], and 6-dimensional rotating black holes in pure Gauss- Bonnet gravity [68]. High-energy collisions near the horizon of axially symmetric black holes were considered for a number of collision scenarios in [119], concluding that the growth of the collision energy can be restricted by the back-reaction effect of the magnetic field on the spacetime geometry. It is worth to note that in [119] black holes surrounded by matter, called "dirty" black holes, were studied, using the Taylor expansion of metric coefficient due to the matter influence near the horizon. In the paper [119] the magnetic field is adopted from Wald [84]. Of course, the presence of matter implies that the background geometry is no longer Ricci-flat, implying corresponding modification of the Maxwell equations. Here we deal with the rotating black hole spacetimes modified by the quintessential field representing one of the alternatives of dark energy. The quintessential rotating black holes [113] are constructed from the exact spherically symmetric Kiselev solution of Einstein equations taking into account the influence of the quintessential scalar field influencing the whole Universe [112]. The main aim of the present study is to consider the contribution of an external magnetic field surrounding quintessential rotating and non-rotating black holes on charged particle motion and collisions.

The most important black hole solution with axial symmetry is the Kerr one [174], which is asymptotically flat, and its anti-de Sitter (AdS) and de Sitter (dS) generalizations were obtained by Carter [175]. The latter case, the dS solution, is more appropriate, for instance, to model a black hole in an expanding universe. Observations [176] suggest that our universe is dominated by an accelerated expansion, described in the ΛCDM model with a positive cosmological constant.

On the other hand, AdS solutions have been used in the so-called AdS correspondence [177].

In the first Randall-Sundrum model (RS-I) [178], the hierarchy problem was considered with the introduction of a warp factor in the bulk metric. In this case, the bulk is described by a five-dimensional AdS spacetime, which has two 3-branes as boundaries (our universe and a hidden universe). The extra dimension is compact and it has a finite radius. On other hand, the second Randall-Sundrum model (RS-II) [179] adopts only a single 3-brane; in this case the extra dimension's radius is infinite.

For astrophysical interests, static and spherically symmetric exterior vacuum solutions of the brane world models were initially proposed by Dadhich et al. [180, 181], which have the mathematical form of the Reissner-Nordstrom solution where a tidal Weyl parameter Q* plays the role of the electric charge squared of the general relativistic solution. The so-called Dadhich-Maartens- Papodopoulos- Rezania [181] solution was obtained by imposing the null energy condition on the three-brane for a bulk having nonzero Weyl curvature. Braneworld corrections to the charged rotating black holes and to the perturbations in the electromagnetic potential around black holes were studied in Refs. [182, 183].

The spherically symmetric solutions have been considered in Refs. [184, 185], where black hole and wormhole solutions have been constructed, assuming a zero value for the cosmological constant in the brane. The authors of Ref. [186] generalized these solutions, considering a negative value of the cosmological constant in the brane. A wormhole solution in an asymptotically de Sitter brane was obtained in Ref. [187]. An axially symmetric vacuum solution of the gravitational field equations in a Randall- Sundrum brane (RSB) for rotating black holes was studied in Ref. [188].

Brane world models of black holes have been studied since the 1990s [180, 189]. In the model presented by Arkani-Hamed, Dimopoulos, and Dvali (ADD) [190, 191], the brane-our universe-is embedded in a $(4 + d)$-dimensional spacetime called the bulk. The d extra dimensions are compact, and all fields are confined on the brane. In the preliminary calculations of Refs. [147, 190], the authors have stressed that for $d > 1$ the extra dimensions have radii in the millimeter scale. One basic motivation for the ADD model was to solve the hierarchy problem, which is the difference between the electroweak scale (~ $\underline{TeV}$) and the 4-dimensional Planck scale (~ $10^{16} TeV$). According to this model, the electroweak scale is the fundamental scale, and the $(4 + d)$-dimensional Planck scale has the same order. Another important option to solve the hierarchy problem was the so-called Randall-Sundrum brane model. The ADD picture evolved to scenarios where the extra dimension can be unbounded. Optical properties of rotating braneworld black holes have been studied in Ref. [192].

In Sec. 3.2, we study the ergosphere and motion of the test particles in the Kerr-Taub-NUT spacetime. The Sec. 3.3 is devoted to study the energy extraction mechanisms through Penrose process in the Kerr-Taub-NUT spacetime. The Sec. 3.4 is devoted to the study of the collision of two particles with the same rest masses moving at the equatorial plane around a rotating black hole in a Randall-Sundrum brane with a nonvanishing effective cosmological constant. We consider in detail the center-of-mass energy for the colliding particles in the fourdimensional brane spacetime, and evaluate the ejected particles' energy from a collision of two accelerating particles near the black hole. In Sec. 3.5, we investigate influence of an external magnetic field of strength $\underline{B}$ on the collision of two particles that both freely fall from large distances (near the static radius), and the collision of freely falling particle with a charged particle following the innermost stable circular orbit of a rotating black hole surrounded by a quintessential energy. We summarize our results and give some concluding remarks in the Sec. 3.6.

§4.2 Properties of ergosphere around rotating black holes

We consider electromagnetic fields of compact astrophysical objects in Keer-Taub-NUT spacetime which in a spherical coordinates (ct,r,θ,φ) is described by the metric [193, 194]

$$
\begin{aligned}
ds^2 &= -\frac{1}{\Sigma}\left(\Delta - a^2\sin^2\theta\right)dt^2 + \frac{2}{\Sigma}\left[\Delta\chi - a(\Sigma + a\chi)\sin^2\theta\right]dtd\varphi \\
&\quad + \frac{\Sigma}{\Delta}dr^2 + \Sigma d\theta^2 + \frac{1}{\Sigma}\left[(\Sigma + a\chi)^2\sin^2\theta - \chi^2\Delta\right]d\varphi^2,
\end{aligned} \tag{4.1}
$$

where parameters Σ, Δ and x are defined by

$$\Sigma = r^2 + (l + a\cos\theta)^2,\ \Delta = r^2 - 2Mr - l^2 + a^2,\ \text{and}\ \chi = a\sin^2\theta - 2l\cos\theta,$$

where M is the total mass, a is the specific angular momentum, and l is the NUT parameter of the central object.

The spacetime (4.1) has a horizon where the 4 velocity of a co-rotating observer turns to null, or the surface $r = const$ becomes null:

$$r_H = M + \sqrt{M^2 + l^2 - a^2}. \tag{4.2}$$

The static limit is defined where the time-translation Killing vector $\xi_{(t)} = \partial/\partial t$ becomes null (i.e. $g_{00} = 0$) and static limit of the black hole can be described as

$$r_{st} = M + \sqrt{M^2 + l^2 - a^2\cos^2\theta}. \tag{4.3}$$

Considering only the outer horizon, r_H and static limit, r_{st}, it can be verified that the static limit always lies outside the horizon. The region between the two is called the ergosphere, where timelike geodesics cannot remain static but can remain stationary due to corotation with the BH with the specific frame dragging angular velocity at the given location in the ergosphere. This is the region of spacetime where timelike particles with negative angular momentum relative to the BH can have negative energy relative to the infinity.

In Fig. 4.1 the dependence of the shape of the ergosphere from small dimensionless parameter $\tilde{l} = l/M$ is shown. From the dependence one can easily see that in the presence of the NUT parameter radius of the event horizon becomes larger. However a relative volume of the ergosphere is decreased.

Due to the existence of an ergosphere around the black hole, it is possible to extract energy from it by means of the Penrose process. Inside the ergosphere, it is possible to have a timelike or null trajectory with negative total energy. As a result, shoot a small particle A into the ergosphere from outside with energy at infinity. When the particle is deep down near the horizon, let it to explode into two parts,

B and C, one of which attains negative energy relative to infinity and

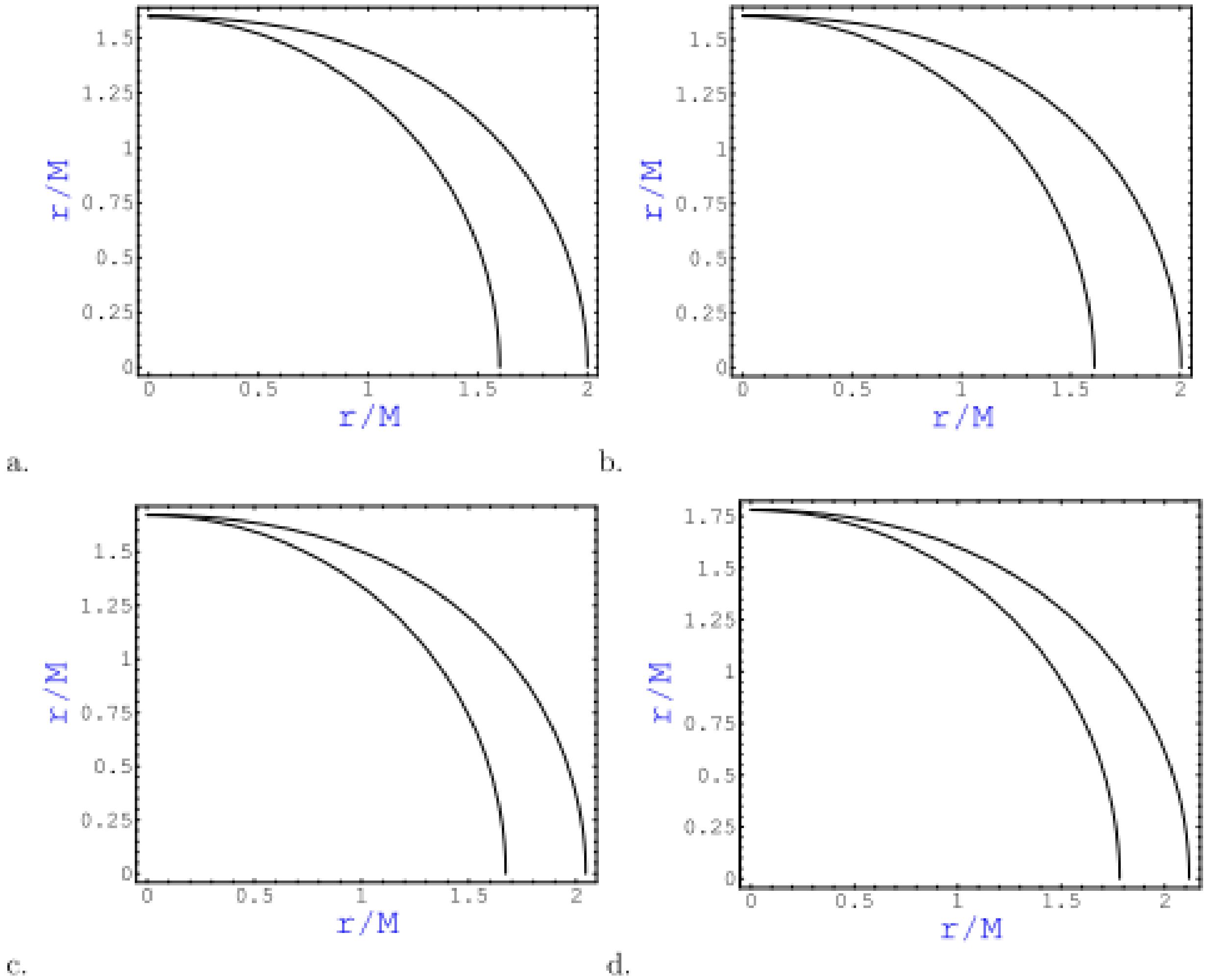

Figure 4.1: The dependence of the shape of the ergosphere from the small dimensionless NUT parameter l: a) $l = 0$, b) $l = 0.1$ c) $l = 0.3$ d) $l = 0.5$.

falls down the hole but other part escapes back to radial infinity by conservation of energy with energy greater than that of the original incident particle. This is how the energy could be extracted from the black hole by axial accretion of particles with the suitable angular momentum and NUT parameters. Consider the equation of motion of such negative energy particle. The Lagrangian for this particle can be written as:

$$\begin{aligned} 2\mathcal{L} &= -\frac{1}{\Sigma}\left(\Delta - a^2\sin^2\theta\right)\dot{t}^2 + \frac{2}{\Sigma}\left[\Delta\chi - a(\Sigma + a\chi)\sin^2\theta\right]\dot{t}\dot{\varphi} \\ &+ \frac{\Sigma}{\Delta}\dot{r}^2 + \Sigma\dot{\theta}^2 + \frac{1}{\Sigma}\left[(\Sigma + a\chi)^2\sin^2\theta - \chi^2\Delta\right]\dot{\varphi}^2, \end{aligned} \tag{4.4}$$

and according to (3.4) the generalized momenta are given by

$$p_t = -\frac{1}{\Sigma}\left(\Delta - a^2\sin^2\theta\right)\dot{t} + \frac{1}{\Sigma}\left(\Delta\chi - a(\Sigma + a\chi)\sin^2\theta\right)\dot{\varphi} = E, \tag{4.5}$$

$$-p_\varphi = -\frac{1}{\Sigma}\left(\Delta\chi - a(\Sigma + a\chi)\sin^2\theta\right)\dot{t} - \frac{1}{\Sigma}\left((\Sigma + a\chi)^2\sin^2\theta - \chi^2\Delta\right)\dot{\varphi} = L, \tag{4.6}$$

$$-p_r = -\frac{\Sigma}{\Delta}\dot{r}, \quad \text{and} \quad -p_\theta = -\Sigma\dot{\theta}, \tag{4.7}$$

where superior dots denote differentiation with respect to an affine parameter τ. (The conservation of p_t and p_φ follows from the independence of the Lagrangian on *t* and *φ* which, in turn, is a manifestation of the stationary and the axisymmetric character of the Kerr- Taub-NUT geometry.)

Then from the expressions (4.5) and (4.6) one can easily obtain the expressions for *φ* and *t* as

$$\dot{\varphi} = \frac{1}{\Delta}\left[\frac{(\Delta - a^2\sin^2\theta)(\chi E - L) - a\Sigma E\sin^2\theta}{\Sigma\sin^2\theta}\right], \tag{4.8}$$

$$\dot{t} = -\frac{1}{\Delta}\left[\frac{\Delta\Sigma L}{\Delta\chi - a(\Sigma + a\chi)\sin^2\theta} + \frac{(\Sigma + a\chi)^2\sin^2\theta - \chi^2\Delta}{\Sigma\left(\Delta\chi - a(\Sigma + a\chi)\sin^2\theta\right)} \times \left((\Delta - a^2\sin^2\theta)(\chi E - L) - a\Sigma E\sin^2\theta\right)\right]. \tag{4.9}$$

It was first shown by [155] for spherical symmetric case (NUT spacetime) and later by [194] for axial symmetric case (Kerr-Taub-NUT spacetime) that the orbits of the test particles are confined to a cone with the opening angle *θ* given by $\cos\theta = 2El/L$. It also follows that in this case the equations of motion on the cone depend on *l* only via l^2 [64, 194]. The main point is that the small value for the upper limit for gravitomagnetic moment has been obtained by comparing theoretical results with experimental data as (i) $l < 10^{-24}$ from the gravitational microlensing [195], (ii) $l < 1.5 \cdot 10^{-18}$ from the interferometry experiments on ultra-cold atoms [149], (iii) and similar limit has been obtained from the experiments on Mach-

Zehnder interferometer [148]. Due to the smallness of the gravitomagnetic charge let us consider the motion in the quasi-equatorial plane when the motion in θ direction changes as $\theta = \pi/2 + \delta\theta(t)$, where $\delta\theta$ (t) is the term of first order in l, then it is easy to expand the trigonometric functions as $\sin\theta = 1 - \delta\theta^2(t)/2 + O(\delta\theta^4(t))$ and $\cos\theta = \delta\theta(t) - O(\delta\theta^3(t))$. Now neglecting the small terms O($\delta\theta^2$(t)), one can

$$\Sigma\dot{r}^2 \;=\; 2(L-aE)^2\frac{(Mr+l^2)}{r^2+l^2}+E^2(r^2+a^2+l^2)-L^2-\delta\Delta. \tag{4.10}$$

As we have noted, $\delta = 0$ for null geodesics and equation for radial motion (4.10) becomes

$$\Sigma\dot{r}^2 = 2(L-aE)^2\frac{(Mr+l^2)}{r^2+l^2}+E^2(r^2+a^2+l^2)-L^2. \tag{4.11}$$

Hereafter, it is more convenient to distinguish the geodesics by the impact parameter $D = L/E$. First, we study the geodesics with the impact parameter

$$D = a, \quad \text{when} \quad L = aE, \tag{4.12}$$

and equations (3.8), (3.9) and (3.11) reduce to

$$\dot{r} = \pm E, \qquad \dot{t} = -(r^2+a^2+l^2)\frac{E}{\Delta}, \quad \text{and} \quad \dot{\varphi} = -\frac{aE}{\Delta}. \tag{4.13}$$

The radial coordinate is uniformly described with respect to the affine parameter while the equations governing t and p are

$$\frac{dt}{dr} = \pm\frac{r^2+a^2+l^2}{\Delta}, \quad \frac{d\varphi}{dr} = \pm\frac{a}{\Delta}. \tag{4.14}$$

§4.3 Energy extraction through Penrose process in the Kerr- Taub-NUT object with gravitomagnetic monopole charge

Let us continue our assumption that the deflection in θ direction is reasonably small and orbits of the particles are in the quasi-equatorial plane $\theta = \pi/2 + \delta\theta(t)$. Using the assumptions mentioned in previous section one can easily rewrite the expressions (4.5) and (4.6) in the approximation $O(\delta\theta^2(t))$ as a quadratic equation in energy:

$$\alpha E^2 - 2\beta E + \gamma + \frac{\Sigma}{\Delta}(p^r)^2 + \Sigma(p^\theta)^2 + m^2 = 0, \tag{4.15}$$

where we have used the following notations

$$\alpha = -\left(1 - 2\frac{Mr + l^2}{r^2 + l^2}\right), \quad \beta = 4a\frac{Mr + l^2}{r^2 + l^2}L,$$
$$\gamma = \left(r^2 + a^2 + l^2 + 2a^2\frac{Mr + l^2}{r^2 + l^2}\right)L^2. \tag{4.16}$$

From Eq. (3.15) one can easily obtain the equation of radial motion in the following form:

$$V_{\rm eff} = E^2 - 2\frac{(Mr + l^2)(L - aE)^2}{\Sigma(r^2 + l^2)} - \frac{E^2(r^2 + a^2 + l^2)}{\Sigma} + \frac{L^2 + \Delta}{\Sigma} \tag{4.17}$$

denotes the effective potential of the radial motion of the test particle around rotating compact object with nonvanishing NUT parameter.

In the Fig. 4.2(a) the radial dependence of the effective potential of radial motion of the massive test particle has been shown for the different values of the dimensionless parameter *l*. Here for the energy and momenta of the particle

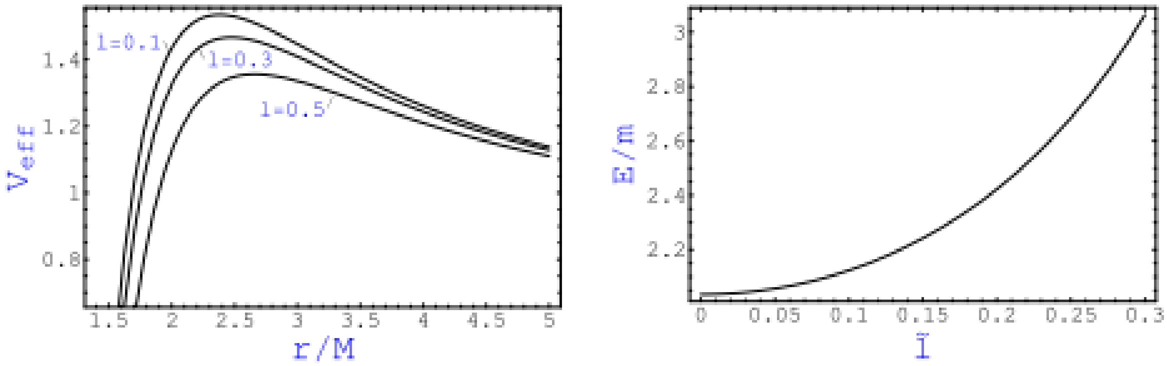

a. b.

Figure 4.2: The radial dependence of the effective potential of radial motion of the particle a) for the different values of the dimensionless NUT parameter *l* and the dependence of the extracted energy from the black hole b) on the NUT parameter.

the following values are taken: E/m = 0.9, L/mM = 4.3. The presence of the parameter l slightly shifts the shape of the effective potential down.

Now, as the particle falls through the horizon, the mass of the black hole will change by $\delta M = E$. There is no upper limit for change of mass of the central black hole. The infalling big number of particles with positive energy can essentially increase the mass of the black hole. But there is a lower limit on δM which could be added to the black hole corresponding to $m = 0$, $p^{\theta} = 0$ and $p^{r} = 0$. Evaluating all of the required quantities at the horizon $r = r_{+}$, we get the limit for the change in black hole mass as

$$\delta M = -\frac{L_z a(Mr_+ + l^2)}{r_+^2 - 2Mr_+} D, \tag{4.18}$$

where

$$\begin{aligned} D \;&=\; 4\Bigg[1 - \Bigg\{1 + \Bigg(1 - \frac{a^2(r_+^2 + 2Mr_+ + 3l^2)}{(r_+^2 + l^2)^2}\Bigg) \\ &\times \;\frac{(r_+^2 - 2Mr_+ - l^2)}{16a^2}\Bigg(\frac{Mr_+ + l^2}{r_+^2 + l^2}\Bigg)^{-2}\Bigg\}^{\frac{1}{2}}\Bigg]. \end{aligned} \tag{4.19}$$

To be able to extract energy from the black hole (δM < 0), we must therefore have

$$\frac{L_z a(Mr_+ + l^2)}{r_+^2 - 2Mr_+} D > 0. \tag{4.20}$$

In the Fig. 4.2(b) the dependence of the extracted energy from the black hole on the small dimensionless parameter l has been shown: with increasing the parameter l the relative extraction of the energy becomes more stronger. The graph shows that the extraction of the energy is directly proportional to the parameter l, that is with increasing l, the extracted energy also increases.

§4.4 Collisional energy through the BSW effect near a rotating black hole in a Randall-Sundrum brane with a cosmological constant

We investigate the center-of-mass energy for collisions of two particles at the equatorial plane and near the horizon of a rotating black hole in a Randall- Sundrum brane with a cosmological constant. The general axially symmetric vacuum solution for a rotating black hole in a Randall-Sundrum brane with a cosmological constant was obtained by Neves and Molina [188] as

$$\begin{aligned} ds^2 &= -\frac{1}{\Sigma}\left(\Delta_r - \Delta_\theta a^2 \sin^2\theta\right) dt^2 - \frac{2a}{\Xi\Sigma}\left[(r^2+a^2)\Delta_\theta - \Delta_r\right]\sin^2\theta dt d\varphi \\ &+ \frac{\Sigma}{\Delta_r}dr^2 + \frac{\Sigma}{\Delta_\theta}d\theta^2 + \frac{1}{\Xi^2\Sigma}\left[(r^2+a^2)^2\Delta_\theta - \Delta_r a^2\sin^2\theta\right]\sin^2\theta d\varphi^2 \ , \end{aligned} \tag{4.21}$$

Here the following notations are introduced:

$$\begin{aligned} \Delta_\theta &= 1 + \frac{\Lambda_{4D}}{3}a^2\cos^2\theta \ , \quad \Sigma = r^2 + a^2\cos^2\theta \ , \quad \Xi = 1 + \frac{\Lambda_{4D}}{3}a^2 \ , \\ \Delta_r &= (r^2+a^2)\left(1 - \frac{\Lambda_{4D}}{3}r^2\right) - 2Mr + \tilde{q} \end{aligned} \tag{4.22}$$

where a is a rotational parameter related to the specific angular momentum of the black hole, the conserved quantity M is the total mass, Λ_{4D} is the four dimensional brane cosmological constant, and $\tilde{q}$ is an induced charge of the black hole on the brane.

Considering colliding particles with rest masses m_1 and m_2, we compute the energy in the center-of-mass frame for this collision according to the calculation method developed in [157]. The four-momentum and the total momenta of the two colliding particles (i = 1, 2) are given by

$$p_i^\alpha = m_0 u_i^\alpha , \tag{4.23}$$

$$p_t^\alpha = \pi_1^\alpha + \pi_2^\alpha \ . \tag{4.24}$$

where u_i^μ is the four velocity of the particle i. The center of mass energy $E_{c.m.}$ of the collision between the two particles is then given by [158]

$$\frac{E_{c.m.}^2}{2m_1m_2} = \frac{m_1^2+m_2^2}{2m_1m_2} - g_{\alpha\beta}u_1^\alpha u_2^\beta\,. \tag{4.25}$$

Here, we assume two particles coming from infinity with $E_1/m_0 = E_2/m_0 = 1$, for simplicity. Using the equations of particle motion around a black hole mentioned in previous chapters one can easily obtain the following relation for the center- of-mass energy of two colliding particles at the equatorial plane of the rotating black hole in the Randall-Sundrum brane spacetime:

$$\begin{aligned}
\frac{E_{\text{c.m.}}^2}{2m_0^2} &= 1 - \frac{\left((a^2+r^2)^2 - a^2\Delta_r\right)\left[aP_1 + (-a+\mathcal{L}_1\Xi)\Delta_r\right]\left[aP_2 + (-a+\mathcal{L}_2\Xi)\Delta_r\right]}{r^6\Delta_r^2\Xi^2} \\
&+ \frac{a\left(a^2+r^2-\Delta_r\right)}{r^6\Delta_r^2\Xi}\Big(2a\left(a^2+r^2\right)P_1P_2 - \left(2a^2+r^2\right)\big[a(P_1+P_2) \\
&- (\mathcal{L}_2P_1 + \mathcal{L}_1P_2)\Xi\big]\Delta_r + 2a(a-\mathcal{L}_1\Xi)(a-\mathcal{L}_2\Xi)\Delta_r^2\Big) \\
&- \frac{\left(a^2-\Delta_r\right)\left[\left(a^2+r^2\right)P_1 + a(-a+\mathcal{L}_1\Xi)\Delta_r\right]}{r^6\Delta_r^2} \\
&\times \left[\left(a^2+r^2\right)P_2 + a(-a+\mathcal{L}_2\Xi)\Delta_r\right] \\
&- \frac{\sqrt{P_1^2 - \left[r^2 + (a-\mathcal{L}_1\Xi)^2\right]\Delta_r}\sqrt{P_2^2 - \left[r^2 + (a-\mathcal{L}_2\Xi)^2\right]\Delta_r}}{r^2\Delta_r},
\end{aligned} \tag{4.26}$$

where $P_1 = r^2 + a^2 - \Xi\,\alpha L_1$ and $P_2 = r^2 + a^2 - \Xi\,\alpha L_2$.

§4.4.1 Classification of $\boldsymbol{E_{c.m.}}$ energy of the colliding particles in 4 dimensional brane spacetime

Considering that one of the colliding particles has the maximum angular momentum L_{max} and other one has the minimum angular momentum L_{min}, we obtain the center of mass energy for the different cases using Eq. (4.26). In all cases mass of BH is taken to be $M = 1$.

First we consider the limiting case when $\tilde{q} = 0$ and $A_{4D} = 0$. The event horizon is located at $r_+ = 1$ in the case when $\alpha = 1$. Center of mass energy is infinite in this case and has the following limit:

$$\frac{E_{\text{c.m.}}^2}{2m_0^2}(r \to r_+) = \frac{\mathcal{L}_2 - 2}{\mathcal{L}_1 - 2} + \frac{\mathcal{L}_1 - 2}{\mathcal{L}_2 - 2}, \tag{4.27}$$

which is indeed finite for generic values of L_1 and L_2.

Next we consider case with a nonvanishing $\tilde{q}$ and $A_{4D} = 0$. Then the event horizon is also located at $r_H = 1 + \sqrt{1 - a^2 - \tilde{q}} = 1$ when the condition $\tilde{q} = 1 - a^2$ is satisfied. In the presence of the brane parameter, Eq. (4.26) reduces to

$$\begin{aligned}\frac{E^2_{\text{c.m.}}}{2m_0^2}(r \to r_H) &= \frac{\mathcal{L}_2 - \mathcal{L}_H}{\mathcal{L}_1 - \mathcal{L}_H} + \frac{\mathcal{L}_1 - \mathcal{L}_H}{\mathcal{L}_2 - \mathcal{L}_H} - \frac{1}{4}\frac{(\mathcal{L}_1 - \mathcal{L}_2)^2}{(\mathcal{L}_1 - \mathcal{L}_H)(\mathcal{L}_2 - \mathcal{L}_H)} \\ &+ \frac{27\sqrt{2}(\mathcal{L}_1 + \mathcal{L}_2) + 2\mathcal{L}_1^2\mathcal{L}_2^2}{(\mathcal{L}_1 - \mathcal{L}_H)(\mathcal{L}_2 - \mathcal{L}_H)} - \frac{3\sqrt{2}(\mathcal{L}_1 + \mathcal{L}_2)\mathcal{L}_1\mathcal{L}_2 + 9\mathcal{L}_1\mathcal{L}_2}{(\mathcal{L}_1 - \mathcal{L}_H)(\mathcal{L}_2 - \mathcal{L}_H)}.\end{aligned} \tag{4.28}$$

where the critical angular momentum $L_H = (a^2 + 1)/a$. Equation (4.28) shows that the infinite center-of-mass energy can be approached if one of the colliding particles has critical angular momentum L_H, ensuring that the particle reaches the outer horizon. Next, we will determine the range of the specific angular momentum $\underline{a}$ with the help of the effective potential

$$V_{eff(\mathcal{L}\to\mathcal{L}_H)} = -\frac{(r-1)^2(r - \frac{1-a^2}{2a^2})}{r^4}. \tag{4.29}$$

As expected, the effective potential $V_{\text{eff}}(L \to L_H)$ approaches 0 at infinity. Here, we can get a condition for the particle falling freely from rest at infinity to reach the horizon,

$$V_{eff(\mathcal{L}\to\mathcal{L}_H)} \leq 0 \quad \text{for} \quad \text{any } r \geq 1. \tag{3.30}$$

Combining this result with the conditions $1 - a^2 > \tilde{q}$ and $-1 < \tilde{q} < 0$, we get the range for the parameter $\underline{a}$ of the rotating black hole as,

$$1 \leq a \leq \sqrt{2}. \tag{4.31}$$

For a fixed $a \in [1,\sqrt{2}]$, one can find that center of mass energy will be infinite if

$L_1 = L_H$ and L_2 is in a proper range. From Fig. 4.3, we find that for the case $a = \sqrt{2}$ and $\tilde{q} = -1$ the center of mass energy at the horizon can be arbitrary high, and it can be unlimited for the two colliding particles with angular momenta $L_1 = L_H = 3/\sqrt{2}$ and $L_2 = -4$. For the case $a = 1.2$, the center of mass energy is unlimited and particle can also reach the horizon. In addition, for a fixed $1 < a < \sqrt{2}$ the particle with the critical angular momentum L_H can reach the horizon and the center-of-mass energy will be unlimited for the two colliding particles coming from infinity when $L = L_H$ and L_2 is in a proper range. In Table 4.1, the radius of the innermost stable circular orbits, and the values of the dimensionless parameter $\xi = (r_{ISCO} - r_H)/r_H$ for the particles moving around the rotating black hole in a Randall-Sundrum brane with a vanishing cosmological constant are shown for different values of the brane parameter. From Table 4.1, one can easily see that the value of the expression ξ will be zero for all cases, which means that for the RSB spacetime the center-of-mass energy for the two colliding particles is indirectly proportional to the value of the parameter ξ. Therefore, the center-of-mass energy can be unlimited regardless of the value of the expression for the parameter ξ .

Table 4.1:

The value of the radii of the innermost stable circular orbits and the values of the dimensionless parameter $(r_{ISCO} - r_H)/r_H$ of the particles moving around the rotating black hole in a Randall-Sundrum brane with a vanishing cosmological constant.

$\tilde{q}$	0	- 0.44	-1
Λ	0	0	*0*
a	1	1.2	$\sqrt{2}$
r_H	1	1	*1*
r_{ISCO}	1	1	*1*
$\xi = (r_{ISCO} - r_H)$	0	0	0

Finally, we consider the case with nonvanishing parameters $\tilde{q}$ and A_{4D}: $\tilde{q} \neq A_{4D} \neq 0$. Then we can easily obtain the expression for the radius of the event horizon as

$$r_H = \frac{-3+\sqrt{3}\sqrt{3-3a^2-3\tilde{q}+a^4\Lambda+a^2\tilde{q}\Lambda}}{-3+a^2\Lambda}. \tag{4.32}$$

For the extreme black hole case, the condition for the angular momentum is

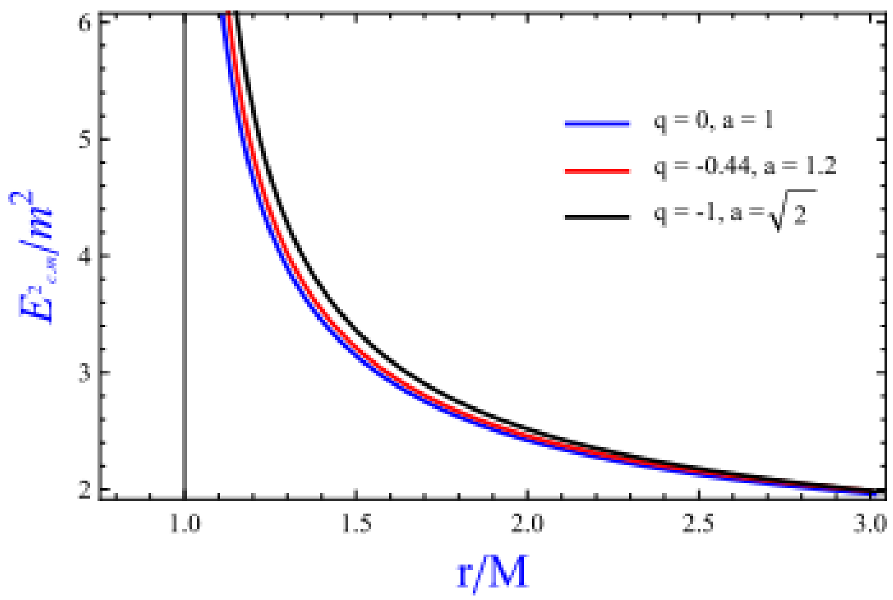

Figure 4.3: Radial dependence of the center-of-mass energy of accelerating particles for the different values of the parameter $\tilde{q}$ in the case of the extreme black hole.

Satisfied as

$$a = \frac{\sqrt{-\tilde{q}+\frac{3}{\Lambda}-\frac{\sqrt{9-12\Lambda+6\tilde{q}\Lambda+\tilde{q}^2\Lambda^2}}{\Lambda}}}{\sqrt{2}}. \tag{4.33}$$

In Fig 4.4 the radial dependence of the center-of-mass energy of the accelerating particles moving around the rotating black hole in a Randall-Sundrum brane for different values of the cosmological constant A_{4D} is shown. From Fig. 4.4 one can easily see that in the RSB spacetime with both negative and positive cosmological constants the particle can be essentially accelerated near the horizon but not to arbitrarily high energies. With an increasing cosmological constant the maximal value of the center-of-mass energy decreases.

Banados, Silk, and West [157] have shown that the total energy of two colliding test particles has no upper limit in their center-of-mass frame in the neighborhood of an extreme Kerr black hole, even if these particles were at rest at infinity in the infinite past. On the contrary, we show here that the energy of two colliding particles in the center-of-mass frame observed from infinity has an upper limit

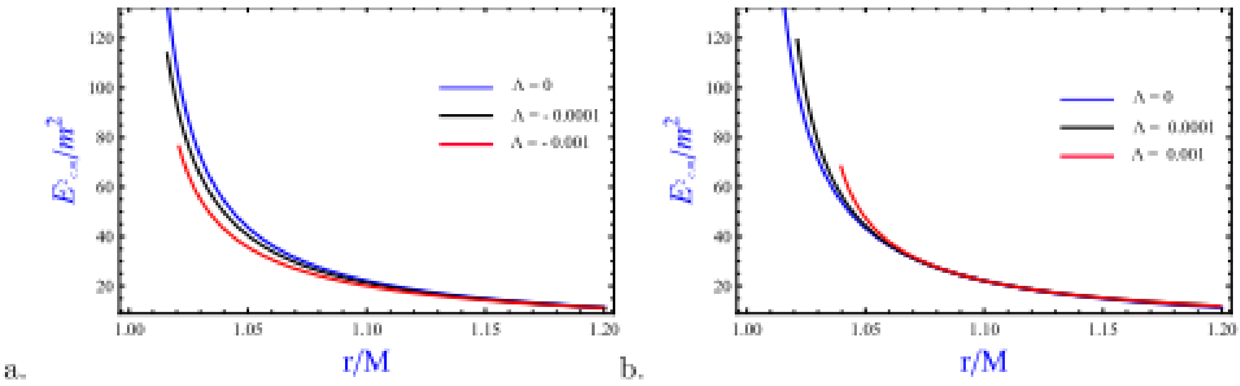

Figure 4.4: Radial dependence of the center-of-mass energy of accelerating particles moving around a rotating black hole in a Randall-Sundrum brane spacetime in the case when (a) $\Lambda_{4D} < 0$, and (b) $\Lambda_{4D} > 0$

near the rotating black hole in the Randall-Sundrum brane spacetime.

In Fig 4.5 the radial dependence of the center-of-mass energy of the accelerating particles moving around a rotating black hole in a Randall-Sundrum brane for different values of the cosmological constant Λ_{4D} are illustrated. From Fig. 4.5 one can easily see that each value of the cosmological constant corresponds to a different horizon, which describes several extremal cases. In this case, particles coming from infinity can be essentially accelerated near the horizon of the rotating black hole in RSB spacetime with a cosmological constant, but they cannot have arbitrarily high energies despite the fact that they collide in different kinds of extremal cases. For the case with a vanishing cosmological constant, the energy of the colliding particles has no upper limit in their center-of-mass frame in an extreme case, whereas there is an upper limit in the presence of a cosmological constant.

In Table 4.2, the radii of the innermost stable circular orbits and the values of the dimensionless parameter $\xi = (r_{ISCO} - r_H)/r_H$ for the particles moving around a rotating black hole in a Randall-Sundrum brane spacetime with a positive cosmological constant for different values of $\tilde{q}$, Λ_{4D}, and a are shown. The results listed

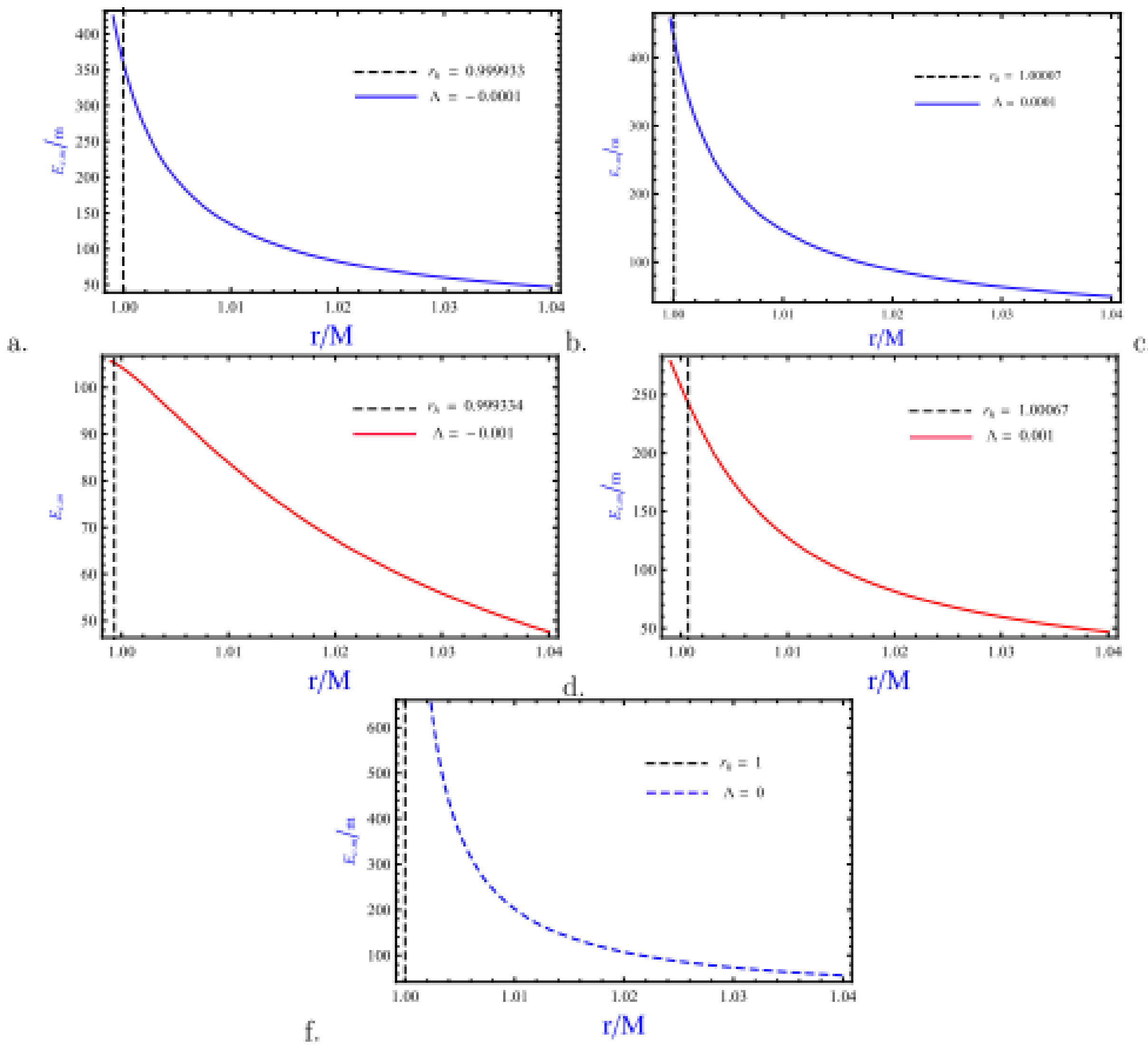

Figure 4.5: The dependence of the event horizon (vertical dashed line) and the radial dependence of the center-of-mass energy (curve line) of accelerating particles moving around a rotating black hole in a Randall-Sundrum brane spacetime on the cosmological constant.

in Table 4.2 explain the behavior of the plots presented in Fig. 4.4(b) and 4.5. By increasing the positive value of the cosmological constant the parameter ξ (which indicates the difference between the ISCO radius and the radius of event horizon) deviates from the null case. Increasing the ISCO radius prevents the value of the center-of-mass energy of the colliding particles from becoming infinite one. Thus the presence of a positive cosmological constant causes the graphs to shift down, which corresponds to a slower rate of acceleration.

Table 4.2:

The value of the radii of the innermost stable circular orbits and the values of the dimensionless parameter $(r_{ISCO} - r_H)/r_H$ of particles moving around a rotating black hole in a Randall-Sundrum brane spacetime with a positive cosmological constant.

$\tilde{q}$	-0.1	-0.1	-0.5	-0.5	-1	-1
Λ	0.00001	0.0001	0.00001	0.0001	0.00001	0.0001
a	1.04881	1.04883	1.22475	1.22477	1.41422	1.41424
r_H	1.0000036	1.00004	1.000005	1.00005	1.0000066	1.00007
r_{ISCO}	1.00028	1.00335	1.00032	1.00689	1.00041	1.00811
$\xi = \frac{r_{ISCO} - r_H}{r_H}$	$2.76 \cdot 10^{-4}$	$3.3 \cdot 10^{-3}$	$3.15 \cdot 10^{-4}$	$6.84 \cdot 10^{-3}$	$4.03 \cdot 10^{-4}$	$8.04 \cdot 10^{-3}$

In the case of nonvanishing Λ_{4D}, parameter one can obtain an upper bound for the ejecta energy from the black hole in the Randall-Sundrum brane spacetime. The expression for the ejected particle can be written as $(\mathrm{E}^2_{\mathrm{c.m}}/2)_{\max} \approx 2 + a^2\Lambda/3$. For the values of parameters a $= 0.98$ and $\Lambda = -0.0001$, one can easily get the maximal value of the factor $\lambda = 1 + m^2/\left(\mathrm{E}^2_{\mathrm{c.m}}/2 - m^2\right) \approx 1.99996$ for the ejected particles, which corresponds to decreasing of energy extraction to nearly 0.1% with compare to one in the Kerr spacetime.

§4.5 Effect of an external magnetic field on particle acceleration by a rotating black hole with quintessential energy

Here, we study the CM energy of two colliding particles moving in the equatorial plane of the quintessential rotating black hole with different angular momenta L_1, L_2 and colliding at a radius $\underline{r}$ near the black hole horizon. The CM energy takes the general form

$$
\begin{aligned}
\frac{E_{c.m.}^2}{2m^2} &= \frac{1}{r\left(r^2-2A(r)r+a^2\right)}\Big[a^2\left(\pi_{t1}\pi_{t2}(2A(r)+r)+r\right) \\
&+ 2aA(r)\left(\pi_{\varphi1}\pi_{t2}+\pi_{t1}\pi_{\varphi2}\right) \\
&- \pi_{\varphi1}\pi_{\varphi2}\left(-2A(r)+r\right)+\left(-2A(r)+r\pi_{t1}\pi_{t2}r\right)r^2 \\
&- \sqrt{2A(r)\left(\pi_{\varphi1}+a\pi_{t1}\right)^2-\pi_{\varphi1}^2 r+2A(r)r^2+r\left(r^2+a^2\right)\left(\pi_{t1}^2-1\right)} \\
&\times \sqrt{2A(r)\left(\pi_{\varphi2}+a\pi_{t2}\right)^2-\pi_{\varphi2}^2 r+2A(r)r^2+r\left(r^2+a^2\right)\left(\pi_{t2}^2-1\right)}\Big],
\end{aligned}
\tag{4.34}
$$

where the parameter $A(r)$ is introduced in the previous chapter by Eq. (2.35) and the generalized momentum $\pi_{\varphi i}$ associated with an external magnetic field is also described in the previous section through Eqs. (2.25-2.27). In the limiting case when both the quintessential parameter, $\tilde{c}=0$, and the magnetic parameter, $\beta = 0$ vanish the general expression (4.34) for the CM energy reduces to the general expression for the Kerr black hole [157]. Let us study the properties of the CM energy, Eq. (4.34), as the radius r approaches the horizon r_H for generic values of the parameters a and $\tilde{c}$. According to the l'Hospital's rule in the linear approximation in the quintessential parameter $\tilde{c}$ (in the particular case when it is small) the limiting value of $E_{c.m.}$ of the two charged particles along the

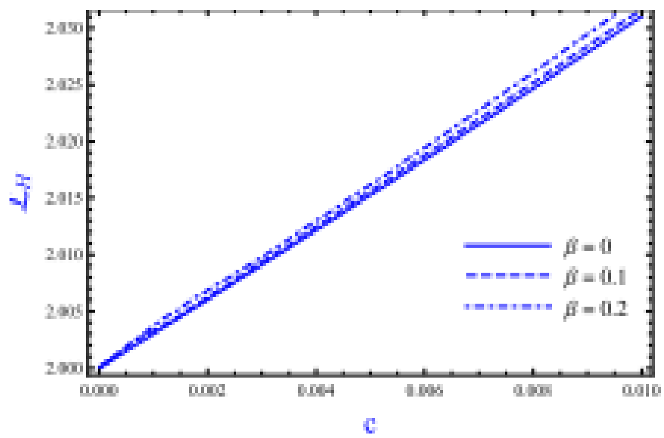

Figure 4.6: The value of the critical angular momentum at the horizon as a

function of quintessential parameter is plotted for the different values of magnetic parameter β for the given matter state parameter $\omega_{\mathrm{q}} = -2/3$.

non-geodesic orbits near the horizon r_H takes the following form

$$\begin{aligned}\frac{E^2_{c.m.}(r\to r_H)}{2m^2} &= \frac{\mathcal{A}_1}{\mathcal{L}_2-\mathcal{L}_H}+\frac{\mathcal{B}_1}{\mathcal{L}_1-\mathcal{L}_H}+\beta^2\left(\frac{\mathcal{A}_2}{\mathcal{L}_2-\mathcal{L}_H}+\frac{\mathcal{B}_2}{\mathcal{L}_1-\mathcal{L}_H}\right)\\ &+\beta\frac{\mathcal{A}_3+\mathcal{B}_3}{(\mathcal{L}_1-\mathcal{L}_H)(\mathcal{L}_2-\mathcal{L}_H)},\end{aligned} \tag{4.35}$$

where the critical value of angular momentum L_H allowing for very large collisional CM energy is given by

$$\mathcal{L}_H = \left[1+2A(r_H)^2 r_H a\left(r_H+\frac{a^2}{r_H}-2A(r_H)\right)\left(1+\frac{cr_H^3}{3M^2}\right)\beta\right]\frac{2A(r_H)r_H}{a}, \tag{4.36}$$

and the functions A_i and B_i are connected with the parameters β, $\tilde{c}$, L_1 and L_2 in a complex way.

We should note that the divergencies of $E_{c\cdot m}.$ in this case is not particular property of this spacetime but is manifestation of universality found in [161]. It was shown that in the fine tuned value of the angular momentum the center of mass energy of the particles diverges [161, 196]. However, there is dependence of the critical angular momentum of the particles on parameter $\tilde{c}$. It is evident that Eq. (3.35) implies ultra-high CM energy if one of the colliding charged particles has the critical angular momentum L_H at the horizon in the presence of a magnetic field [157, 161]. As a consequence, we can say that the $E_{c.m.}$ is divergent for the extremal quintessential rotating black holes with extremely small parameter $\tilde{c} << 1$ due to the external magnetic field accelerating charged particles faster as compared to those accelerated in vicinity of the Kerr back holes. However, with increasing quintessential parameter $\tilde{c}$, the critical value of angular momentum L_H also starts increasing respectively. This, in turn, requires that one of the colliding charged particles must reach the critical value so as for CM energy to be divergent at the horizon. In Table 4.3, we present values of the radii of the innermost stable circular orbits r_{ISCO} the values of the dimensionless distance parameter $\xi = (r_{ISCO} - r_H)/r_H$ of the ISCO radius from the event horizon radius, and the range of the allowed values of the angular momentum L for the several values of the parameter $\tilde{c}$ of extremal quintessential rotating black holes immersed in an external asymptotically uniform magnetic field. We can see that the dimensionless parameter ξ increases with increasing quintessential parameter $\tilde{c}$; consequently, the radius r_{ISCO} is tending away from the horizon radius r_H due to the increasing repulsive effect of the quintessential field, as pointed out previously in Fig. 2.4. This implies lowering of acceleration of two charged particles near the black hole horizon due to increasing quintessential field parameter $\tilde{c}$. We have to say that the finite $E_{c.m.}$ energy is obtained since the r_{ISCO} radius or any observable collisional event does not coincide with the event horizon radius r_H. Hence, the quintessential parameter $\tilde{c}$ implies suppression of the ultra-high energy collisions, while the magnetic parameter β implies enhancement of the BSW effect.

Fig. 4.6 shows the dependence the critical angular momentum on the quintessential parameter c for various values of the magnetic parameter β in general case. As can be seen from Fig. 4.6, the magnetic field accelerates the charged particles as compared to the case of the vanishing magnetic parameter β.

Finally, we study the amount of energy extracted due to a charged particle moving towards the black hole horizon in the presence of external magnetic field. For the BSW effect it is essential to be aware of the energy of the charged particle at the innermost stable circular orbit of the quintessential rotating black hole. Therefore, we estimate the total amount of (binding) energy released by a charged particle starting at large distance, say near the static radius, at a stable circular orbit at r_c and descends towards the innermost stable circular orbit at r_{ISCO}.

Table 4.3:

The value of the radii of the innermost stable circular orbits and the values of the dimensionless parameter ξ of charged particles and the range of the angular momentum L for different values of parameter $\tilde{c}$ for the extremal quintessential rotating black hole immersed in an external uniform magnetic field with strength B.

			$\beta = 0$			
$\tilde{c}$	a	r_H	$\mathcal{L}_{min}$	$\mathcal{L}_{max}$	r_{ISCO}	$\xi = \frac{r_{ISCO}-r_H}{r_H}$
0.00001	1.00001	1.000015	-4.82913	2.00001	1.0007523	736×10^{-6}
0.00005	1.00003	1.000075	-4.83193	2.00011	1.0011836	110×10^{-5}
0.00010	1.00005	1.000150	-4.83546	2.00026	1.0035802	342×10^{-5}
0.00050	1.00025	1.000750	-4.86344	2.00151	1.0108539	10×10^{-3}
0.00100	1.00050	1.001500	-4.89816	2.00312	1.0176548	2×10^{-2}
			$\beta = 0.1$			
0.00001	1.00001	1.000015	-4.89628	2.00005	1.0007504	725×10^{-6}
0.00005	1.00003	1.000075	-4.91299	2.00025	1.0011794	108×10^{-5}
0.00010	1.00005	1.000150	-4.93454	2.00034	1.0035422	338×10^{-5}
0.00050	1.00025	1.000750	-5.13971	2.00251	1.0105272	9×10^{-3}
0.00100	1.00050	1.001500	-5.52526	2.00503	1.0173182	1.5×10^{-2}

The energy efficiency of the binding energy release is then given by the

$$\zeta_{B_{energy}} = \frac{\mathcal{E}(r_C) - \mathcal{E}(r_{ISCO})}{\mathcal{E}(r_C)} \times 100\% \,. \tag{4.37}$$

The upper values of the efficiency of the binding energy ζB_{energy} (%) for the extremal black hole immersed in an external uniform magnetic field are tabulated in Table 4.3 for various values of the quintessential parameter $\tilde{c}$ and the spin parameter a. In Table 4.3, one may observe that the energy extraction decreases with increasing quintessential parameter $\tilde{c}$. One can obtain the maximal efficiency as large as 42% in the case of $\tilde{c} = 0$ for the extremal rotating black hole. The magnetic field, although small, can have a strong influence on the efficiency magnitude. For given value of the parameter $\tilde{c}$, the efficiency increases with increasing magnetic parameter β as can be seen in Table 4.3.

Table 4.4:

The efficiency of the binding energy ζB_{energy} (%) for the extremal quintessential rotating black hole placed in an magnetic field with strength B through the BSW mechanism for different values of the quintessential parameter c and spin parameter a for the minimum collision distance r_c from horizon.

		$\beta = 0$		$\beta = 0.1$		$\beta = 0.2$	
$\tilde{c}$	a	r_c	ζB_{energy}	r_c	ζB_{energy}	r_c	ζB_{energy}
0.00000	1.00000	1.000000	42.2650	1.000000	45.2147	1.000000	47.4120
0.00001	1.00001	1.000752	40.7253	1.000750	43.8409	1.000749	46.1728
0.00005	1.00003	1.001183	39.6673	1.001179	42.9013	1.001178	45.3280
0.00010	1.00005	1.003580	39.0188	1.003542	42.3273	1.003541	44.8131
0.00050	1.00025	1.010853	36.8991	1.010527	40.4622	1.010523	43.1467
0.00100	1.00050	1.017654	35.6603	1.017318	39.3779	1.017312	42.1832

We note that the magnetic field plays crucial role in the amount of binding energy released by the charged particle. The magnetic field also causes an increase in the value of the upper bound of the efficiency up to 50% for the extremal rotating black hole as compared to the upper bound 42% for the extremal Kerr black hole.

§4.5.1 Collision of a freely falling charged particle with a charged particle plunging from the ISCO to the horizon of the magnetized quintessential rotating black hole

We consider collision of a charged particle plunging from the ISCO to the horizon with a freely falling charged particle, and determine the $E_{c.m.}$ energy near the black hole horizon. We focus attention on the investigation of the combined effect of the magnetic and quintessential fields on the energy obtained in collision process.

First, we give the specific energy and specific angular momentum of the charged particles at the ISCO, solving Eq. (2.37) through the radial function $R(E, L, \mathrm{a}, \tilde{\mathrm{c}}, \beta)$ given by (2.34). As in previous sections, we again give approximative analytic form of E and L by imposing the restrictive condition for infinitesimal quintessential parameter c. The specific energy and specific angular momentum are then given by

$$\begin{aligned}
\mathcal{E}^2 &= 1-\frac{2(1+\frac{\tilde{c}r^2}{2})}{3r}-\frac{\beta^2(1+\frac{\tilde{c}r^3}{3})}{6}\Bigg[(2+\tilde{c}r^2)^2-5r^2-a^2\Bigg(3-\frac{2(1+\frac{\tilde{c}r^2}{2})}{r} \\
&+ \frac{4(1+\frac{\tilde{c}r^2}{2})^2}{3r^2}\Bigg)\Bigg]-\beta\left(1+\frac{\tilde{c}r^3}{3}\right)\left(1-\frac{2(1+\frac{\tilde{c}r^2}{2})}{3r}\right) \\
&\times \Bigg[\frac{2(1+\frac{\tilde{c}r^2}{2})}{3r}(3r^2-a^2)+\frac{\beta^2(1+\frac{\tilde{c}r^3}{3})^2}{4}\left(5r^4-4(1+\frac{\tilde{c}r^2}{2})r^2\left(r-(1+\frac{\tilde{c}r^2}{2})^2\right)\right. \\
&+ \left.\frac{2}{3}a^2\left(5r^2-6(1+\frac{\tilde{c}r^2}{2})r+2(1+\frac{\tilde{c}r^2}{2})^2\right)+a^4\left(1+\frac{4(1+\frac{\tilde{c}r^2}{2})^2}{9r^2}\right)\right)\Bigg]^{1/2}
\end{aligned} \tag{4.38}$$

and

$$\begin{aligned}
\mathcal{L} &= \Bigg[\frac{2(1+\frac{\tilde{c}r^2}{2})}{3r}(3r^2-a^2)+\frac{\beta^2(1+\frac{\tilde{c}r^3}{3})^2}{4}\left(5r^4-4(1+\frac{\tilde{c}r^2}{2})r^2\left(r-(1+\frac{\tilde{c}r^2}{2})^2\right)\right. \\
&+ \left.\frac{2}{3}a^2\left(5r^2-6(1+\frac{\tilde{c}r^2}{2})r+2(1+\frac{\tilde{c}r^2}{2})^2\right)+a^4\left(1+\frac{4(1+\frac{\tilde{c}r^2}{2})^2}{9r^2}\right)\right)\Bigg]^{1/2} \\
&- \beta\left(1+\frac{\tilde{c}r^3}{3}\right)\left(3r^2-a^2\right)\frac{1+\tilde{c}r^2}{6r},
\end{aligned} \tag{4.39}$$

respectively. From the expressions (4.38) and (4.39) we determine the radius of the ISCO assuming the quintessential parameter $\tilde{c}_* = \tilde{c}M << 1$ and the spin parameter $a_* = a/M \simeq 1$. We can then find the solution of Eq. (2.38) for the ISCO radius in the following form

$$
\begin{aligned}
r_{ISCO} &= 1 + 2^{2/3}(1+\tilde{c}_* - a_*)^{1/3} \\
&+ \frac{63 - \beta^2(2\tilde{c}_*+3)\left(8\beta^2(2\tilde{c}_*+3) + 2\beta(\tilde{c}_*+3)\sqrt{12\beta^2(2\tilde{c}_*+3)+27} - 15\right)}{6^{5/3}\left(3+\beta^2(2\tilde{c}_*+3)\right)} \\
&\times\ 3^{2/3}(1+\tilde{c}_* - a_*)^{2/3} + \mathcal{O}(1+\tilde{c}_* - a_*)\,. \qquad (4.40)
\end{aligned}
$$

From Eq. (4.40) one can see that in the limit of $\tilde{c} = 0$, it is in agreement with the expression for the ISCO radius obtained in [118]. Eq. (4.40) gives the ISCO radius associated with the combined effect of the quintessential field and the external magnetic field. The corresponding radius of the event horizon will have the

$$
r_H = 1 + 3(1+\tilde{c}_* - a_*) + \mathcal{O}(\tilde{c}^2)\ .
$$

$$
r_H = 1 + 3(1+\tilde{c}_* - a_*) + \mathcal{O}(\tilde{c}^2)\ . \qquad (4.41)
$$

Applying the ISCO radius expression (4.40) in Eqs. (4.38) and (4.39), one can obtain the following forms for the specific energy E_{ISCO} and the specific angular momentum L_{ISCO} of the charged particles revolving at the ISCO

$$
\begin{aligned}
\mathcal{E}_{ISCO} &= \left(\frac{\sqrt{4\beta^2+3}-\beta}{3} + \frac{3\left(\frac{5\beta}{18\sqrt{4\beta^2+3}} + \frac{13\beta^3}{216\sqrt{4\beta^2+3}} - \frac{23\beta^2}{54} - \frac{1}{3}\right)\tilde{c}_*}{2\left(\sqrt{4\beta^2+3}-\beta\right)} + \mathcal{O}(\tilde{c}_*)^2\right) \\
&+ \left(\frac{2^{2/3}\left(\sqrt{4\beta^2+3}-\beta\right)^2}{3\sqrt{4\beta^2+3}}\right. \\
&- \frac{2^{1/3}3\beta\left[312 + \beta\left(\beta\left(1648 - 763\beta\sqrt{4\beta^2+3}\right) - 228\sqrt{4\beta^2+3}\right)\right]\tilde{c}_*}{8\left(4\beta^2+3\right)^{3/2}\left(5\beta^2 - 2\beta\sqrt{4\beta^2+3}+3\right)^{3/2}} \\
&+ \left.\mathcal{O}(\tilde{c}_*)^2\right)(1+\tilde{c}_* - a_*)^{1/3} + \mathcal{O}(1+\tilde{c}_* - a_*)^{2/3}\,, \qquad (4.42)
\end{aligned}
$$

And

$$
\begin{aligned}
\mathcal{L}_{ISCO} &= \left(\frac{2(\sqrt{4\beta^2+3}-\beta)}{3}+\frac{\left(115\beta^2-16\sqrt{4\beta^2+3}\beta+36\right)\tilde{c}_*}{72\sqrt{4\beta^2+3}}+\mathcal{O}(\tilde{c}_*)^2\right)\\
&+ \left(\frac{2^{5/3}\left(\sqrt{4\beta^2+3}-\beta\right)^2}{3\sqrt{4\beta^2+3}}\right.\\
&+ \left.\frac{2^{2/3}\left[4(2\beta^2+1)^2-\beta(4\beta^2+3)^{3/2}\right]\tilde{c}_*}{(4\beta^2+3)^{3/2}}+\mathcal{O}(\tilde{c}_*)^2\right)(1+\tilde{c}_*-a_*)^{1/3}\\
&+ \mathcal{O}(1+\tilde{c}_*-a_*)^{2/3}, \qquad (4.43)
\end{aligned}
$$

respectively. The behaviour of Eqs (4.42) and (4.43) coincides with the results of Ref. [118] in the limiting case when the quintessential field parameter $\tilde{c}\to 0$.

In what follows, we calculate the CM energy of the colliding two charged particles near the horizon and evaluate how strong is the effect of the quintessential field on the CM energy. We consider collision between a charged particle with $E = E_{ISCO}$ and $L = L_{ISCO}$ leaving the ISCO, with a charged particle freely moving from the static radius; the collision occurs near the black hole horizon. Following [119] and imposing assumption of a nearly maximally rotating quintessential black hole, $\Delta\to 0$, we apply the l'Hopital's rule to Eq. (4.34) associated with energy $E = E_{ISCO}$ and angular momentum $L = L_{ISCO}$. The resulting $E_{c.m.}$ energy of the colliding two charged particles takes the following form

$$
\begin{aligned}
\frac{E^2_{c.m.}(r\to r_H)}{m^2} &\simeq \left[\left(\frac{\mathcal{E}_2\mathcal{L}_1-\mathcal{E}_1\mathcal{L}_2}{2A(r)}-\beta A(r)(1+\frac{\tilde{c}r_H^3}{3})\right.\right.\\
&\times \left.\left(\frac{a\mathcal{L}_1}{2A(r)r_H}-\frac{a\mathcal{L}_2}{2A(r)r_H}-\mathcal{E}_1+\mathcal{E}_2\right)\right)^2\\
&+ \left.\left(\frac{a\mathcal{L}_2}{2A(r)r_H}-\frac{a\mathcal{L}_1}{2A(r)r_H}+\mathcal{E}_1-\mathcal{E}_2\right)^2\right]\\
&\times \frac{1}{\left(\mathcal{E}_1-\frac{a\mathcal{L}_1}{2A(r)r_H}\right)\left(\mathcal{E}_2-\frac{a\mathcal{L}_2}{2A(r)r_H}\right)}, \qquad (4.44)
\end{aligned}
$$

where the function $A(r)$ is introduced in the previous section and related to the quintessential parameter $\tilde{c}$. Applying Eqs (4.42) and (4.43) in Eq. (4.44) and assuming the quintessential parameter $\tilde{c} \ll 1$, we obtain the corresponding approximate value for the $E_{c.m.}$ energy in the form

$$\frac{E^2_{c.m.}(r \to r_H)}{m^2} \simeq \frac{F(\beta, \tilde{c}_*, \mathcal{E}_2, \mathcal{L}_2)}{(1+\tilde{c}_* - a_*^2)^{1/2}} . \tag{4.45}$$

In the case when $\tilde{c} = 0$, Eq. (4.45) takes the approximate form

$$\frac{E^2_{c.m.}(r \to r_H)}{m^2} \simeq \frac{F(\beta, \mathcal{E}_2, \mathcal{L}_2)}{(1 - a_*^2)^{1/2}} , \tag{4.46}$$

which covers the results given in [118] and [119].

The $E_{c.m.}$ energy becomes non-divergent with increasing quintessential parameter c. This implies suppression effect of the quintessential field on the ultra-high energy collisions. However, the magnetic field in the black hole vicinity enhances the high-energy collisions, serving as an accelerator.

§4.6 Conclusion

We have studied the properties of the ergosphere of the black hole in the Kerr-Taub-NUT spacetime. The dependence of the shape of the ergosphere from small dimensionless NUT parameter shows that the radius of the event horizon becomes larger. However the relative volume of the ergosphere is decreased and the extracted energy from the black hole is raised up by the small dimensionless parameter $\tilde{l}$.

We have also studied the properties of the ergosphere of the rotating black hole in the Randall-Sundrum brane spacetime with nonvanishing and vanishing cosmological constants. The dependence of the shape of the ergosphere on the parameter c for both cases with nonvanishing and vanishing cosmological constant shows that the radius of the event horizon becomes larger. However, the relative volume of the ergosphere is decreased.

Many additional mechanisms and effects (e.g., astrophysical restrictions on the spin of black hole, radiative energy losses, significant fine-tuning to get sensible cross sections for particles, etc.) prevent particles from accelerating to arbitrarily high energies. Here we have shown that the influence of the cosmological constant and the brane parameter is also very sufficient and that they may also cause a limitation for the center-of-mass energy of the colliding particles. The mechanism of this limitation is related to splitting the ISCO radius from the event horizon.

We have also calculated the range of angular momentum for which a charged particle approaches the horizon r_H as well as we have also found that this range could be extendable for the external magnetic field surrounding black hole. The center of mass energy has been studied around quintessential rotating black hole, and we have found that it reaches infinite energy in the case in which one of the colliding charged particles has the critical angular momentum L_{H} for the infinitesimal quintessential parameter. On the other hand, the center of mass energy starts becoming finite once the value of quintessential parameter c increases even for the extremal quintessential rotating black hole. For center of mass energy to be infinite again at the horizon it requires that one of the colliding charged particles must reach its critical value. Thus, in the presence of quintessential field, the $E_{c.m.}$ depends not only on the parameter a but also on the quintessential field parameter c . We have shown that the magnetic field gives rise to an increase in the value of the upper bound of the efficiency up to 50% the for the extremal quintessential rotating black hole as compared to the upper bound 42% for the extremal Kerr black hole.

MAIN RESULTS AND CONCLUSIONS

The main conclusions of the dissertation work are the following:

1. Expressions for the center-of-mass energy of the particles colliding near the horizon of black holes immersed in the external magnetic field have been obtained. It has been demonstrated that due to the existence of quintessential field intensity parameter $\tilde{c}$ charged particles are prevented from acceleration to infinitely high energies. It has been also shown that the magnetic field, although small, can have a strong influence on the efficiency magnitude for the extracted energy, noting that the magnetic field serve as a crucial role in the amount of binding energy released by the charged particles and also causes an increase in the value of the upper bound of the efficiency up to 50 % for the extremal rotating black hole as compared to the upper bound 42 % for the extremal Kerr black hole.
2. We have developed isofrequency pairing of non-geodesic orbits under the gravitational field of the Schwarzschild black hole immersed in external asymptotically uniform magnetic field and the dependence of the surface of region where isofrequency pairing of non-geodesic orbits occur around Schwarzschild black hole from the external magnetic field has been found. As a result, a decrease in the surface of the isofrequency pairing of nongeodesic orbits as nearly (7-10) % for the maximal values of the external uniform magnetic field $\mathrm{B} \sim 10^6 - 10^7$Gauss has been found.
3. We have shown that a test magnetic field can affect the process of destroying black holes and restore the cosmic censorship in the astrophysical context. It has been also shown that a test magnetic field would act as a cosmic censor beyond a certain threshold value $B_{cr} = 0.6872$.
4. The analytical expressions for the vacuum electromagnetic fields of a quintessential rotating black hole in the external asymptotically uniform magnetic field has been obtained.
5. Expressions for the innermost stable circular orbits (ISCO) and the specific

angular momentum of charged particles in the quintessential rotating black hole vicinity in the presence of external magnetic field with strength B have been obtained. It has been shown that the ISCO radius is slightly shifted outwards due to the effect of the quintessential parameter $\tilde{c}$. However, once the magnetic parameter $\beta \to \infty$, the ISCO radius reaches its minimum irrespective of presence of the parameter $\tilde{c}$.

6. It has been shown that the influence of the cosmological constant and the brane parameter may also cause a limitation for the high efficiency of the ultrahigh-energy of the colliding particles; it has been established that the mechanism of this limitation is related to splitting the ISCO radius from the event horizon.

7. It has been shown that energy extraction through Penrose process is more realistic process for the energy extraction from the rotating black hole in the Kerr-Taub-NUT spacetime. The dependence of the extracted energy from compact object on NUT parameter has been found. It has been shown that the relative volume of the ergosphere is decreased and the extracted energy from the black hole is raised up due to the small dimensionless NUT parameter $\tilde{l}$.

BIBLIOGRAPHY

1. Abdujabbarov A. A., Ahmedov B. J., Shaymatov S. R., and Rakhmatov A. S. Penrose process in Kerr-Taub-NUT spacetime // *Astrophys Space Sci*. -2011.-vol. 334.- pp. 237-241.
2. Shaymatov S. R., Ahmedov B. J., and Abdujabbarov A. A. Particle acceleration near a rotating black hole in a Randall-Sundrum brane with a cosmological constant // *Phys. Rev. D*.-2013.-vol. 88.- p. 024016.
3. Atamurotov F., Ahmedov B., and Shaymatov S. Formation of black holes through BSW effect and black hole-black hole collisions // *Astrophys. Space Sci*.-2013- vol. 347.- pp. 277-281.
4. Shaymatov S., Atamurotov F., and Ahmedov B. Isofrequency pairing of circular orbits in Schwarzschild spacetime in the presence of magnetic field // *Astrophys Space Sci*.-2014-vol. 350.- pp. 413-419.
5. Shaymatov S., Patil M., Ahmedov B., and Joshi P. S. Destroying a nearextremal Kerr black hole with a charged particle: Can a test magnetic field serve as a cosmic censor? // *Phys. Rev. D*.-2015.- vol. 91.- p. 064025.
6. Shaymatov S.R., Atamurotov F.S. and Hakimov A.A. Solar system effects by potentials of galaxy // *Uzbek Journal of Physics*.-2015.- vol. 17, no. 2.- pp. 75-78.
7. Shaymatov S., Ahmedov B., Stuchlik Z. and Abdujabbarov A. Effect of an external magnetic field on particle acceleration by a rotating black hole surrounded by quintessential energy // *International Journal of Modern Physics D*.-2018.-vol. 27.-pp. 1741011-187.
8. Warburton N., Barack L. and Sago N. Isofrequency pairing of geodesic orbits in Kerr geometry // *Phys. Rev. D*.-2013.- vol. 87.- p. 084012.
9. K. Schwarzschild, “ ¨Uber das Gravitationsfeld einer Kugel aus inkompressibler

Fl¨ussigkeit nach der Einsteinschen Theorie," in Sitzungsberichte der K¨oniglich Preussischen Akademie der Wissenschaften zu Berlin, Phys.- Math. Klasse,-1916. 424-434, Mar.

10. R. Genzel, F. Eisenhauer, and S. Gillessen, "The Galactic Center massive black hole and nuclear star cluster, // Reviews of Modern Physics-2010. vol. 82. -pp. 3121–3195.
11. M. Schmidt, "3C 273 : A Star-Like Object with Large Red-Shift, // Nature-1963. vol. 197, p. 1040.
12. C. W. Misner, K. S. Thorne, and J. A. Wheeler, Gravitation. San Francisco: W. H. Freeman, 1973.
13. B. P. Abbott and et al. (VIRGO and LIGO Scientific Collaborations), "Observation of Gravitational Waves from a Binary Black Hole Merger,// Phys. Rev. Lett.- 2016.- vol. 116.-p. 061102.
14. B. P. Abbott and et al. (VIRGO and LIGO Scientific Collaborations), GW151226: Observation of Gravitational Waves from a 22-Solar-Mass Binary Black Hole Coalescence, // Phys. Rev. Lett.- 2016.- vol. 116. -p. 241103.
15. S. S. Doeleman, J. Weintroub, A. E. E. Rogers, R. Plambeck, and et al., "Event-horizon-scale structure in the supermassive black hole candidate at the Galactic Centre, // Nature-2008.- vol. 455. -pp. 78–80.
16. V. L. Fish, S. S. Doeleman and et al., "1.3 mm Wavelength VLBI of Sagittarius A*: Detection of Time-variable Emission on Event Horizon Scales, // Astrophys. J. Lett. -2011.- vol. 727. -p. L36.
17. S. S. Doeleman, V. L. Fish, D. E. Schenck, C. Beaudoin, and et al., "Jet-Launching Structure Resolved Near the Supermassive Black Hole in M87, // Science-2012.- vol. 338. -p. 355.
18. M. D. Johnson, V. L. Fish, S. S. Doeleman, D. P. Marrone, R. L. Plambeck, and et al., "Resolved magnetic-field structure and variability near the event horizon of Sagittarius A*, // Science-2015. -vol. 350. -pp. 1242–1245.

19. R. Penrose, “Gravitational Collapse: the Role of General Relativity, // Nuovo Cimento Rivista Serie-1969. -vol. 1. - p. 252.

20. I. Collaboration, “Neutrino emission from the direction of the blazar txs 0506+056 prior to the icecube-170922a alert, // Science-2018.

21. I. Collaboration, “Multimessenger observations of a flaring blazar coincident with high-energy neutrino icecube-170922a, // Science.

22. C. Kopper and E. Blaufuss, “IceCube-170922A - IceCube observation of a high-energy neutrino candidate event., // GRB Coordinates Network, Circular Service, No. 21916, #1-2017.-vol. 21916.

23. R. Narayan, “Black holes in astrophysics, // New J. Phys. 2005. -vol. 7. -p. 199.

24. C. Bambi, “Testing black hole candidates with electromagnetic radiation, // Rev. Mod. Phys. 2017. -vol. 89. -p. 025001.

25. L. Brenneman, Measuring the Angular Momentum of Supermassive Black Holes. 2013.

26. D. J.Walton, E. Nardini, A. C. Fabian, L. C. Gallo, and R. C. Reis, “Suzaku observations of ‘bare’ active galactic nuclei, // Mon. Not. R. Astron. Soc. 2013.-vol. 428. -pp. 2901–2920.

27. A.R. Patrick, J. N. Reeves, D. Porquet, A. G. Markowitz, A. P. Lobban, and Y. Terashima, “Iron line profiles in Suzaku spectra of bare Seyfert galaxies, // Mon. Not. R. Astron. Soc., vol. 411, pp. 2353–2370.

28. A.R. Patrick, J. N. Reeves, A. P. Lobban, D. Porquet, and A. G. Markowitz, “Assessing black hole spin in deep Suzaku observations of Seyfert 1 AGN, // Mon. Not. R. Astron. Soc.- 2011. - vol. 416. -pp. 2725–2747.

29. L. W. Brenneman and C. S. Reynolds, “Constraining Black Hole Spin via X-Ray Spectroscopy,” // Astrophys. J.- 2006. -vol. 652. -pp. 1028–1043.

30. G. Risaliti, G. Miniutti, M. Elvis, G. Fabbiano, M. Salvati, A. Baldi, V. Braito, S. Bianchi, G. Matt, J. Reeves, R. Soria, and A. Zezas, “Variable Partial

Covering and A Relativistic Iron Line in NGC 1365, // Astrophys. J.- 2009. -vol. 696. -pp. 160–171.

31. G. Risaliti, F. A. Harrison, K. K. Madsen, D. J. Walton, S. E. Boggs, F. E. Christensen, W. W. Craig, B. W. Grefenstette, C. J. Hailey, E. Nardini, D. Stern, and W. W. Zhang, “A rapidly spinning supermassive black hole at the centre of NGC 1365, // Nature-2013.- vol. 494. -pp. 449–451.
32. A.Zoghbi, A. C. Fabian, P. Uttley, G. Miniutti, L. C. Gallo, C. S. Reynolds, J. M. Miller, and G. Ponti, “Broad iron L line and X-ray reverberation in 1H0707-495, // Mon. Not. R. Astron. Soc.- 2010. -vol. 401. -pp. 2419–2432.
33. Y. Tan, J. X. Wang, X. W. Shu, and Y. Zhou, “A Possible Ultra Strong and Broad Fe K_ Emission Line in Seyfert 2 Galaxy IRAS 00521-7054, // Astrophys. J.- 2012. -vol. 747. -p. L11.
34. A.M. Lohfink, C. S. Reynolds, S. G. Jorstad, A. P. Marscher, E. D. Miller, H. Aller, M. F. Aller, L. W. Brenneman, A. C. Fabian, J. M. Miller, R. F. Mushotzky, M. A. Nowak, and F. Tombesi, “An X-Ray View of the Jet Cycle in the Radio-loud AGN 3C120, // Astrophys. J.- 2013. -vol. 772. -p. 83.
35. L. C. Gallo, A. C. Fabian, T. Boller, and W. Pietsch, “A possible line-like emission feature at 8 keV in the Seyfert 1.2 UGC 3973,” // Mon. Not. R. Astron. Soc.- 2005. -vol. 363. -pp. 64–70.
36. L. C. Gallo, G. Miniutti, J. M. Miller, L. W. Brenneman, A. C. Fabian, M. Guainazzi, and C. S. Reynolds, “Multi-epoch X-ray observations of the Seyfert 1.2 galaxy Mrk 79: bulk motion of the illuminating X-ray source,” // Mon. Not. R. Astron. Soc.- 2011 -vol. 411. -pp. 607–619.
37. T. M. Belloni, “States and Transitions in Black Hole Binaries,” in Lecture Notes in Physics, Berlin Springer Verlag (T. Belloni, ed.), vol. 794 of Lecture Notes in Physics, Berlin Springer Verlag-2010. -p. 53.
38. J. E. McClintock, R. Narayan, and J. F. Steiner, “Black Hole Spin via Continuum Fitting and the Role of Spin in Powering Transient Jets,” // Space

Sci. Space Sci. Rev.- 2014. -vol. 183. -pp. 295–322.

39. J. E. McClintock, R. Shafee, R. Narayan, R. A. Remillard, S. W. Davis, and L.-X. Li, “The Spin of the Near-Extreme Kerr Black Hole GRS 1915+105,” // Astrophys. J.- 2006. -vol. 652. -pp. 518–539.

40. L. Gou, J. E. McClintock, M. J. Reid, J. A. Orosz, J. F. Steiner, R. Narayan, J. Xiang, R. A. Remillard, K. A. Arnaud, and S. W. Davis, “The Extrem Spin of the Black Hole in Cygnus X-1,” Astrophy. J.- 2011. -vol. 742, -p. 85.

41. L. Gou, J. E. McClintock, R. A. Remillard, J. F. Steiner, M. J. Reid, J. A. Orosz, R. Narayan, M. Hanke, and J. Garc´ıa, “Confirmation via the Continuum-fitting Method that the Spin of the Black Hole in Cygnus X-1 Is Extreme,” // Astrophys. J.- 2014 -vol. 790. -p. 29.

42. J. F. Steiner, J. E. McClintock, and M. J. Reid, “The Distance, Inclination, and Spin of the Black Hole Microquasar H1743-322,” // Astrophys. J.- 2012. -vol. 745, -p. L7.

43. L. Gou, J. E. McClintock, J. F. Steiner, R. Narayan, A. G. Cantrell, C. D. Bailyn, and J. A. Orosz, “The Spin of the Black Hole in the Soft X-ray Transient A0620-00,” // Astrophys. J.- 2010. -vol. 718. -pp. L122–L126.

44. M. Kolehmainen and C. Done, “Limits on spin determination from disc spectral fitting in GX 339-4,” Mon. Not. R. Astron. Soc.- 2010. -vol. 406. -pp. 2206–2212.

45. R. Shafee, J. E. McClintock, R. Narayan, S. W. Davis, L.-X. Li, and R. A. Remillard, “Estimating the Spin of Stellar-Mass Black Holes by Spectral Fitting of the X-Ray Continuum,” // Astrophys. J. Lett.-2006. -vol. 636. -pp. L113–L116.

46. J. F. Steiner, D. J.Walton, J. A. Garc´ıa, J. E. McClintock, S. G. T. Laycock, M. J. Middleton, R. Barnard, and K. K. Madsen, “On the Spin of the Black Hole in IC 10 X-1,” // Astrophys. J.- 2016 -vol. 817, -p. 154.

47. J. F. Steiner, R. C. Reis, J. E. McClintock, R. Narayan, R. A. Remillard, J. A.

Orosz, L. Gou, A. C. Fabian, and M. A. P. Torres, “The spin of the black hole microquasar XTE J1550-564 via the continuum-fitting and Fe-line methods,” // Mon. Not. R. Astron. Soc.- 2011. -vol. 416. -pp. 941–958.

48. J. F. Steiner, J. E. McClintock, J. A. Orosz, R. A. Remillard, C. D. Bailyn, M. Kolehmainen, and O. Straub, “The Low-spin Black Hole in LMC X-3,” // Astrophys. J.- 2014. -vol. 793. -p. L29.

49. R. C. Reis, J. M. Miller, M. T. Reynolds, A. C. Fabian, and D. J. Walton, “Suzaku Observation of the Black Hole Candidate Maxi J1836-194 in a Hard/Intermediate Spectral State,” // Astrophys. J.- 2012. -vol. 751, -p. 34.

50. R. C. Reis, A. C. Fabian, R. R. Ross, and J. M. Miller, “Determining the spin of two stellar-mass black holes from disc reflection signatures,” // Mon. Not. R. Astron. Soc.- 2009. -vol. 395. -pp. 1257–1264.

51. R. C. Reis, J. M. Miller, A. C. Fabian, E. M. Cackett, D. Maitra, C. S. Reynolds, M. Rupen, D. T. H. Steeghs, and R. Wijnands, “Multistate observations of the Galactic black hole XTE J1752-223: evidence for an intermediate black hole spin,” // Mon. Not. R. Astron. Soc. 2011. -vol. 410, -pp. 2497–2505.

52. D. J. Walton, R. C. Reis, E. M. Cackett, A. C. Fabian, and J. M. Miller, “The similarity of broad iron lines in X-ray binaries and active galactic nuclei,” Mon. Not. R. Astron. Soc. -2012. -vol. 422, -pp. 2510–2531.

53. C.-Y. Chiang, R. C. Reis, D. J. Walton, and A. C. Fabian, “Re-examining the XMM-Newton spectrum of the black hole candidate XTE J1652-453,” Mon. Not. R. Astron. Soc.- 2012. -vol. 425, -pp. 2436–2442.

54. Warburton N., Barack L. and Sago N. Isofrequency pairing of geodesic orbits in Kerr geometry // *Phys. Rev. D*.-2013.- vol. 87.- p. 084012.

55. Barack L. and Sago N. Beyond the geodesic approximation: Conservative effects of the gravitational self-force in eccentric orbits around a Schwarzschild black hole // *Phys. Rev. D*.-2011.- vol. 83.- p. 084023.

56. Frolov V. P., and Shoom A. A. Motion of charged particles near a weakly

magnetized Schwarzschild black hole // *Phys. Rev. D.*-2010.- vol. 82.- p. 084034.

57. Gal'tsov D. V. and Petukhov V. I. Black hole in an external magnetic field // *Soviet Journal of Experimental and Theoretical Physics*.-1978.- vol. 47.- p. 419.

58. de Felice F. and Sorge F. Magnetized orbits around a Schwarzschild black hole // *Classical and Quantum Gravity*.-2003.- vol. 20.- pp. 469-481.

59. de Felice F., Sorge F. and Zilio S. Magnetized orbits around a Kerr black hole // *Classical and Quantum Gravity*.-2004.- vol. 21.- pp. 961-973.

60. Frolov V. P. Weakly magnetized black holes as particle accelerators // *Phys. Rev. D*.-2012.- vol. 85.- p. 024020.

61. Prasanna A. R. General-relativistic analysis of charged-particle motion in electromagnetic fields surrounding black holes // *Nuovo Cimento Rivista Serie*.-1980.-vol. 3.- pp. 1-53.

62. Abdujabbarov A. and Ahmedov B. Test particle motion around a black hole in a braneworld // *Phys. Rev. D*.-2010.- vol. 81.- p. 044022.

63. Chellathurai V., Dhurandhar S. V. and Dadhich N. Charged particle orbits in the field of two charges placed symmetrically near a Schwarzschild black hole // *Pramana*.-1986.- vol. 27.- pp. 485-495.

64. Abdujabbarov A. A., Ahmedov B. J. and Kagramanova V. G. Particle motion and electromagnetic fields of rotating compact gravitating objects with gravitomagnetic charge // *General Relativity and Gravitation.*2008.- vol. 40.- pp. 2515-2532.

65. Abdujabbarov A. A., Ahmedov B. J. and Jurayeva N. B. Charged-particle motion around a rotating non-Kerr black hole immersed in a uniform magnetic field // *Phys. Rev. D*.-2013.- vol. 87.- p. 064042.

66. Abdujabbarov A. A., Tursunov A. A., Ahmedov B. J. and Kuvatov A. Acceleration of particles by black hole with gravitomagnetic charge immersed in magnetic field,” *Astrophys Space Sci*,-2013.- vol. 343.- pp. 173-179.

67. Aliev A. N. and Ozdemir N. Motion of charged particles around a rotating black hole in a magnetic field // *Mon. Not. R. Astron. Soc*.-2002.-vol. 336.- pp. 241-248.

68. Abdujabbarov A., Atamurotov F., Dadhich N., Ahmedov B. and Stuchlik Z. Energetics and optical properties of 6-dimensional rotating black hole in pure Gauss-Bonnet gravity // *European Physical Journal C*.-2015.- vol. 75.- p. 399.

69. Kolos M., Stuchlik Z. and Tursunov A. Quasi-harmonic oscillatory motion of charged particles around a Schwarzschild black hole immersed in a uniform magnetic field // *Classical and Quantum Gravity*.-2015.- vol. 32.- p. 165009.

70. Stuchlik Z. and Kolos M. Acceleration of the charged particles due to chaotic scattering in the combined black hole gravitational field and asymptotically uniform magnetic field // *European Physical Journal C*.-2016.- vol. 76.- p. 32.

71. Tursunov A., Stuchlik Z. and Kolos M. Circular orbits and related quasi-harmonic oscillatory motion of charged particles around weakly magnetized rotating black holes // *Phys. Rev. D*.-2016.- vol. 93.- p. 084012.

72. Kovar J., Stuchlik Z. and Karas V. Off-equatorial orbits in strong gravitational fields near compact objects // *Classical and Quantum Gravity*.-2008.- vol. 25.- p. 095011.

73. Kovar J., Kopacek O., Karas V. and Stuchlik Z. Off-equatorial orbits in strong gravitational fields near compact objects II: halo motion around magnetic compact stars and magnetized black holes // *Classical and Quantum Gravity*.-2010.- vol. 27.- p. 135006.

74. Miller J. M., Raymond J., Fabian A., Steeghs D., Homan J., Reynolds C., van der Klis M., and Wijnands R. The magnetic nature of disk accretion onto black

holes," *Nature*.-2006.- vol. 441.- pp. 953-955.

75. de Kool M., Bicknell G. V. and Kuncic Z. Magnetic Fields in Accretion Disks* // *Publications of the Astronomical Society of Australia*.-1999.- vol. 16.- pp. 225-233.

76. Baczko A.K., Schulz R., Kadler M., Ros E., Perucho M., Krich- baum T. P., Bock M., Bremer M., Grossberger C., Lindqvist M., Lobanov A. P., Mannheim K., Marti-Vidal I., Muller C., Wilms J. and Zensus J. A., // A highly magnetized twin-jet base pinpoints a supermassive black hole // *Astronomy and Astrophysics*.-2016.- vol. 593.- p. A47.

77. Piotrovich M. Y., Silant'ev N. A., Gnedin Y. N. and Natsvlishvili T. M. Magnetic Fields of Black Holes and the Variability Plane // *ArXiv e-prints*.-2010.

78. Eatough R. P., Falcke H., Karuppusamy R., Lee K. J., Champion D. J., Keane E. F., Desvignes G., Schnitzeler D. H. F. M., Spitler L. G., Kramer M., Klein B., Bassa C., Bower G. C., Brunthaler A., Cognard I., Deller A. T., Demorest P. B., Freire P. C. C., Kraus A., Lyne A. G., Noutsos A., Stap- pers B., and N. Wex A strong magnetic field around the supermassive black hole at the centre of the Galaxy // *Nature*.2013.p- vol. 501.- pp. 391-394.

79. Shannon R. M. and Johnston S. Radio properties of the magnetar near Sagittarius A* from observations with the Australia Telescope Compact Array // *Mon. Not. R. Astron. Soc*.-2013.- vol. 435.- pp. L29-L32.

80. Tursunov A., Kolos M., Ahmedov B. and Stuchlik Z. Dynamics of an electric current-carrying string loop near a Schwarzschild black hole embedded in an external magnetic field // *Phys. Rev. D*.-2013.- vol. 87.- p. 125003.

81. Tursunov A., Kolos M., Abdujabbarov A., Ahmedov B. and Stuchlik Z. Acceleration of particles in spacetimes of black string // *Phys. Rev. D*.-2013.- vol. 88.- p. 124001.

82. Ginzburg O. L. M. V. L. // *Zh. Eksp. Teor. Fiz*.-1964.- vol. 47.- p. 1030.

83. Anderson J. L. and Cohen J. M. Gravitational Collapse of Magnetic Neutron Stars //*Astrophys. Space Sci*.-1970.- vol. 9.- pp. 146-152.

84. Wald R. M. Black hole in a uniform magnetic field // *Phys. Rev. D*.-1974.- vol. 10.- pp. 1680-1685.

85. Aliev A. N., Galtsov D. V. and Petukhov V. I. Negative absorption near a magnetized black hole - Black hole masers // *Astrophys. Space Sci*.-1986.- vol. 124.- pp. 137-157.

86. Aliev A. N. and Gal'tsov D. V. REVIEWS OF TOPICAL PROBLEMS: "Magnetized" black holes // *Soviet Physics Uspekhi*.-1989.- vol. 32.- pp. 75-92.

87. Schmidt W. Celestial mechanics in Kerr spacetime // *Classical and Quantum Gravity*.-2002.- vol. 19.- pp. 2743-2764.

88. Drasco S. and Hughes S. A. Rotating black hole orbit functionals in the frequency domain // *Phys. Rev. D*.-2004.- vol. 69.- p. 044015.

89. Peebles P. J. and Ratra B. The cosmological constant and dark energy // *Reviews of Modern Physics*.-2003.- vol. 75.- pp. 559-606.

90. Stuchlik Z. Influence of the RELICT Cosmological Constant on Accretion Discs // *Modern Physics Letters* A.-2005.- vol. 20.- pp. 561-575.

91. Stuchlik Z. The motion of test particles in black-hole backgrounds with non-zero cosmological constant // *Bulletin of the Astronomical Institutes of Czechoslovakia*.-1983.- vol. 34.- pp. 129-149.

92. Stuchlik Z. An Einstein-Strauss-de Sitter model of the universe // *Bulletin of the Astronomical Institutes of Czechoslovakia*.-1984.- vol. 35.- pp. 205-215.

93. Kagramanova V., Kunz J. and Lammerzahl C. Solar system effects in Schwarzschild de Sitter space time // *Physics Letters B*.-2006.- vol. 634.- pp. 465470.

94. Stuchlik Z., Slany P. and Hledik S. Equilibrium configurations of perfect fluid orbiting Schwarzschild-de Sitter black holes // *Astronomy and Astrophysics*.-

2000.- vol. 363.- pp. 425-439.

95. Stuchlik Z. and Hledik S. Equatorial photon motion in the Kerr-Newman spacetimes with a non-zero cosmological constant // *Classical and Quantum Gravity*.-2000.- vol. 17.- pp. 4541-4576.

96. Cruz N., Olivares M. and Villanueva J. R. The geodesic structure of the Schwarzschild anti-de Sitter black hole // *Classical and Quantum Gravity*.-2005.- vol. 22.- pp. 1167-1190.

97. Kraniotis G. V. Precise relativistic orbits in Kerr and Kerr (anti) de Sitter spacetimes // *Classical and Quantum Gravity*.-2004.- vol. 21.- pp. 4743-4769.

98. Kraniotis G. V. Periapsis and gravitomagnetic precessions of stellar orbits in Kerr and Kerr de Sitter black hole spacetimes // *Classical and Quantum Gravity*.-2007.- vol. 24.- pp. 1775-1808.

99. Stuchlik Z., Slany P., and Kovar J. Pseudo-Newtonian and general relativistic barotropic tori in Schwarzschild-de Sitter spacetimes // *Classical and Quantum Gravity*.-2009.- vol. 26.- p. 215013.

100. Stuchlik Z. and Schee J. Influence of the cosmological constant on the motion of Magellanic Clouds in the gravitational field of Milky Way // *Journal of Cosmology and Astroparticles*.-2011.- vol. 9.- p. 18.

101. Grenon C. and Lake K. Generalized Swiss-cheese cosmologies: Mass scales // *Phys. Rev. D*.-2010.- vol. 81.- p. 023501.

102. Uzan J.-P., Ellis G. F. R. and Larena J. A two-mass expanding exact space-time solution // *General Relativity and Gravitation*.-2011.- vol. 43.- pp. 191205.

103. Grenon C. and Lake K Generalized Swiss-cheese cosmologies. II. Spherical dust // *Phys. Rev. D*.-2011.- vol. 84.- p. 083506.

104. Rezzolla L., Zanotti O. and Font J. A. Dynamics of thick discs around Schwarzschild-de Sitter black holes // *Astronomy and Astrophysics*.-2003.- vol. 412.- pp. 603-613.

105. Arraut I. On the astrophysical scales set by the Cosmological Constant, Black Hole thermodynamics and non-linear massive gravity // *ArXiv e-prints*.-2013.

106. Arraut I. On the black holes in alternative theories of gravity: The case of nonlinear massive gravity //*International Journal of Modern Physics D*.-2015.- vol. 24.- p. 1550022.

107. Faraoni V., ed. // *Cosmological and Black Hole Apparent Horizons*.-2015.- vol. 907 of *Lecture Notes in Physics, Berlin Springer Verlag*.

108. Faraoni V. and Cardini A. M. Analogues of glacial valley profiles in particle mechanics and in cosmology // *ArXiv e-prints*.-2016.

109. Stuchlik Z., Hledik S. and Novotny J. General relativistic polytropes with a repulsive cosmological constant // *Phys. Rev. D*.-2016.- vol. 94.- p. 103513.

110. Wetterich C. Cosmology and the fate of dilatation symmetry // *Nuclear Physics B*.-1988.- vol. 302.- pp. 668-696.

111. Caldwell R. and Kamionkowski M. Cosmology: Dark matter and dark energy // *Nature*.-2009.- vol. 458.- pp. 587-589.

112. Kiselev V. V. Quintessence and black holes // *Classical and Quantum Gravity*.-2003.- vol. 20.- pp. 1187-1197.

113. Toshmatov B., Stuchlik Z. and Ahmedov B. Rotating black hole solutions with quintessential energy // *ArXiv e-prints: 1512.01498*.-2015.

114. Darwin C. The Gravity Field of a Particle. II // *Proceedings of the Royal Society of London Series A*.-1961.- vol. 263.- pp. 39-50.

115. Cutler C., Kennefick D. and Poisson E. Gravitational radiation reaction for bound motion around a Schwarzschild black hole *Phys. Rev. D*.-1994.- vol. 50.- pp. 3816-3835.

116. Stuchlik Z. and Hledik S. Some properties of the Schwarzschild-de Sitter and Schwarzschild-anti-de Sitter spacetimes // *Phys. Rev. D*.-1999.- vol. 60.- p. 044006.

117. Bicak J., Suchlik Z. and Balek V. The motion of charged particles in the field of rotating charged black holes and naked singularities // *Bulletin of the Astronomical Institutes of Czechoslovakia*.-1989.- vol. 40.- pp. 65-92.

118. Igata T., Harada T. and Kimura M. Effect of a weak electromagnetic field on particle acceleration by a rotating black hole // *Phys. Rev. D*.-2012.- vol. 85.- p. 104028.

119. Zaslavskii O. B. Innermost stable circular orbit near dirty black holes in magnetic field and ultra-high-energy particle collisions // *European Physical Journal C*.-2015.- vol. 75.- p. 403.

120. Wald R. Gedanken experiments to destroy a black hole. // *Annals of Physics*.-1974.- vol. 82.- pp. 548-556.

121. Jacobson T. and Sotiriou T. P. Destroying black holes with test bodies in *Journal of Physics Conference Series*, vol. 222 of *Journal of Physics Conference Series*, p. 012041, Apr. 2010.

122. Hubeny V. E. Overcharging a black hole and cosmic censorship // *Phys. Rev. D*.-1999.- vol. 59.- p. 064013.

123. Saa A. and Santarelli R. Destroying a near-extremal Kerr-Newman black hole // *Phys. Rev. D*.-2011.- vol. 84.- p. 027501.

124. Barausse E., Cardoso V. and Khanna G. Test Bodies and Naked Singularities: Is the Self-Force the Cosmic Censor? // *Physical Review Letters*.-2010.- vol. 105.- p. 261102.

125. Zimmerman P., Vega I., Poisson E. and Haas R. Self-force as a cosmic censor // *Phys. Rev. D*.-2013 vol. 87.- p. 041501.

126. Rocha J. V. and Cardoso V. Gravitational perturbation of the BTZ black hole induced by test particles and weak cosmic censorship in AdS spacetime // *Phys. Rev. D*.-2011.- vol. 83.- p. 104037.

127. Li Z. and Bambi C. Destroying the event horizon of regular black holes // *Phys.*

Rev. D.-2013.- vol. 87.- p. 124022.

128. Semiz I. Dyonic Kerr-Newman black holes, complex scalar field and cosmic censorship // *General Relativity and Gravitation*.-2011.- vol. 43.- pp. 833-846.

129. Duztas K. and Semiz I. Cosmic censorship, black holes and integer-spin test fields // *Phys. Rev. D*.- vol. 88.- p. 064043.

130. Karas V. and Kopacek O. Magnetic layers and neutral points near a rotating black hole // *Classical and Quantum Gravity*.-2009.- vol. 26.- p. 025004.

131. Karas V., Kopacek O. and Kunneriath D. Influence of frame-dragging on magnetic null points near rotating black holes // *Classical and Quantum Gravity*.-2012.- vol. 29.- p. 035010.

132. Lyutikov M. Schwarzschild black holes as unipolar inductors: Expected electromagnetic power of a merger // *Phys. Rev. D*.-2011.- vol. 83.- p. 064001.

133. Morozova V. S., Rezzolla L. and Ahmedov B. J. Nonsingular electrodynamics of a rotating black hole moving in an asymptotically uniform magnetic test field // *Phys. Rev. D*.-2014.- vol. 89.- p. 104030.

134. Gimon E. G. and Horava P. Astrophysical violations of the Kerr bound as a possible signature of string theory *Physics Letters B*.-2009.- vol. 672.- pp. 299-302.

135. Patil M. and Joshi P. Kerr naked singularities as particle accelerators // *Classical and Quantum Gravity*.-2011.- vol. 28.- p. 235012.

136. Patil M. and Joshi P. S. High energy particle collisions in superspinning Kerr geometry // *Phys.Rev. D*.-2011.- vol. 84.- p. 104001.

137. Patil M. and Joshi P. S. Finite escape fraction for ultrahigh energy collisions around Kerr naked singularity // *Pramana*.-2015.- vol. 84.- pp. 491-501.

138. Patil M., Joshi P. S., Kimura M. and Nakao K.-i. Acceleration of particles and shells by Reissner-Nordstrom naked singularities // *Phys. Rev. D*.-2012.- vol. 86.- p. 084023.

139. Nakao K.-i., Kimura M., Patil M. and Joshi P. S. Ultrahigh energy collision with neither black hole nor naked singularity // *Phys. Rev. D*.-2013.- vol. 87.- p. 104033.

140. Joshi P. S. // *Global aspects in gravitation and cosmology*.-1993.

141. Goswami R., Joshi P. S. and Singh P. Quantum Evaporation of a Naked Singularity // *Physical Review Letters*.-2006.- vol. 96.- p. 031302.

142. Harada T., Iguchi H. and Nakao K. Physical Processes in Naked Singularity Formation // *Progress of Theoretical Physics*.-2002- vol. 107.- pp. 449-524.

143. Joshi P. S. Gravitational collapse: The story so far // *Pramana*.-2000.- vol. 55.- p. 529.

144. Ernst F. J. Black holes in a magnetic universe // *Journal of Mathematical Physics*.-1976.- vol. 17.- pp. 54-56.

145. Gibbons G. W., Mujtaba A. H. and Pope C. N. Ergoregions in magnetized black hole spacetimes // *Classical and Quantum Gravity*.-2013.- vol. 30.- p. 125008.

146. Newman E., Tamburino L. and Unti T. Empty-Space Generalization of the Schwarzschild Metric // *Journal of Mathematical Physics*.-1963.- vol. 4.- pp. 915923.

147. Nouri-Zonoz M. Electromagnetic waves in NUT space: solutions to the Maxwell equations // *Classical and Quantum Gravity*.-2004.- vol. 21.- pp. 471-482.

148. Kagramanova V., Kunz J. and Lammerzahl C. Charged particle interferometry in Plebanski Demianski black hole spacetimes // *Classical and Quantum Gravity*.-2008.- vol. 25.- p. 105023.

149. Morozova V. S. and Ahmedov B. J. Quantum Interference Effects in Slowly Rotating Nut Space-Time // *International Journal of Modern Physics D*.-2009.- vol. 18.- pp. 107-118.

150. Aliev A. N., Cebeci H. and Dereli T. Kerr-Taub-NUT spacetime with Maxwell and dilaton fields // *Phys. Rev. D*.-2008.- vol. 77.- p. 124022.

151. Morozova V. S., Ahmedov B. J. and Kagramanova V. G. General Rela- tivistic Effects of Gravitomagnetic Charge on Pulsar Magnetospheres and Particle Acceleration in the Polar Cap // *Astrophys. J*.-2008.- vol. 684.- pp. 13591365.

152. Gariel J., MacCallum M. A. H., Marcilhacy G. and Santos N. O. Kerr geodesics, the Penrose process and jet collimation by a black hole // *Astronomy and Astrophysics*.-2010.- vol. 515.- p. A15.

153. Bhat M., Dhurandhar S. and Dadhich N. Energetics of the Kerr-Newman black hole by the Penrose process // *Journal of Astrophysics and Astronomy*.-1985.- vol. 6.- pp. 85-100.

154. Prabhu K. and Dadhich N. Energetics of a rotating charged black hole in 5-dimensional supergravity // *Phys. Rev. D*.-2010.- vol. 81.- p. 024011.

155. Zimmerman R. L. and Shahir B. Y. Geodesics for the NUT metric and gravitational monopoles // *General Relativity and Gravitation*.-1989.- vol. 21.- pp. 821-848.

156. Kagramanova V., Kunz J., Hackmann E. and Lammerzahl C. Analytic treatment of complete and incomplete geodesics in Taub-NUT space-times *Phys. Rev. D*.-2010.- vol. 81.- p. 124044.

157. Banados M., Silk J. and West S. M. Kerr Black Holes as Particle Accelerators to Arbitrarily High Energy // *Physical Review Letters*.-2009.- vol. 103.- p. 111102.

158. Grib A. A. and Pavlov Y. V. On particle collisions near rotating black holes // *Gravitation and Cosmology*.-2011.- vol. 17.- pp. 42-46.

159. Harada T. and Kimura M. Collision of an innermost stable circular orbit particle around a Kerr black hole // *Phys. Rev. D*.- vol. 83.- p. 024002.

160. Wei S.-W., Liu Y.-X., Guo H. and Fu C.-E. Charged spinning black holes as particle accelerators // *Phys. Rev. D*.-2010.- vol. 82.- p. 103005.

161. Zaslavskii O. B. Acceleration of particles as a universal property of rotating black holes // *Phys. Rev. D*.- vol. 82.- p. 083004.

162. Zaslavskii O. B. Acceleration of particles by nonrotating charged black holes? // *Soviet Journal of Experimental and Theoretical Physics Letters*.- vol. 92.- pp. 571-574.

163. Zaslavskii O. B. Acceleration of particles by black holes - a general explanation // *Classical and Quantum Gravity*.-2011.- vol. 28.- p. 105010.

164. Kimura M., Nakao K.-I. and Tagoshi H. Acceleration of colliding shells around a black hole: Validity of the test particle approximation in the Banados-Silk-West process // *Phys. Rev. D*.-2011.- vol. 83.- p. 044013.

165. Banados M., Hassanain B., Silk J. and West S. M. Emergent flux from particle collisions near a Kerr black hole // *Physical Review D*.-2011.- vol. 83.- p. 023004.

166. Liu C., Chen S., Ding C. and Jing J. Particle acceleration on the background of the Kerr-Taub-NUT spacetime // *Physics Letters B*.-2011.- vol. 701.- pp. 285-290.

167. Stuchlik Z., Hledik S., and Truparova K. Evolution of Kerr superspinars due to accretion counterrotating thin discs // *Classical and Quantum Gravity*.-2011.- vol. 28.- p. 155017.

168. Stuchlik Z. and Schee J. Observational phenomena related to primordial Kerr superspinars // *Classical and Quantum Gravity*.-2012.- vol. 29.- p. 065002.

169. Stuchlik Z. and Schee J. Circular geodesic of Bardeen and Ayon-Beato-Garcia regular black-hole and no-horizon spacetimes // *International Journal of Modern Physics D*.-2015.- vol. 24.- p. 50020.

170. Stuchlik Z. and Schee J. Ultra-high-energy collisions in the superspinning Kerr geometry // *Classical and Quantum Gravity*.-2013.- vol. 30.- p. 075012.

171. Stuchlik Z., Schee J. and Abdujabbarov A. Ultra-high-energy collisions of particles in the field of near-extreme Kehagias-Sfetsos naked singularities and

their appearance to distant observers // *Phys. Rev. D.*-2014.- vol. 89.- p. 104048.

172. Toshmatov B., Abdujabbarov A., Ahmedov B. and Stuchlik Z. Motion and high energy collision of magnetized particles around a Horava-Lifshitz black hole," *Astrophys Space Sci*.-2015.- vol. 360.- p. 19.

173. Toshmatov B., Abdujabbarov A., Ahmedov B. and Stuchlik Z. Particle motion and Penrose processes around rotating regular black hole // *Astrophys Space Sci*.-2015.- vol. 357.- p. 41.

174. Kerr R. P. Gravitational field of a spinning mass as an example of algebraically special metrics // *Phys. Rev. Lett.*-1963.- vol. 11.- pp. 237-238.

175. Carter B. Global Structure of the Kerr Family of Gravitational Fields // *Physical Review*.-1968.- vol. 174.- pp. 1559-1571.

176. Riess A. G., Filippenko A. V. and et al. Observational Evidence from Supernovae for an Accelerating Universe and a Cosmological Constant," *Astrophys. J.*.-1998.- vol. 116.- pp. 1009-1038.

177. Hawking S. W., Hunter C. J. and Taylor-Robinson M. M. Rotation and the AdS-CFT correspondence," *Phys. Rev. D*.-1999.- vol. 59.- p. 064005.

178. Randall L. and Sundrum R. Large Mass Hierarchy from a Small Extra Dimension // *Physical Review Letters*.-1999.- vol. 83.- pp. 3370-3373.

179. Randall L. and Sundrum R. An Alternative to Compactification // *Physical Review Letters*.-1999.- vol. 83.- pp. 4690-4693.

180. Maartens R. Brane-World Gravity // *Living Reviews in Relativity*.-2004.- vol. 7.- p. 7.

181. Dadhich N., Maartens R., Papadopoulos P. and Rezania V. Black holes on the brane," *Physics Letters B*.-2000.- vol. 487.- pp. 1-6.

182. Aliev A. N. and Gumrukcuoglu A. E. Charged rotating black holes on a 3-brane // *Phys. Rev. D*.-2005.- vol. 71.- p. 104027.

183. da Rocha R. and Coimbra-Araujo C. H. Physical Effects of Extra Dimension and Concomitant Map between Photons and Gravitons in Randall- Sundrum Brane-World Scenario // *ArXiv General Relativity and Quantum Cosmology e-prints*.-2006.

184. Casadio R., Fabbri A. and Mazzacurati L. New black holes in the brane world?," *Phys. Rev. D*.-2002.- vol. 65.- p. 084040.

185. Bronnikov K., Melnikov V. and Dehnen H. General class of brane-world black holes," *Phys. Rev. D*.-2003.- vol. 68.- p. 024025.

186. Molina C. and Neves J. C. S. Black holes and wormholes in AdS branes // *Phys. Rev. D*.-2010.- vol. 82.- p. 044029.

187. Molina C. and Neves J. C. S. Wormholes in de Sitter branes // *Phys. Rev. D*.-2012.- vol. 86.- p. 024015.

188. Neves J. C. S. and Molina C. Rotating black holes in a Randall-Sundrum brane with a cosmological constant // *Phys. Rev. D*.-2012.- vol. 86.- p. 124047.

189. Clifton T., Ferreira P. G., Padilla A. and Skordis C. Modified gravity and cosmology," *Phys. Rep*.-2012.- vol. 513.- pp. 1-189.

190. Arkani-Hamed N., Dimopoulos S. and Dvali G. The hierarchy problem and new dimensions at a millimeter // *Physics Letters B*.-1998.- vol. 429.- pp. 263-272.

191. Antoniadis I., Arkani-Hamed N., Dimopoulos S. and Dvali G. New dimensions at a millimeter to a fermi and superstrings at a TeV // *Physics Letters B*.-1998.- vol. 436.- pp. 257-263.

192. Schee J. and Stuchlik J. Optical Phenomena in the Field of Braneworld Kerr Black Holes // *International Journal of Modern Physics D*.-2009.- vol. 18.- pp. 983-1024.

193. Dadhich N. and Turakulov Z. Y. The most general axially symmetric electrovac spacetime admitting separable equations of motion // *Classical and Quantum Gravity*.-2002.- vol. 19.- pp. 2765-2775.

194. Bini D., Cherubini C., Jantzen R. T. and Mashhoon B. Gravitomagnetism in the Kerr-Newman-Taub-NUT spacetime // *Classical and Quantum Gravity*.-2003.- vol. 20.- pp. 457-468.

195. Rahvar S. and Habibi F. Possibility of Magnetic Mass Detection by the Next Generation of Microlensing Experiments // *Astrophys. J*.-2004.- vol. 610.- pp. 673-678.

196. Oteev T., Abdujabbarov A., Stuchlik Z. and Ahmedov B. Energy extraction and particle acceleration around a rotating black hole in quintessence *Astrophys Space Sci*.-2016.- vol. 361.- p. 269.

197. Abdujabbarov A., Ahmedov B. and Hakimov A. Particle motion around black hole in Horava-Lifshitz gravity // *Phys.Rev. D*.-2011.- vol. 83.- p. 044053.

Appendix

Appendix —1. A uniform magnetic field in the vicinity of quintessential rotating black hole

Here we assume that the quintessential rotating black hole is placed in the external magnetic field aligned along its symmetry axis.

Consider quintessential black hole in an external asymptotically uniform magnetic field. In order to find the related vector potential of the electromagnetic field we apply the Wald method that uses the Killing vectors of the spacetime [84]. The Killing vector field ξ^{μ}, being an infinitesimal generator of an isometry, fulfills the equation

$$\xi_{\alpha;\beta} + \xi_{\beta;\alpha} = 0 \ . \tag{A.1.1}$$

The equation (A.1.1) implies the equation

$$\xi_{\alpha;\beta;\gamma} - \xi_{\alpha;\gamma;\beta} = -\xi^{\lambda} R_{\lambda\alpha\beta\gamma} \tag{A.1.2}$$

where $R_{\lambda\alpha\beta\gamma}$ is the Riemann curvature tensor. we have relation for the Killing vectors

$$\xi^{\alpha;\beta}_{;\beta} = R^{\alpha}_{\mu}\xi^{\mu}. \tag{A.1.3}$$

In the Lorentz gauge the source free Maxwell equations take the form [39]

$$A^{\alpha;\beta}_{;\beta} = 0. \tag{A.1.4}$$

Since the quintessential black hole spacetime is not Ricci flat ($R_{\alpha\beta} \neq 0$) the external magnetic field surrounding the quintessential black hole will be modified. In order to find the solution for the potential of electromagnetic field one may use the following anzatz:

$$A^{\alpha} = C_1\xi^{\alpha}_{(t)} + C_2\xi^{\alpha}_{(\phi)} - a^{\alpha} \tag{A.1.5}$$

where a^{a} is the correction due to the non-zero Ricci tensor in the presence of quintessence. It can be found from the equations

$$a^{\alpha;\beta}{}_{;\beta} = \left(C_1\xi^{\gamma}_{(t)} + C_2\xi^{\gamma}_{(\phi)}\right) R^{\alpha}{}_{\gamma}\ . \tag{A.1.6}$$

The first two terms in this equation are related to the homogeneous solution of the equation that is directly related to the Killing vectors of the spacetimes. The third term is the partial solution related to the Ricci tensor of the spacetime. The constants related to the Killing vectors can be found easily - the constant $C_2 = B/2$, if we have the gravitational source immersed in the uniform magnetic field **B** that is parallel to the axis of rotation corresponding to the axial symmetry of the spacetime. The remaining constant C_1 has to vanish as can be easily shown due to the asymptotic properties of the KS spacetimes at the infinity [64, 84, 197]. Finally, the covariant components of the four-vector potential of the electromagnetic field can be written in the form

$$\begin{aligned} A_t &= -\frac{1}{\Sigma}\Bigg\{aB\left[\left(\Delta + \frac{r^2-a^2-\Delta}{2}\sin^2\theta\right)\right.\\ &+ \left.\left.\tilde{c}r^3\frac{r^2+a^2-\Delta}{6}\sin^2\theta\right]\right\},\\ A_r &= A_\theta = 0\ ,\\ A_\varphi &= -\frac{B}{2\Sigma}\Bigg\{\left(r^2+a^2-\Delta\right)a^2\left(1+cos^2\theta\right) - \left(r^2+a^2\right)\Sigma\\ &- \left.\frac{\tilde{c}r^3}{3}\left(\Sigma(r^2+a^2) + (r^2+a^2-\Delta)a^2\sin^2\theta\right)\right\}\sin^2\theta\ . \end{aligned} \tag{A.1.7}$$

The components of the four-velocity for zero angular momentum observers (ZAMOs) take the form

$$\begin{aligned} (u^\alpha)_{\text{ZAMO}} = \Bigg\{&\left(\frac{\Sigma(r^2+a^2)+a^2\Xi\sin^2\theta}{(r^2+a^2)(\Sigma-\Xi)+\Xi a^2\sin^2\theta}\right)^{1/2},0,0,\\ &\left.\frac{a\Xi}{\Sigma(r^2+a^2)+a^2\Xi\sin^2\theta}(u^t)_{\text{ZAMO}}\right\}, \end{aligned} \tag{A.1.8}$$

$$(u_\alpha)_{\text{ZAMO}} = \left\{-\left(\frac{(r^2+a^2)(\Sigma-\Xi)+\Xi a^2\sin^2\theta}{\Sigma(r^2+a^2)+a^2\Xi\sin^2\theta}\right)^{1/2},0,0,0\right\}, \tag{A.1.9}$$

Where the parameter $\Xi = r^2 + a^2 - \Delta$.

The nonvanishing components of the Faraday tenor measured by zero angular momentum observers (ZAMO) with the help of four velocity components are given as follows

$$
\begin{aligned}
F_{rt} &= \frac{aB}{\Sigma}\left\{\frac{\Sigma'}{\Sigma}\left[\Delta+\left(\frac{r^2-a^2-\Delta}{2}+\frac{\Xi}{6}cr^3\right)\sin^2\theta\right]\right.\\
&- \left.\left[\Delta'+\left(r-\frac{\Delta'}{2}+\frac{1}{2}\left(\Xi'\frac{\tilde{c}r^3}{3}+\Xi\tilde{c}r^2\right)\right)\sin^2\theta\right]\right\}, \qquad (A.1.10)\\
F_{\theta t} &= -\frac{aB}{\Sigma}\left(r^2-a^2-\Delta+\frac{\Xi}{3}\tilde{c}r^3\right)\sin\theta\cos\theta\,, \qquad (A.1.11)\\
F_{r\phi} &= \frac{B}{2\Sigma}\left\{\left(\frac{\Sigma'}{\Sigma}\left(r^2+a^2-\Delta\right)-2r+\Delta'\right)a^2\left(1+\cos^2\theta\right)\right.\\
&+ 2r\Sigma-\frac{\Sigma'}{\Sigma}\frac{\tilde{c}r^3}{3}\left(\Sigma(r^2+a^2)+(r^2+a^2-\Delta)a^2\sin^2\theta\right)\\
&+ \tilde{c}r^2\left[\left(\Sigma(r^2+a^2)+(r^2+a^2-\Delta)a^2\sin^2\theta\right)\right.\\
&\quad \left.\left.+\frac{r}{3}\left(\Sigma'(r^2+a^2)+2r\Sigma+(2r-\Delta')a^2\sin^2\theta\right)\right]\right\}\sin^2\theta\,, \qquad (A.1.12)\\
F_{\theta\phi} &= \frac{B}{\Sigma}\left\{\Sigma\left(r^2+a^2\right)-2\left(r^2+a^2-\Delta\right)a^2\cos^2\theta+\frac{\tilde{c}r^3}{3}\left(\Sigma(r^2+a^2)\right.\right.\\
&+ \left.\left.2(r^2+a^2-\Delta)a^2\sin^2\theta\right)\right\}\sin\theta\cos\theta\,. \qquad (A.1.13)
\end{aligned}
$$

It is uncomplicated to carry out the expressions for the orthonormal components of the electromagnetic fields measured by the ZAMO observers with the help of the four-velocity components of zero angular momentum observer (A.1.8) and

$$
\begin{aligned}
E^{\hat{r}} &= \frac{aB}{\Sigma}\left\{\frac{\Sigma\,'}{\Sigma}\left(\Delta-\frac{r^2-a^2-\Delta}{2}\sin^2\theta\right)-\left(\Delta'-(r-\frac{\Delta'}{2})\sin^2\theta\right)\right.\\
&+ \frac{1}{2}\left[\left(\frac{\Sigma'}{\Sigma}\Xi-2r+\Delta'\right)a^2(1+\cos^2\theta)+2r\Sigma\right]\\
&\quad \left.\times\frac{\Xi\sin^2\theta}{\Sigma(r^2+a^2)+\Xi a^2\sin^2\theta}+\frac{(r^2+a^2)(\Sigma'\,\Xi-\Sigma\,\Xi')+2r\,\Sigma\,\Xi\,\tilde{c}r^3}{\Sigma(r^2+a^2)+a^2\Xi\sin^2\theta}\frac{\tilde{c}r^3}{6}\sin^2\theta\right\}\\
&\quad \times\left(\frac{\Sigma(r^2+a^2)+\Xi a^2\sin^2\theta}{(r^2+a^2)(\Sigma-\Xi)+\Xi a^2\sin^2\theta}\frac{\Delta}{\Sigma}\right)^{1/2}, \qquad (A.1.14)
\end{aligned}
$$

$$
\begin{aligned}
E^{\hat{\theta}} &= \frac{B}{\Sigma}\Bigg\{ a\left(r^2-a^2-\Delta\right) + \left[\Sigma(r^2+a^2) - 2\Xi a^2\cos^2\theta + \frac{\Xi}{3}a^3\tilde{c}r^3\right] \\
&\times \frac{\Xi\sin^2\theta}{\Sigma(r^2+a^2)+\Xi a^2\sin^2\theta}\Bigg\} \\
&\times \left(\frac{\Sigma(r^2+a^2)+\Xi a^2\sin^2\theta}{\cdots} - \frac{1}{\cdots}\right)^{1/2}\sin\theta\cos\theta
\end{aligned}
\tag{A.1.15}
$$

$$
\begin{aligned}
B^{\hat{r}} &= -\frac{B}{\Sigma}\left(\frac{\Sigma(r^2+a^2)-2\Xi a^2\cos^2\theta-\tilde{c}r^3(\Sigma(r^2+a^2)+2\Xi a^2\cos^2\theta)}{\Sigma(r^2+a^2)+\Xi a^2\sin^2\theta}\right)\Sigma^{1/2} \\
&\times\left(\frac{(r^2+a^2)(\Sigma-\Xi)+\Xi a^2\sin^2\theta}{\Delta-a^2\sin^2\theta}\right)^{1/2}\cos\theta\,,
\end{aligned}
\tag{A.1.16}
$$

$$
\begin{aligned}
B^{\hat{\theta}} &= \frac{B}{2\Sigma}\Bigg[\left(\frac{\Sigma'}{\Sigma}\Xi-2r+\Delta'\right)a^2(1+\cos^2\theta)+2r\Sigma \\
&- \frac{\tilde{c}r^2}{3}\Big(-a^2r\sin^2\theta\,\Xi\Sigma'+\Sigma^2(3(r^2+a^2)+r\Sigma') \\
&+a^2\Sigma\sin^2\theta(3\Xi+r\Xi')\Big)\Bigg]\frac{1}{\Sigma(r^2+a^2)+\Xi a^2\sin^2\theta} \\
&\times\left(\frac{(r^2+a^2)(\Sigma-\Xi)+\Xi a^2\sin^2\theta}{\Delta-a^2\sin^2\theta}\,\frac{\Delta}{\Sigma}\right)^{1/2}\sin\theta\,.
\end{aligned}
\tag{A.1.17}
$$

In fact, the radial and polar components of the electric field can appear due to the dragging of inertial frames with dependence on angular momentum of the

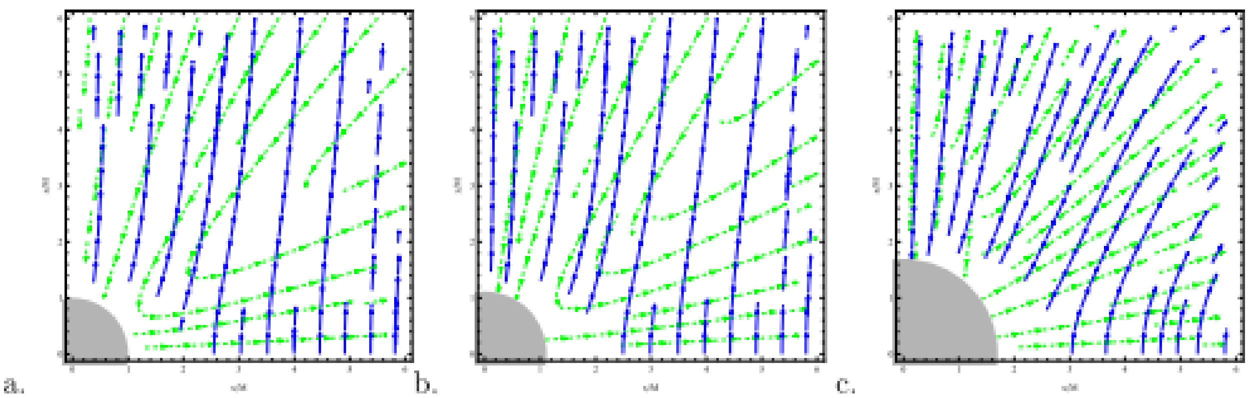

Figure A.1.1: The configuration of electromagnetic field lines in the vicinity of a quintessential rotating black hole. Blue and green lines describe field lines of the magnetic and electric field, respectively. Meanwhile, the horizon is shown as a gray-shaded area. Given the figures correspond to the various values of the quintessential parameter (a) c = 0.0001, (b) c = 0.01, and (c) c = 0.1 in the case in which magnetic field B = 0.5. Also, spin and matter state parameters are considered as $\alpha = 1$ and ω_q= —2/3, respectively, for all cases.

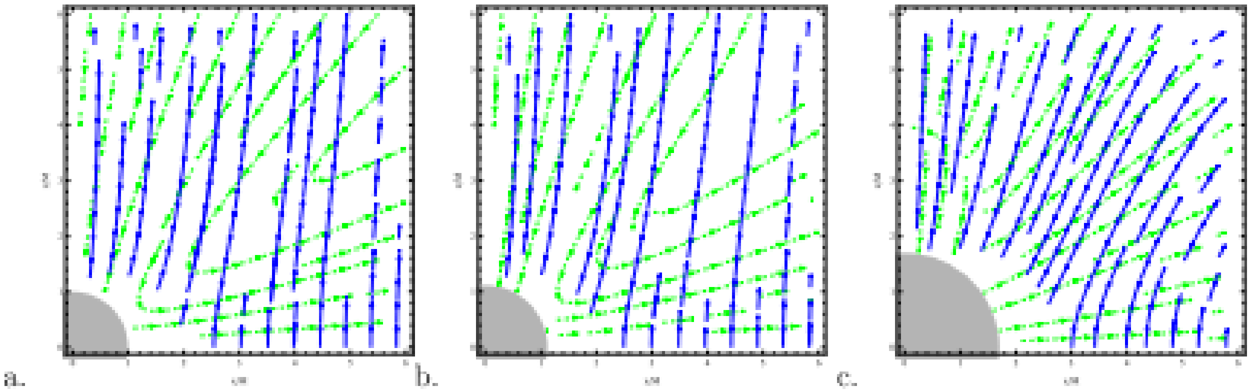

Figure A.1.2: The configuration of electromagnetic field lines in the vicinity of a quintessential rotating black hole. Blue and green lines describe field lines of the magnetic and electric field, respectively. Meanwhile, the horizon is shown as a gray-shaded area. Given the figures correspond to the various values of the quintessential parameter (a) $\tilde{c} = 0.0001$, (b) $\tilde{c} = 0.01$, and (c) $\tilde{c} = 0.1$ in the case in which magnetic field B = 1. Also, spin and matter state parameters are considered as $\alpha = 1$ and $\omega_q = -2/3$, respectively, for all cases.

black hole. In the limit of flat spacetime, i.e., for $M/r \to 0$, $M\alpha/r^2 \to 0$, and $c \to 0$, expressions (A.1.14-A.1.17) give

$$\lim_{M/r,\ Ma/r^2\to 0,\ \tilde{c}\to 0} B^{\hat{r}} = -B\cos\theta\,,$$

$$\lim_{M/r,\ Ma/r^2\to 0,\ \tilde{c}\to 0} B^{\hat{\theta}} = B\sin\theta\,,$$

$$\lim_{M/r,\ Ma/r^2\to 0,\ \tilde{c}\to 0} E^{\hat{r},\hat{\theta}} = 0\,, \tag{A.1.18}$$

as was expected, they coincide with the solutions for the homogeneous magnetic field in a Minkowski spacetime. The configuration of electromagnetic field lines in the vicinity of a quintessential rotating black hole is plotted in Fig.s A.1.1 and A.1.2.